AUTOPHAGY AND THE NRF2/KEAP1 PATWAY IN GLIA

ROLE OF AUTOPHAGY AND THE NRF2/KEAP1 PATHWAY IN THE GLIA DURING OXIDATIVE STRESS IN THE *DOSOPHILA* BRAIN

By: MARIA PESEVSKI, B.SC.

A Thesis submitted to the School of Graduate Studies in Partial Fulfilment of the Requirement for the Degree Master of Science

McMaster University MASTER OF SCIENCE (2015) Hamilton, Ontario (Biology)

TITLE: Role of Autophagy and the NRF2/Keap1 Pathway in the Glia During Oxidative Stress in the *Drosophila* Brain AUTHOR: Maria Pesevski, B.Sc. (McMaster University) SUPERVISOR: Professor A.R. Campos NUMBER OF PAGES: xiii, 145

Lay Abstract

Excessive levels of reactive oxygen species (ROS) damage cellular components and leads to oxidative stress (Finkel & Holbrook, 2000). Oxidative stress is a major cause of aging, neurodegenerative disease, cardiovascular disease and cancer (Finkel & Holbrook, 2000). Two stress response pathways that help cells cope with oxidative stress are the NRF2/Keap1 pathway, involved in the direct regulation of antioxidants, and the autophagy pathway, the recycling pathway of the cell (Essick & Sam, 2010; Singh, Vrishni, Singh, Rahman, & Kakkar, 2010). Although autophagy can clean up damage in cells during oxidative stress, it is also involved in autophagic cell death, especially during highly stressful conditions (Maiuri, Zalckvar, Kimchi, & Kroemer, 2007). It was hypothesized that down regulation of autophagy and activation of the NRF2/Keap1 pathway in the glia would provide protection of the *Drosophila* brain from these forms of stress. In this thesis, it was demonstrated that down regulation of autophagy in the glia, provides some protection of the *Drosophila* brain from oxidative stress. This was not observed for the NRF2/Keap1 pathway.

Abstract

Excessive levels of reactive oxygen species (ROS) damage cellular components and leads to oxidative stress (Finkel & Holbrook, 2000). Oxidative stress is a major cause of aging, neurodegenerative disease, cardiovascular disease and cancer (Finkel & Holbrook, 2000). Two stress response pathways that help cells cope with oxidative stress are the NRF2/Keap1 pathway, involved in the direct regulation of antioxidants, and the autophagy pathway, the recycling pathway of the cell (Essick & Sam, 2010; Singh et al., 2010). Although autophagy can clean up damage in cells during oxidative stress, it can cause autophagic cell death, especially during highly stressful conditions (Maiuri et al., 2007). In this thesis, the roles of autophagy and the NRF2/Keap1 pathway were examined in the glia during acute oxidative stress, and the role of autophagy was examined during thermal stress and aging. It was hypothesized that down regulation of autophagy and activation of the NRF2/Keap1 pathway in the glia would provide protection of the *Drosophila* brain from these forms of stress. The results show that down regulation of autophagy provides protection of survival and locomotor ability but there were inconclusive results regarding the protection of dopaminergic neurons after exposure to oxidative stress. Activation of the NRF2/Keap1 Pathway in the glia did not provide any protection to survival or locomotor ability of flies. Furthermore, down regulation of autophagy in the glia did not provide protection from thermal stress nor did it provide extension of the lifespan or delay in age-dependent decline of locomotor ability. In conclusion, only the down regulation of autophagy in the glia provides some protection of the *Drosophila* brain from oxidative stress.

Acknowledgements

I want to express my deepest gratitude to my supervisor Dr. Ana R. Campos, for being an incredible mentor and a role model. Thank you for accepting me into your lab family and providing me with the opportunity to work on this project. You have helped me learn many valuable lessons about science and about life. Because of your mentorship, I have become a better critical thinker and a more detail oriented researcher. I also look up to you, as you are one of my most influential role models. I will never forget this valuable experience and my time in your lab. I want to also thank Dr. Roger Jacobs for his mentorship and guidance as the second member of my supervisory committee. Thank you for your time and valuable input towards my thesis and the knowledge I have gained through the process. I also want to than Dr. Juliet Daniel for accepting to be the chair for my defense despite the short notice. I would also like to give a very special thanks to former Campos lab members Jonathan Tsou and Nadia Iftekharuddin for your help, support and most importantly your friendship. I will never forget you, and I hope to stay friends with you for a really long time. I would also like to thank all of the Jacob's lab former and current members. You have enhanced my entire experience and have helped my research with your useful input during lab meetings and engaging talks while fly pushing. I want to give a special mention to Duygu Cevik, thank you for being an incredible friend, and being there during the hard parts when I needed you. Finally, I want to give a very special thanks to the two volunteers Ana Stosic and Rachel Lee who have helped me greatly by obtaining the thermal stress data, as well as for their help with the general lab maintenance and stocks.

Table of Contents

Table of Figures:

List of Abbreviations

AD	Alzheimer's Disease
ALS	Amyotrophic lateral sclerosis
ARE	Antioxidant Response Element
Atg	Autophagy Related
BBB	Blood Brain Barrier
Bcl2	B-Cell lymphoma 2
CAT	Catalase
CncC	Cap'n'collar C
CNS	Central Nervous System
DA	Dopamine
ERK	Extracellular-signal regulated Kinase
EST	Expressed Sequence Tag
ETC	Electron Transport Chain
GPx	Glutathione Peroxidase
GSH	Glutathione
HD	Huntington's Disease
JNK	c-Jun amino-terminal kinase
KEAP1	Kelch-like ECH-associated Protein 1
LC3	Microtubule-associated protein 1A/1B-light chain 3
Maf	Musculo-aponeurotic fibroscaroma
MAPK	Mitogen-activated protein kinase

MPTP	1-methyl-4-phenyl-1,2,3,6-tetrahydropyridine
ND	Neurodegenerative Disease
NF-kB	Nuclear factor kappa-light-chain-enhancer of activated B cells
NRF2	NF-E2 Related Factor 2
PAL	Paired anterior lateral
PAM	Paired anterior medial
PAS	Pre-autosomal structure
PD	Parkinson's Disease
PE	Phosphatidylethanolamine
PI3K	Phosphatidylinostol 3-kinase
PI3P	Phosphatidylinostol 3-phosphate
PNG	Perineurial glia
PPL1 and 2	Paired posterior lateral 1 and 2
PPM1/2 and 3	Paired posterior medial 1/2 and 3
ROS	Reactive Oxygen Species
SOD	Superoxide Dismutase
SPG	Subperineurial Glia
TH	Tyrosine hydroxylase
Tor	Target of Rapamycin

1 Introduction

1.1 Oxidative stress: The tipping point of ROS balance

Oxidative stress is a cellular state that occurs when high levels of oxygen free radicals or other partially reduced oxygen intermediates, also known as reactive oxygen species (ROS), cause cellular damage (Finkel & Holbrook, 2000; Kohen & Nyska, 2002; Runchel, Matsuzawa, & Ichijo, 2011). High levels of ROS can be the result of aerobic respiration or external sources such as ultraviolet light, ionizing radiation, chemotherapeutics and other environmental toxins (Finkel & Holbrook, 2000; Kohen & Nyska, 2002). Aerobic respiration provides an advantage to cells compared to anaerobic respiration due to the greater and more efficient production of energy (Blackstone, 1995). Aerobic respiration, however, comes at a cost. It requires electrophilic molecular oxygen, which, during the process of aerobic respiration, is converted into superoxide ions (O_2^-), hydrogen peroxide (H_2O_2) or hydroxyl radicals (HO^-) (Kohen & Nyska, 2002; Mittler, 2002; Miwa & Brand, 2003). ROS can cause damage to important cell components and macromolecules including proteins, lipids and DNA (Finkel & Holbrook, 2000; Kohen & Nyska, 2002). This damage includes intracellular modifications that can lead to denaturation, inactivation, fragmentation or degradation of proteins, lipid peroxidation leading to compromised integrity and leakiness of lipid membranes, and finally base modification and single- or double-strand breakage of DNA molecules (Kohen & Nyska, 2002). Since the origin of aerobic respiration, organisms have evolved many different cellular mechanisms aimed to protect the cell from the burden of ROS production and oxidative stress (Blackstone, 1995; Harman, 1992). Such mechanisms include repair systems for damaged macromolecules,

stabilization of biological sites, control of endogenous sources of ROS and, most importantly, the production of enzymatic and non-enzymatic antioxidants, molecules and enzymes involved in scavenging and neutralization of ROS (Kohen & Nyska, 2002). All of these defense mechanisms, including the production of antioxidants, are governed by several conserved stress response pathways including the c-Jun-N-terminal kinase (JNK) pathway, p38 pathway, extracellular-signal regulated kinase (ERK) pathway, Nrf2/Keap1 (NF-E2 Related Factor 2/Kelch-like ECH-associated Protein 1) pathway and autophagy among others, which will be discussed in detail in section *1.1.2* (Finkel & Holbrook, 2000; Harman, 1992; Nguyen, Sherratt, & Pickett, 2003; Runchel et al., 2011). The balance between ROS and antioxidant production, referred to as the redox potential, is very tightly regulated by the cell. (Finkel & Holbrook, 2000; Kohen & Nyska, 2002). At equilibrium, a baseline, controlled production of ROS is essential for normal cell function (Finkel & Holbrook, 2000). It is required for many different cell signaling pathways involved in cell proliferation, cell differentiation and apoptosis, as well as in immunity and cellular host defenses (Finkel & Holbrook, 2000; Kohen & Nyska, 2002; Mates, Pérez-Gómez, & De Castro, 1999). When the balance between ROS production and the antioxidant scavengers is disturbed, the cells undergo either oxidative stress or reductive stress. Reductive stress is the cellular state in which there is cellular malfunction due to lack of oxidizing agents and an abundance of reducing agents such as antioxidants (Kohen & Nyska, 2002; Rajasekaran et al., 2007). In both cases, this eventually leads to abnormal cell function or cell death (Finkel & Holbrook, 2000; Kohen & Nyska, 2002; Runchel et al., 2011). In the case of oxidative stress, the consequences include neurodegenerative disease (ND), cardiac

disease, cancer and aging (Essick & Sam, 2010; Finkel & Holbrook, 2000; Kohen & Nyska, 2002).

1.1.1 Aging: Consequence of chronic oxidative stress

One of the most popular theories explaining the cause of aging is the "Free Radical Theory", first proposed in the mid 1950's by Dr. Denham Herman (Harman, 1956, 1992). Dr. Herman's theory states that lifespan is strongly correlated with the rate of metabolism. This is because metabolism is the primary endogenous mechanism for production of ROS (Harman, 1956, 1992). This theory goes further to suggest that chronic exposure to ROS leads to chronic cellular oxidative stress which leads to aging, disease and death (Harman, 1956, 2002). Over the years this theory has gained tremendous popularity and support, and it is now widely accepted that ROS and oxidative stress are major causes of aging and age-associated pathologies such as neurodegenerative and cardiovascular diseases and cancer (Finkel & Holbrook, 2000; Harman, 1992; Kohen & Nyska, 2002).

1.1.2 Oxidative stress response: The defense mechanisms

Cells have developed several different defense mechanisms in order to counteract the negative effects of ROS and oxidative stress (Finkel & Holbrook, 2000; Kohen & Nyska, 2002; Mates et al., 1999). As discussed above, the most important cellular defense mechanism against oxidative stress is the array of enzymatic and non-enzymatic antioxidants (Finkel & Holbrook, 2000; Kohen & Nyska, 2002; Mates et al., 1999). Enzymatic antioxidants include superoxide dismutase (SOD), catalase (CAT), and glutathione peroxidase (GPx) all of which are found both in the mitochondria and in the cytoplasm (Kohen & Nyska, 2002; Mates et al., 1999). These enzymatic antioxidants deal

with ROS produced by the electron transport chain (ETC) during aerobic respiration (Kohen & Nyska, 2002; Mates et al., 1999). More specifically, during aerobic respiration, molecular oxygen is used as an electrophile that receives the electrons passing through the ETC at ubiquinine-cytochrome C reductase (Complex III) (Turrens, 1997, 2003). This process converts molecular oxygen into a superoxide ion (O_2^-) (Turrens, 1997, 2003). SOD converts superoxide ions (O_2^-) into hydrogen peroxide (H_2O_2). H_20_2 is converted into water (H_2O) by CAT and GPx (Mates et al., 1999; Turrens, 1997, 2003). Additionally, there are several non-enzymatic antioxidants that can be characterized by their low molecular weight and their ability to directly scavenge ROS that can come from endogenous or exogenous sources (Kohen & Nyska, 2002; Mates et al., 1999). These include glutathione (GSH), histidine dipeptides, uric acid, ascorbic acid (vitamin C), alpha-tocopherol (vitamin E), beta-carotene and vitamin A (Finkel & Holbrook, 2000; Kohen & Nyska, 2002; Mates et al., 1999).

There are several stress response pathways that govern the cellular response to damage caused by ROS (Essick & Sam, 2010; Finkel & Holbrook, 2000; Martindale & Holbrook, 2002; Runchel et al., 2011). These include the highly conserved mitogen-activated protein kinase (MAPK) signaling cascades such as extracellular signal-regulated kinase 1 and 2 (ERK) pathways, involved in promoting proliferation and survival, c-Jun amino-terminal kinase (JNK) and p38 mitogen-activated protein kinase (p38MAPK), both involved in general cellular stress response and promotion of apoptosis (Finkel & Holbrook, 2000; Martindale & Holbrook, 2002; Runchel et al., 2011). In addition, there are several non-MAPK pathways that are activated during oxidative stress and these

include phosphoinositide 3-kinase (PI3K)/Akt pathway, another proliferation promoting pathway involved in starvation, the nuclear factor NF-kB (Nuclear factor kappa-light-chain-enhancer of activated B cells), transcription factor involved in general stress response and promoting the expression of immunity, inflammation, and apoptosis genes, p53, the tumor-suppressing, DNA-damage-sensing protein, the heat shock response transcription factor, involved in protein damage response, as well as, the NRF2/Keap1, the oxidative stress-specific signaling pathway, and autophagy, the recycling pathway of the cell. (Essick & Sam, 2010; Finkel & Holbrook, 2000; Martindale & Holbrook, 2002; Runchel et al., 2011; X. Wang, Martindale, Liu, & Holbrook, 1998). For the purpose of this report, only the NRF2/Keap1 pathway and autophagy will be discussed in further detail in sections *1.3* and *1.4*.

1.1.3 Paraquat: Experimental induction of oxidative stress

Paraquat (1,1'dimethyl-4-4'-bipyridynium dichloride), also referred to as methyl viologen, is an herbicide with highly toxic effect on most animals (Smith, Rose, & Wyatt, 1978). Upon its reaction with molecular oxygen, it reduces the O_2 molecule into O_2^-, one of the most potent ROS (Smith et al., 1978). Paraquat has been linked to acute pathology upon ingestion and inhalation of high concentration, including lung, mouth, esophagus, kidney, liver and brain damage (Smith et al., 1978). Paraquat has also been linked to the development and progression of Parkinson-like symptoms in many organisms including *Drosophila*, rats and humans (McCormack et al., 2002; Nisticò, Mehdawy, Piccirilli, & Mercuri, 2011; Tanner et al., 2011). Because of its property to rapidly produce of ROS, as well as its ability to penetrate the blood brain barrier (BBB), paraquat is often used in

many studies for the induction of oxidative stress, especially studies using *Drosophila* as a model organism (Shimizu et al., 2001; Smith et al., 1978). *Drosophila* studies using paraquat will be described in more detail in section *1.1.4*

1.1.4 Aging and oxidative stress: Studies in Drosophila

One study in *Drosophila* investigated whether gene expression during aging is similar to the gene expression during oxidative stress (Zou, Meadows, Sharp, Jan, & Jan, 2000). This study used a microarray technique and tested 8000 different ESTs (Expressed sequence tags) representing 4500 different genes (Zou et al., 2000). They tested flies ranging in age from 3 days old to 50 days old and compared them to 3 day old flies treated with paraquat (Zou et al., 2000). Although they found a lot of genes that are regulated independently by age or by oxidative stress, 42 genes were regulated by both processes (Zou et al., 2000). The majority of the genes regulated by both oxidative stress and age were of unknown function (Zou et al., 2000). However, some of the genes downregulated by both processes are involved in energy production and mitochondrial function, and some of the genes upregulated by both processes are involved in redox balance, antioxidant production and detoxification (Zou et al., 2000). The authors of the study concluded that this evidence supports the "Free radical theory of aging" (Zou et al., 2000).

Another study looked at age-related changes on the levels of different enzymatic and non-enzymatic antioxidants, as well as different indicators of oxidative stress in *Drosophila* (Sohal, Arnold, & Orr, 1990). This study found that activities of CAT and GPx as well as the concentration of reduced glutathione decreased with age, while SOD activity increased with age (Sohal et al., 1990). As for the oxidative stress markers,

NADPH/NADP+ ratios and thiobarbituric acid-reactants decreased with age, while NADH/NAD+ ratios and inorganic peroxides increased with age (Sohal et al., 1990). This study concluded that, although these antioxidants and oxidative stress markers are selective and and tend to vary in different tissues, there is an overall trend in increase of oxidative stress as the flies age (Sohal et al., 1990).

Several different studies looked at the effects of overexpression of enzymatic antioxidants in *Drosophila* and found that independent overexpression of SOD and CAT yielded either a small or an insignificant effect on fly lifespan (Orr & Sohal, 1992, 1993). CAT overexpression did not provide protection to hyperoxia or paraquat treatment but it did provide resistance to H_2O_2 (Orr & Sohal, 1992). SOD, on the other hand, showed resistance to hyperoxia but not paraquat exposure (Orr & Sohal, 1993). When these two proteins were co-overexpressed in *Drosophila*, it extention of the fly's lifespan was observed by 1/3, and these flies had lower oxidative damage and delayed age-dependent decline in locomotor ability (Orr & Sohal, 1994).

Finally, a study examined the effects of exogenous antioxidants such as, SOD mimetic drugs Euk-8 and Euk-134 and mitochondria-targeted mitoquinone, on *Drosophila* lifespan and oxidative stress resistance and found that these drugs had a positive effect on immediate oxidative stress resistance but failed to provide significant lifespan extension to the exposed flies (Magwere et al., 2006).

All of these studies show evidence that support the "Free-radical theory of aging" and stress the importance of ROS, oxidative stress and antioxidant balance on normal cell function.

1.2 Oxidative stress in the brain: Neurodegeneration

Neurodegenerative diseases (NDs) are a large group of diseases that are characterized by gradual, usually age-related, loss of neuronal function (Jaiswal, Sandoval, Zhang, Bayat, & Bellen, 2012). The most common NDs include Alzheimer's disease (AD), Parkinson's disease (PD), polyglutamine diseases such as Huntington disease (HD), and amyotrophic lateral sclerosis (ALS) (Jaiswal et al., 2012; Martinez-Vicente & Cuervo, 2007; Simonian & Coyle, 1996). Although these ND are distinct and affect different types of neurons, they all have very similar characteristics: they have a late onset, they are usually caused by accumulation of protein aggregates and the progression of these NDs is highly linked to oxidative stress (Beal, 1995; Jaiswal et al., 2012; Martinez-Vicente & Cuervo, 2007). In fact, many of these NDs are linked to proteins involved in mitochondrial function and ROS metabolism (Lin & Beal, 2006). Most of these NDs have been modeled in different organisms such as *C. elegans*, *Drosophila*, and mice (Jaiswal et al., 2012). The mechanisms by which oxidative stress leads to NDs are outlined in section 1.2.1 and a detailed discussion of PD is outlined in 1.2.2.

1.2.1 Neurons: Neurodegeneration as a consequence of oxidative stress

The brain and neurons have a greater susceptibility for oxidative stress than other tissues because they have a high metabolic rate and are in a the post-mitotic state (Andersen, 2004). It has been suggested that the increased level of ROS with aging, due to age-related progressive mitochondrial dysfunction, insufficient production of antioxidants and exogenous exposure to ROS and toxins, cause oxidative alteration to proteins associated with NDs (Andersen, 2004). This causes these proteins to misfold and

aggregate in neurons resulting in progression of NDs (Andersen, 2004). Interestingly many of the proteins that are associated with NDs have some function in mitochondrial function (Lin & Beal, 2006). Some examples of mutant proteins associated with NDs that have mitochondrial function include α-synuclein, parkin and PINK1 in PD, and SOD1 in ALS (Lin & Beal, 2006). All of this evidence suggests that there is an intimate link between oxidative stress, aging and neurodegeneration. For the purposes of this report, this connection between oxidative stress and neurodegeneration and how this can be studied in *Drosophila* as a model organism, will be explored further through discussion of PD in section *1.2.2*.

1.2.2 Parkinson's disease and Drosophila: Oxidative stress and dopaminergic neurons

PD is caused by gradual loss of dopaminergic neurons due to the accumulation of protein aggregates called Lewy Bodies that contain α-synuclein and ubiquitin (Feany & Bender, 2000; Hirth, 2010; Lin & Beal, 2006). Symptoms of PD include progressive rigidity, bradykinesia and tremor (Lin & Beal, 2006). Dopaminergic neurons are particularly sensitive to oxidative stress because dopamine (DA) metabolism involves production of high levels of ROS (Andersen, 2004; Simonian & Coyle, 1996). The progressive increase in ROS and decrease of antioxidant defenses with age causes oxidative damage of α-synuclein in the Dopaminergic neurons (Andersen, 2004). This leads to misfolding of this protein making it unrecognizable to the ubiquitin-proteasome degradation system. Eventually, this process leads to aggregation of misfolded α-synuclein and formation of Lewy bodies in dopaminergic neurons (Andersen, 2004). This

process triggers the apoptotic signaling pathway and leads to programed cell death of dopaminergic neurons (Tompkins, Basgall, Zamrini, & Hill, 1997).

Studying PD-like phenotypes has been developed extensively in *Drosophila* (Barone & Bohmann, 2013; Feany & Bender, 2000; Hirth, 2010). Studying PD-like phenotypes in *Drosophila* has proven very useful for understanding the mechanism by which neurodegeneration occurs, as well as, for the search of new drugs that may be used as treatment or cure for PD in humans (Botella, Bayersdorfer, Gmeiner, & Schneuwly, 2009; Feany & Bender, 2000; Whitworth, Wes, & Pallanck, 2006). *Drosophila melanogaster* is one of the best studied model organisms and there are many different easy techniques that can be used to test PD-like phenotypes (Barone & Bohmann, 2013; Botella et al., 2009; Friggi-Grelin et al., 2003). One of the most common ways to test for PD-like phenotypes in *Drosophila* is the negative geotaxis assay (Barone & Bohmann, 2013; Feany & Bender, 2000). This method assesses the locomotor performance of flies, which can linked to the number and health of dopaminergic neurons (Barone & Bohmann, 2013). Another method for assessing PD-like phenotypes in *Drosophila* is immunostaining of the dopaminergic neurons using Tyrosine Hydroxylase (TH) antibody in order to quantify the number of dopaminergic neurons in whole brain mounts (Barone & Bohmann, 2013). The *Drosophila* brain contains more than 100 dopaminergic neurons organized in several different clusters (PPL1, PPL2, PPM1/2, PPM3, PAL and PAM) (Barone & Bohmann, 2013; White, Humphrey, & Hirth, 2010). These techniques provide an easy way to study the role of oxidative stress and aging, as well as the involvement of glia in neurodegeneration in *Drosophila*.

1.2.3 Glia: The protectors of the brain

Glia are a subset of central nervous system (CNS) cells that are involved in general maintenance of neurons (Edwards & Meinertzhagen, 2010). They are involved in neuronal insulation, axon pathfinding signaling, trophic support, cellular maintenance of neurons, clearance and recycling of excess neurotransmitters among other functions (Edwards & Meinertzhagen, 2010). The *Drosophila* CNS is comprised of 90% neurons and 10% glial cells (Edwards & Meinertzhagen, 2010). Although their numbers in *Drosophila* are much lower compared to mammals, glial cells still play a very important role in maintenance, protection and overall integrity of the fly's CNS (Edwards & Meinertzhagen, 2010). There are several different types of glia in the *Drosophila* CNS including surface glia, cortex glia and neurpile glia (Edwards & Meinertzhagen, 2010).

Surface glia are flattened cells that form the outermost layer of the *Drosophila* brain (Edwards & Meinertzhagen, 2010). They form the BBB, which protects the brain from harmful toxins that may be found in the haemolymph (Edwards & Meinertzhagen, 2010). The BBB is comprised of two types of surface glia, the perineurial glia (PNG) and subperineurial glia (SPG) (Edwards & Meinertzhagen, 2010). The exact function of the PNG has not been fully investigated (Edwards & Meinertzhagen, 2010). The SPG, on the other hand, act as the major component of the BBB as they contain septate junctions that prevent the leakage of haemolymph components into the brain (Edwards & Meinertzhagen, 2010). The septate junctions between the SPG are very similar to the tight junctions found in the vascular endothelial cells of capillaries in the CNS of vertebrates (Edwards & Meinertzhagen, 2010). There are several genetic tools that can be

used in *Drosophila* for tissue specific expression of proteins of interest in glia (Stork, Bernardos, & Freeman, 2012). Repo-Gal4 can be used for tissue-specific expression of proteins in all of the glia and Moody-Gal4 can be used for tissue-specific expression in the SPG (Stork et al., 2012).

Glial cells have a major role in the progression of NDs (Andersen, 2004; Hirsch et al., 2006; Rojo, 2010; Valori, Brambilla, & Rossi, 2014). Glial cell activation can occur in response to oxidative stress in neurons (Andersen, 2004; Hirsch et al., 2006; Maragakis & Rothstein, 2006). This glial activation often involves the release of ROS, nitric oxide and proinflammatory cytokines involved in nonspecific removal of damaged cells (Andersen, 2004; Hirsch et al., 2006). This can lead to further neuronal oxidative damage and neurodegeneration (Andersen, 2004). On the other hand, some researchers believe that glia can have neuroprotective roles during oxidative stress (Gao et al., 2015). They suggest that glial cells can excrete antioxidants and other therapeutic agents that the neurons can then use in order to protect themselves from damage (Gao et al., 2015). This supports the idea that glial cells are an important factor when it comes to protection of the brain from oxidative stress and neuronal antioxidant support. It is very important and beneficial to understand how glia may contribute in neuroprotective and neurodegenerative processes in greater detail and in order to do this it is important to study this in various different models. Glial support of neurons during neurodegeneration and oxidative stress has been studied to some extent in mice and will be discussed in greater detail in *1.2.4* , such research is lacking in other model organisms especially in *Drosophila.*

1.2.4 Oxidative stress and neurodegeneration: Studies in Drosophila and other model organisms

Evidence about the role ROS and oxidative stress play in neurodegeneration is very abundant. Post-mortem analysis of human ND patients has shown that tissues that have undergone neurodegeneration carry various oxidative stress markers (Andersen, 2004; Butterfield, Castegna, Lauderback, & Drake, 2002; Dexter et al., 1989; Hensley et al., 1998). Additionally, studies have shown that activities and concentrations of enzymatic and non-enzymatic antioxidants are significantly lower in affected brain regions in NDs (Andersen, 2004; Gabbita, Aksenov, Lovell, & Markesbery, 2002; Pappolla, Omar, Kim, & Robakis, 1992; Perry, Godin, & Hansen, 1982; Zemlan, Thienhaus, & Bosmann, 1989). Measurements of oxidative stress biomarkers were performed in living PD patients, and a systematic increase in these biomarkers was discovered in PD patients compared to a healthy control group (Seet et al., 2010). Studies in mice show that null mutants of enzymatic antioxidants show increased sensitivity to PD-causing chemical N-Methyl-4-Phenyl-1,2,3,6-Tetrahydropyridine (MPTP), while overexpression of these antioxidants cause resistance to MPTP (Andersen, 2004; Klivenyi et al., 1998; J. Zhang, Graham, Montine, & Ho, 2000). This evidence shows that oxidative stress and neurodegeneration overlap and it suggests that oxidative stress is a major cause of neurodegeneration.

There are also lots of studies that use *Drosophila* as a model organism, that support this claim. One study has shown that ingestion of paraquat caused PD-like movement symptoms in *Drosophila* by observing a significant decrease in climbing assay

performance of treated flies compared to controls (Chaudhuri et al., 2007). Additionally, paraquat ingestion caused a selective loss of dopaminergic neuron clusters, with the PPL1 cluster being most sensitive and the PPM1 cluster being the least sensitive (Chaudhuri et al., 2007). They also observed morphological changes of dopaminergic neurons including retraction of neuronal processes, as well as a greater aggregation and rounding of the cell bodies (Chaudhuri et al., 2007). Another study has shown that up-regulation of the enzymatic antioxidant glutathione S-transferase S1(GstS1) in the dopaminergic neurons of *Drosophila* model of PD expressing a mutant form of the parikin protein showed rescue of PD-like phenotypes (Whitworth et al., 2005). This evidence also suggests that antioxidants have therapeutic potential in the treatment of PD, as well as other neurodegenerative diseases.

There is also evidence that glial cells play an important role in both the progression of NDs as well as in protection of neurons from neurodegeneration (Gao et al., 2015; Hirsch et al., 2006; Maragakis & Rothstein, 2006). Studies in mice have shown that depletion of mutant SOD1 in astrocytes in mice models of ALS slowed the progression of ALS (Valori et al., 2014; Yamanaka et al., 2008). In addition, one study genetically manipulated astrocytes in wildtype mice to express mutant SOD1 and showed that this alone can trigger the progression of ALS (Papadeas, Kraig, O'Banion, Lepore, & Maragakis, 2011; Valori et al., 2014). Additionally, in mouse model of PD, they found that glial activation and inflammation contributed to a faster progression of the disease (Rojo, 2010). This was exaggerated in mice that were hypersensitive to oxidative stress achieved by the knockdown of the NRF2 pathway, a major oxidative stress response

pathway upstream of important antioxidant metabolism genes that will be discussed in greater detail in section *1.3* (Rojo, 2010). These studies show that glia are very important in the maintenance of the neurons and any defects in glia can cause a rapid progression of NDs. On the other hand, there is evidence that suggests that glial cells can provide antioxidant support to neurons during oxidative stress (Gao et al., 2015). An in vitro study of mixed mammalian neuron and glial cell culture has shown that neurons express lower levels of NRF2 protein than glial cells, and they showed that when introducing NRF2-overexpressing glia into naive mixed cultures there was an overall protection of both glia and neurons from hydrogen peroxide (Shih et al., 2003). This study also shows that there was an increase in both intracellular and secreted GSH in cell cultures with enriched NRF2-overexpressing glial cells (Shih et al., 2003). Another study has shown that astrocyte specific expression of NRF2 in mice protected the brain from the harmful effects of oxidative stress (Calkins, Vargas, Johnson, & Johnson, 2010). This evidence supports the claim that glia play an important neuroprotective role in the brain during oxidative stress.

1.3 NRF2/Keap1 pathway: Major defense mechanism against oxidative stress

The NRF2/Keap1 pathway is one of the major redox sensitive pathways that gets activated in response to elevated ROS and oxidative stress (Singh et al., 2010). The NRF2/Keap1 pathway is upstream of genes involved in antioxidant production, ROS scavenging, glutathione homeostasis, drug metabolism and other genes involved in oxidative stress response (Nguyen et al., 2003; Singh et al., 2010).

1.3.1 NRF2/Keap1 pathway: The major players

NRF2 (NF-E2-Related Factor 2) is a transcription factor that binds to promoters and enhancers containing an antioxidant response element (ARE), a DNA motif found in regulatory sequences of genes involved in endogenous antioxidant metabolism (Nguyen et al., 2003; Singh et al., 2010). Under normal conditions, NRF2 is kept in the cytosol by the protein Keap1 (Kelch-like ECH-associated Protein 1). Keap1 attaches to NRF2 in a latch and hinge formation and targets NRF2 for degradation by ubiquitination (Singh et al., 2010; Sykiotis & Bohmann, 2008; D. D. Zhang, 2006). Keap1 contains reactive cysteine residues that can sense changes in the redox environment (Singh et al., 2010; Sykiotis & Bohmann, 2008; D. D. Zhang, 2006). In the event of oxidative stress, Keap1 goes under a conformational change and opens the latch formation of NRF2/Keap1 complex. This stops the ubiquitination of NRF2 by Keap1. The hinge formation of this complex still remains intact (Singh et al., 2010; D. D. Zhang, 2006). Since NRF2 is no longer targeted for degradation, Keap1 becomes saturated and cannot sequester newly synthesized NRF2 in the cytosol (Singh et al., 2010). This allows the newly synthesized NRF2 to freely translocate to the nucleus where it dimerizes with small Maf (Musculo-Aponeurotic Fibroscaroma) proteins, that help NRF2 bind to DNA (Singh et al., 2010). The NRF2/Maf dimers bind to ARE motifs promoting the expression of antioxidant response genes (Singh et al., 2010).

1.3.2 NRF2/Keap1 pathway, oxidative stress and neurodegeneration: studies in Drosophila and other model organisms

Several studies have shown that the NRF2/Keap1 pathway provides protection to

cells from oxidative stress in different model organisms both *in vivo* and *in vitro*. In mouse models, up-regulation of NRF2 in glial cells has been shown to provide neuronal protection from oxidative stress and alleviation from neurodegenerative phenotypes (Calkins et al., 2005; Shih et al., 2005; Vargas, Johnson, Sirkis, Messing, & Johnson, 2008; Williamson, Johnson, & Johnson, 2012). NRF2 mouse null mutants and NRF2 knockout astrocyte mouse cell lines have been shown to be more sensitive to mitochondrial complex II inhibitors and oxidative stress inducers that cause neurodegenerative phenotypes in mice than wildtype mice and astrocyte cell lines (Calkins et al., 2005; Shih et al., 2005). In addition, in primary mouse astrocyte cultures, down-regulation of Keap1 via siRNA resulted in upregulation of NRF2-dependent transcription of an ARE-containing reporter and it conferred protection from tert-butyl hydroperoxide (tBOOH) induced oxidative stress (Williamson et al., 2012). Furthermore, targeted up-regulation of NRF2 in mouse astrocytes in mouse models of ALS has shown protection of motor neurons and slowed progression of the disease (Vargas et al., 2008). In *C. elegans*, SKN-1, a homologue of the mammalian NRF2, has been identified to be important in the protection of dopaminergic neurons in worms exposed to methylmercury, a toxin linked to PD and a known oxidative stress inducer, by the increased expression of glutathione metabolism genes (Vanduyn, Settivari, Wong, & Nass, 2010) . Homologues of the NRF2/Keap1 pathway components also found in *Drosophila* (Sykiotis & Bohmann, 2008). CncC (cap'n'collar C, homologue of NRF2) and Keap1, regulate antioxidant genes via the ARE motif in *Drosophila* as well (Sykiotis & Bohmann, 2008). Sykiotis & Bohmann (2008) have shown that up-regulation of CncC

and down-regulation of Keap1 in the whole fly significantly increases lifespan of flies exposed to paraquat, therefore indicating that these genes regulate resistance to oxidative stress in *Drosophila* (Sykiotis & Bohmann, 2008). In addition, in a transgenic *Drosophila* model of familial PD, where the human α-synuclein protein is expressed in the dopaminergic neurons, upregulation of CncC in the dopaminergic neurons either via the direct overexpression of CncC or by partial loss of Keap1, improved the performance of the flies in a negative geotaxis assay and delayed the locomotor deficit that was observed in flies expressing α-synuclein only (Barone, Sykiotis, & Bohmann, 2011). The same study showed that upregulation of CncC via partial loss of Keap1 as well as upregulation of MafS, the only Maf homologue in *Drosophila*, in the dopaminergic neurons caused a rescue in the loss of dopaminergic neurons of old flies expressing α-synuclein (Barone et al., 2011). A separate similar study, found that flies expressing mutant α-synuclein in neurons showed that there was a significant increase in ROS levels in the fly brains and that the ROS levels were correlated with the severity of PD-like symptoms such as locomotor dysfunction and loss of dopaminergic neurons (B. Wang, Liu, Shan, Xia, & Liu, 2015). These symptoms were attenuated by the introduction of the NRF2 signaling pathway activator CDDO-Me, and this activation of the NRF2 pathway significantly decreased the ROS levels in the fly brains (B. Wang et al., 2015). All of this data shows the importance of the NRF2/Keap1 pathway during oxidative stress in the *Drosophila* brain. Although there are studies investigating the role of NRF2 during oxidative stress in glial cells in *in vitro* and *in vivo* in mammals as discussed at the end of section *1.2.4* , such studies in *Drosophila* are lacking.

1.4 Autophagy: The cellular recycling plant

Autophagy is the process by which cytosolic components are degraded via the lysosome (Mizushima, 2007). There are three types of autophagy, macroautophagy, microautophagy and chaperone-mediated autophagy (Martinez-Vicente & Cuervo, 2007; Mizushima, 2007). Macroautophagy, the most studied type of autophagy and often referred to simply as autophagy, is the non-selective, bulk degradation of cytoplasmic components via specialized organelles called autophagosomes (Martinez-Vicente & Cuervo, 2007). Unlike macroautophagy, microautophagy does not require specialized organelles, and it is performed directly by the lysosome (Martinez-Vicente & Cuervo, 2007). In microautophagy, the lysosome isolates sections of the cytoplasm via invagination and engulfs the components that are then degraded (Martinez-Vicente & Cuervo, 2007). This process is also non-selective and involves bulk degradation (Martinez-Vicente & Cuervo, 2007). The only selective type of autophagy is chaperone-mediated autophagy (Martinez-Vicente & Cuervo, 2007). Chaperones selectively bind to specific cytosolic proteins with lysosome target motifs and carry them to the surface of the lysosome where they interact with receptor proteins and get imported into the lysosome for degradation (Martinez-Vicente & Cuervo, 2007). In addition, autophagy can be classified in two different categories, induced autophagy or basal autophagy (Mizushima, 2007). Induced autophagy is usually initiated by stress signals such as starvation (Mizushima, 2007). Basal autophagy is the constitutive degradation for the purpose of turnover of cellular components (Mizushima, 2007). In this report, the focus will be directed towards macroautophagy, and it will be referred to as autophagy.

1.4.1 Autophagy: The pathway and its regulation by oxidative stress response

The process of autophagy has three steps, induction, formation and elongation of the autophagosome, and degradation (Mizushima, 2007).

The first step of the autophagy pathway is induction (Mizushima, 2007). The best known pathway for induction of autophagy is the TOR (target of rapamycin) pathway activated by starvation and nutrient deficiency (Mizushima, 2007). When starvation occurs TOR is inhibited through dephosphorylation (Essick & Sam, 2010; Mizushima, Yoshimori, & Ohsumi, 2011; Mizushima, 2010). This prevents TOR from phosphorylating the autophagy related protein 13 (Atg13) (Essick & Sam, 2010; Mizushima et al., 2011; Mizushima, 2010). This allows Atg13 to bind to Atg1, a serine/threonine protein kinase, and activate the Atg1 kinase activity which leads to initiation of autophagy (Essick & Sam, 2010; Mizushima et al., 2011; Mizushima, 2010). Atg1is part of the Atg1 kinase complex that also includes Atg13, Atg17, Atg29 and Atg31 among other proteins (Mizushima, 2010). This complex is at the top of the autophagy pathway hierarchy and is essential for the initiation of the preautophagosomal structure (PAS) formation (Mizushima, 2010). The Atg1 kinase complex has two roles, kinase-independent recruitment of downstream Atg proteins as well as kinase-dependent activation of the downstream proteins, 1888 in total, via phosphorylation (Mizushima, 2010). The Beclin-1/ B-cell lymphoma 2 (Bcl-2) pathway is another starvation sensing pathway by which autophagy is regulated (Feng, He, Yao, & Klionsky, 2014; Feng, Yao, & Klionsky, 2015; Mizushima, 2007). In the case of starvation the Beclin1/Bcl-2 interaction is dissociated and this allows for Beclin 1, also known as Atg6 or vacuolar

protein sorting 30 (Vps30), to form a Class III P13K complex with Atg14 and other proteins, which produces phosphatidylinositol 3-phosphate (PI3P), a lipid molecule essential to autophagy, in the PAS (Feng et al., 2014, 2015; Mizushima et al., 2011; Mizushima, 2007). The beclin-1/Blc-2 pathway is also sensitive to hypoxia and oxidative stress conditions (Scherz-Shouval & Elazar, 2011). BNIP3 and NIX, targets of the hypoxia-inducible factor 1 (HIF1), both of which positively regulate autophagy by binding to Blc2 and releasing beclin-1 (Scherz-Shouval & Elazar, 2011). Additionally, increased ROS and oxidative stress activates the ubiquitin-proteasome system which degrades Blc-2, and allows for the activation of beclin-1, which eventually leads to autophagic cell death (Essick & Sam, 2010).

The second step of autophagy, formation and elongation of the autophagosome, begins with the formation of a phagophore or isolation membrane, which is a flat double membrane structure (Mizushima, 2007). The phagophore starts elongating around molecules and organelles that are to be degraded (Mizushima, 2007). When it has fully sequestered the cargo and it fuses at both ends it forms the autophagosome (Mizushima, 2007). The elongation process involves about 18 different Atg proteins, among which are Atg18 and Atg8 (Mizushima, 2007). Atg18 is a PI3P-binding protein and it is a part of the Atg2-Atg18 complex (Mizushima et al., 2011; Nair, Cao, Xie, & Klionsky, 2010; Polson et al., 2010). It is involved in proper formation and shaping of the autophagosome by recruiting Atg8-PE to the PAS (Mizushima et al., 2011; Nair et al., 2010; Polson et al., 2010). Atg8-PE, also known as LC3, is a ubiquitin-like protein covalently bound to the lipid phosphatidylethanolamine (PE) and it is found on the inner autophagosome

membrane (Geng & Klionsky, 2008; Mizushima et al., 2011). The Atg2-Atg18 complex also prevents the Atg4-driven deconjugation of Atg8-PE from the autophagosome membrane by interaction with Atg4 (Mizushima et al., 2011; Nair et al., 2010; Tamura et al., 2013). Atg8-PE is involved in the proper elongation of the phagophore and closure of the phagophore membrane to form the autophagosome (Geng & Klionsky, 2008; Mizushima et al., 2011; Xie, Nair, & Klionsky, 2008). The Atg8 protein is covalently bound to PE in the phagophore membrane by Atg7 and Atg3 and it is removed from the membrane by Atg4 which breaks the bond between Atg8 and PE (Geng & Klionsky, 2008; Mizushima et al., 2011). Interaction between the elongation process of autophagy and ROS has been well established (Essick & Sam, 2010; Scherz-Shouval & Elazar, 2007, 2011; Scherz-Shouval et al., 2007). One such interaction is between starvation-induced elevation of ROS and Atg4 (Scherz-Shouval et al., 2007). Atg4 is deactivated via oxidation by H_2O_2 during starvation allowing for conjugated Atg8-PE to continue with autophagosome formation (Scherz-Shouval et al., 2007). Other more indirect ways by which ROS and oxidative stress interact with the elongation process of autophagy involve oxidative stress response pathways such as the p53, FOXO3, JNK and NRF2/Keap1 among others (Essick & Sam, 2010; Pietrocola et al., 2013; Scherz-Shouval & Elazar, 2007, 2011). For the purpose of this report only JNK and the NRF2/Keap1 pathway will be discussed further. JNK signaling induces the transcript levels of Atg1, Atg4, Atg6, Atg8a and Atg18 (Wu, Wang, & Bohmann, 2009). This was parallel to the increased transcript level of Atg1 and Atg18 seen during exposure to paraquat (Wu et al., 2009). Additionally, the interaction between autophagy elongation components and JNK is also

confirmed by the discovery of the regulative role that Atg9, an essential autophagy transmembrane protein involved in lipid transport, plays in JNK activation (Tang et al., 2013). Atg9 activates the JNK signaling which has protective role during oxidative stress (Tang et al., 2013). The interaction between the NRF2/Keap1 pathway and autophagy will be discussed in detail in section *1.5*.

The third and final step of autophagy is degradation, which involves the fusion of the autophagosome to a lysosome to form the autophagolysosome where the autophagosome cargo and the inner membrane of the autophagosome are degraded (Mizushima, 2007). The monomeric units that result from this degradation are shuffled out into the cytosol to be reused for several different metabolic processes (Mizushima, 2007).

1.4.2 Balance of autophagy in oxidative stress and neurodegeneration: Studies in Drosophila and other model organisms

Autophagy has been well established as a major pathway in oxidative stress (Essick & Sam, 2010; Scherz-Shouval & Elazar, 2007, 2011). Autophagy is also involved in disease progression and prevention, particularly in neurodegenerative diseases (Cherra & Chu, 2008; Essick & Sam, 2010; Mariño, Madeo, & Kroemer, 2011; Martinez-Vicente & Cuervo, 2007; Mizushima, Levine, Cuervo, & Klionsky, 2008; Scherz-Shouval & Elazar, 2011; Winslow & Rubinsztein, 2008). Studies have shown that loss of essential autophagy proteins in the central nervous system of both mice and *Drosophila* resulted in neurodegenerative phenotypes and decreased lifespan (Komatsu et al., 2006; Simonsen et al., 2008). Overexpression of Atg8a in *Drosophila* neurons increased the adult fly

lifespan and prevented accumulation of protein aggregates (Simonsen et al., 2008). Atg8a mutants showed an increased sensitivity to H_2O_2 induced oxidative stress measured by lifespan profiles, while pan-neural overexpression of Atg8a allowed for greater resistance to the same exposure of H_2O_2 (Simonsen et al., 2008). In addition, an increased amount of ubiquitin-positive inclusion bodies were found in different brain regions of autophagy-deficient mice (Komatsu et al., 2006). In human PD cell line models, upregulation of autophagy by rapamycin showed that α-synuclein is degraded by both the proteasome system and autophagy (Webb, Ravikumar, Atkins, Skepper, & Rubinsztein, 2003). Autophagy has also been associated with the degradation of other proteins, including polyglutamine and polyalanine aggregate-prone proteins, involved in the development of neurodegenerative diseases such as HD (Ravikumar, 2002). This research suggests that autophagy is a very important pathway with regards to dealing with oxidative stress and has therapeutic potential for the treatment of neurodegenerative disease.

On the other hand, autophagy and lysosomal degradation can have negative effects on cells that are dealing with oxidative stress (Kiffin, Bandyopadhyay, & Cuervo, 2006). During oxidative stress, the oxidized macromolecules that are delivered by autophagy to the lysosome for degradation, often crosslink with other proteins, lipids, carbohydrates and other molecules due to their high reactivity (Kiffin et al., 2006). This makes them highly resistant to hydrolytic degradation and they turn into an indestructible byproduct called lipofuscin (Kiffin et al., 2006). Lipofuscin accumulates in the lysosome in post-mitotic cells as they age and can be used as a biomarker for aging because it has autofluorescence properties (Kiffin et al., 2006; Terman & Brunk, 2004). This

accumulation of lipofuscin makes cells even more susceptible to oxidative stress and lysosomal breakage, which leads to leakage of degradation enzymes into the cytosol and causes immeasurable damage to the cell (Kiffin et al., 2006; Terman, Dalen, & Brunk, 1999). This is observed at a greater frequency during acute and persistent oxidative stress (Kiffin et al., 2006). In addition, uncontrolled and excessive autophagy can lead to autophagic stress and cause cell death (Cherra & Chu, 2008). Autophagic stress is the cellular state characterized by an accumulation of cargo-carrying autophagosomes (Cherra & Chu, 2008). This accumulation can occur when there is an increase in induction of autophagy to a level that it overwhelms the degradation step of the autophagy process (Cherra & Chu, 2008). It can also be caused by impairment in the maturation and degradation process during basal levels of autophagy (Cherra & Chu, 2008). Furthermore, autophagic stress can be caused by inefficient replacement of essential organelles that have been removed by autophagy (Cherra & Chu, 2008). Autophagic stress has been observed in many neurodegenerative diseases including Lysosomal storage diseases (LSDs) and AD (Cherra & Chu, 2008; Martinez-Vicente & Cuervo, 2007). Increased autophagy and autophagic stress can lead to cell death either by degradation of essential components or by the induction of the apoptotic pathway (Maiuri et al., 2007). In general, a right balance and efficiency of the autophagy pathway is required for normal cell function and cytoprotection from oxidative stress.

1.5 Autophagy and The NRF2/Keap1 pathway

Autophagy and the NRF2/Keap1 pathway have both been established to have major roles in oxidative stress response. Only recently, however, a link between these two

pathways was discovered (Scherz-Shouval & Elazar, 2011). Studies have found that Atg8 binds to the ubiquitin binding protein p62, which is commonly found in ubiquitinated protein aggregates, and targets the p62-containing aggregates the for sequestration into the autophagosome and the eventual degradation in the lysosome (Pankiv et al., 2007). Research shows that the role of p62 is conserved among species, as the *Drosophila* homologue of p62, Ref(2)P, has the same selective autophagy function in *Drosophila* (Nezis et al., 2008). Additionally, it was found that p62 is under the transcriptional control of NRF2 (Jain et al., 2010). Extensive promoter analysis of the p62 gene showed that it contains an ARE sequence (Jain et al., 2010). p62 is involved in further activation of NRF2 via inactivation of Keap1 (Jain et al., 2010; Komatsu et al., 2010; Lau et al., 2010). p62 binds to the NRF2-binding site of Keap1 and prevents the Keap1 dependent degredation of NRF2 (Komatsu et al., 2010). This process forms a positive feedback loop between NRF2 and p62 (Jain et al., 2010; Komatsu et al., 2010; Lau et al., 2010). This data suggests that NRF2/Keap1 promotes selective autophagy. Additionally has an autophagy an interesting upstream position of the NRF2/Keap1 pathway (Komatsu et al., 2010; Riley et al., 2010). A study shows that when autophagy is artificially repressed, it allows for the accumulation of p62 which then competes with NRF2 for the binding affinity of Keap1 (Komatsu et al., 2010; Riley et al., 2010). This eventually leads to an increased amount of stabilized NRF2 that can travel to the nucleus and promote expression of genes under the control of ARE-containing promoters among which is the p62 gene (Komatsu et al., 2010; Riley et al., 2010). This puts p62 in a central position in the oxidative stress response and its link to autophagy.

1.6 Hypothesis

Alteration of the levels of autophagy and the NRF2/Keap1 pathway in the glia affects the *Drosophila*'s sensitivity to oxidative stress. Down regulation of autophagy provides protection of viability and locomotor performance from oxidative stress. Activation of the NRF2/Keap1 pathway provides protection of viability and locomotor performance from oxidative stress. Down regulation of autophagy in the glia provides protection of the dopaminergic neurons from oxidative stress. Down regulation of autophagy in the glia provides protection of viability after thermal stress. Down regulation of autophagy in the glia provides extension of lifespan and a delay in age-related decline in locomotor ability.

1.7 Thesis objective and specific aims

The objective of this thesis is to explore the role autophagy and NRF2/Keap1 pathway have in the protection of the *Drosophila melanogaster* brain from neurodegeneration phenotypes during induced acute oxidative stress, induced acute thermal stress and chronic exposure to stress via aging, while these pathways are upregulated or downregulated in either all glial cells or specifically in SPG cells.

1.7.1 Specific aim 1: Acute oxidative stress

As previously stated, oxidative stress is one of the major causes of neurodegenerative diseases (Andersen, 2004). It has been well established that oxidative stress in *Drosophila* causes neurodegenerative phenotypes such as decline in locomotor performance in a negative geotaxis assay (Chaudhuri et al., 2007). Oxidative stress has also been implicated as one of the major causes in the decline of dopaminergic neuron

number in Parkinson's disease (Chaudhuri et al., 2007). Although research exists regarding the protective role of upregulation of NRF2 in glia on adjacent neurons in mice, activation of the NRF2/Keap1 pathway in the glia of *Drosophila* has not been previously studied in the context of oxidative stress (Calkins et al., 2005). In addition, such studies regarding the effects of glial upregulation or down regulation of autophagy are lacking for all model organisms. The first goal of this thesis is to assess whether upregulation or down regulation of the NRF2/Keap1 pathway and autophagy in the glia and SPG has a protective effect on the *Drosophila* brain during acute oxidative stress. This is assessed by examining flies in which autophagy is downregulated in the glia and testing the survival, negative geotaxis assay performance and the shape and number of dopaminergic neurons of flies that are undergoing acute oxidative stress caused by the exposure to paraquat. This is also tested by examining flies in which the NRF2/Keap1 pathway is activated and measuring the for the viability and negative geotaxis assay performance of flies that are undergoing acute oxidative stress.

1.7.2 Specific aim 2: Thermal stress

Thermal stress is another form of acute stress that activates similar stress response pathways as oxidative stress. One such pathway is the NF-kB pathway that gets activated by both oxidative stress and heat shock (Essick & Sam, 2010). In order to broaden the scope of the role of autophagy to acute stress in general, the second goal of this thesis is asses the effects of down regulation of autophagy in the glia and SPG on viability after acute thermal stress exposure.

1.7.3 Specific aim 3: Lifespan and chronic exposure to stress

It has been well established that aging is caused by the long-term chronic exposure to oxidative stress. In order to examine role of autophagy in the context of aging, the third goal of this thesis is to assess whether down regulation of autophagy in the glia or SPG causes an increased lifespan and delay in the development of aging phenotypes such as a delay in age-dependent decline in locomotor ability.

2 Materials and methods

2.1 Fly strains

The fly strains used in this project include the white eye mutant w^{1118}; Gal4 strains: Repo-Gal4/TM3.Sb (BSC# 7415) and Moody-Gal4 (provided by Dr. Michael O'Donnell, McMaster University); UAS strains: UAS-$Atg1^{RNAi}$ (VDRC# v16133), UAS-$Atg18^{RNAi}$ (VDRC# v22646), UAS-Atg8a (BSC# 10107), UAS-$Atg8a^{RNAi}$ (BSC# 28989), UAS-CncC, UAS-Keap1 and UAS-$Keap1^{RNAi}$ (provided by Dr. Dirk Bohmann, University of Rochester). Repo-Gal4 is a pan-glial driver and it was crossed with the UAS lines in order to express the appropriate RNAi or cDNA sequences in all glial cells. Moody-Gal4 is a SPG driver and it was crossed with UAS lines to express the appropriate RNAi and cDNA sequences in the SPG. Parental controls were created by crossing the stock strains with the w1118 flies.

2.2 Paraquat exposure

Paraquat (*N*,*N*′-dimethyl-4,4′-bipyridinium dichloride, Sigma Aldrich, Cat# 856177) exposure was performed in male progeny that were first collected from crosses grown at 25^0 C for 1-2 days. They were placed in a 29^0 C incubator and were aged on standard *Drosophila* food medium at for 3 days. The flies were starved for 6 hours in vials containing 1% agar and filter paper discs soaked with 150 µL ddH_2O. After the starvation, the flies were transferred in vials containing filter paper discs soaked in 250 µL 5% sucrose solution, 20 mM paraquat in 5% sucrose solution or 25 mM paraquat in 5% sucrose solution. The flies were exposed to these solutions for 24 hours at 25^0 C

covered in aluminum foil to eliminate exposure to light.

2.3 Thermal stress exposure

The collection and aging of flies was performed in the exact same way as for the paraquat exposure outlined in section 2.2. After the aging period, flies were flipped into fresh food that has been previously warmed to the exposure temperature. The vials were securely placed in wire boxes and were submerged in a 37^0 C water bath up to the level of the cotton ball used to prevent the flies from escaping. The flies were exposed to this temperature for 2 h. A subset of flies was left in the 29^0 C during this time to serve as a non-exposed control. The surviving and dead flies were counted immediately after exposure. The surviving flies were also counted 24h after exposure in order to make sure that the flies considered to be dead were not just knocked out by the heat shock.

2.4 Survival assay

Survival assays were performed on flies that were exposed to 5% sucrose solution, 20 mM paraquat solution or 25 mM paraquat solution after a 24-hour exposure. The number of dead and alive flies was counted and recorded for each vial. Each vial of 20 flies was considered a single sample.

2.5 Negative geotaxis assay

Negative geotaxis assay was performed on flies that were exposed to 5% sucrose solution and 25 mM paraquat solution after a 24-hour exposure. The flies were distributed into negative geotaxis vials created in the lab by marking standard *Drosophila* vials with lines at 2.35 cm, 4.70 cm and 7.05 cm forming 4 quadrants. Each vial

containing 20 flies was considered as a single sample. The negative geotaxis vials were placed in a specialized rack that fits 6 vials. The vial-containing rack was tapped strongly a single time and the flies were photographed with Cannon EOS M camera 4 seconds after the tap. This was repeated 3 times for each set of 6 vials leaving 30 second rest between each tap. The negative geotaxis assay for each experiment was performed in the same room, under the similar temperature, humidity and light conditions and at the same time of the day (between 5pm and 8pm). The images that were taken were then analyzed in order to score and quantify the behavior and locomotion of the flies. The number of flies in each quadrant was counted and the Climbing Index (CI) score was calculated using the following formula:

$$CI = \big((0 \times Q0) + (0.25 \times Q1) + (0.5 \times Q2) + (0.75 \times Q3) + (1 \times Q4)\big) \div n$$

, where Q0 represents the number of flies remaining on the bottom of the vial, Q1 represents the number of flies in the first quadrant, Q2 represents the number of flies in the second quadrant, Q3 represents the number of flies in the third quadrant, Q4 represents the number of flies in the fourth quadrant and n represents the total number of flies in the vial. The CI was averaged for the three replicates per sample to produce the Sample Climbing Index (SCI) and then the SCI for all samples was averaged to produce the Mean Climbing Index (MCI).

2.6 Immunostaining of dopaminergic neurons

Immunostaining of the dopaminergic neurons was performed on flies exposed to 5% sucrose solution and 25 mM paraquat solution after a 24-hour exposure. The CNS of these flies was dissected and extracted in 1xPBS (Phosphate buffered saline pH= 7.2-

7.4). The brains were kept on ice in screw-cap round-bottomed tubes (Fisher Scientific test tube Cat# 14-959-35B, cap Cat# 03-340-77D). The brains were then fixed in 4% formaldehyde overnight at 4^0 C while spinning on a rotator. After the fixation, the brains were washed in 0.5% PBS-T (1xPBS + 0.5% triton) 3 times, 10 minutes each time on a shaker. The 0.5% PBS-T was then aspirated and the brains were blocked for 2 h in 10% NGS (10% normal goat serum in 0.5% PBS-T). The brains were then incubated overnight in primary antibody rabbit anti-tyrosine hydroxylase (Millipore, Cat# AB152MI) that was diluted to 1:500. The next day, the brains were washed in 0.2% PBS-T (1xPBS + 0.2% triton) 3 times, 10 minutes each time on a shaker. The brains were once again blocked for 2 h in 10% NGS. They were incubated overnight with the secondary antibody 1:200 diluted Alexa 488-conjugated goat anti-rabbit IgG (Life Technologies, Cat# A-11008). The next day the flies were once again washed in 0.2% PBS-T 3 times, 10 minutes each time on a shaker. The brains were then submerged in 1xPBS and kept at 4^0 C until imaging. The brains were imaged using confocal microscopy using consistent settings at a Leica Confocal SP5II microscope.

2.7 Longevity assay

The longevity assay was stared with collecting male flies from the desired genotypes, 60 flies per vial, and placing them at 29^0 C. Every day the flies were counted and the number of living flies was recorded. The flies transferred into new food vials every 2-3 days to prevent death due to runny or bad food. The counting was performed until all of the flies in the vial died.

2.8 Age-dependent negative geotaxis assay

The lifespan negative geotaxis assay was started with collecting male flies from desired genotypes, 60 flies per vial, and placing them at 29^0 C. At 3 days, 10 days, 20 days and 30 days a subset of the flies was taken and tested using a negative geotaxis assay. The negative geotaxis assay involved placing 12 flies in 5 different negative geotaxis vials marked with lines at 2.35 cm, 4.70 cm and 7.05 cm forming 4 quadrants. The flies were placed on a specialized rack. They were tapped strongly a single time and the flies were photographed with Cannon EOS M camera 4 seconds after the tap. This was repeated 3 times for each set of 5 vials leaving 30 second rest between each repetition. The negative geotaxis assay for each experiment was performed in the same room, under the similar temperature, humidity and light conditions and at the same time of the day. The images that were taken were then analyzed in order to score and quantify the behavior and locomotion of the flies. The same scoring system was used as in the acute oxidative stress negative geotaxis.

2.9 Statistical analysis

Statistical analysis was performed using the program IMB SPSS Statistics (Version 21). For the survival data, negative geotaxis data, and quantification of the dopaminergic neurons, one-way ANOVA was used to test for statistical significance. The post-hock Tukey test was used for pairwise comparisons. The longevity data was analyzed using the Kaplan-Meyer survival analysis, and the Log Rank statistic was used to determine statistical significance.

3 Results

3.1 What is the effect of acute oxidative stress on viability and locomotor ability?

Oxidative stress is one of the major causes of neurodegeneration (Andersen, 2004). In *Drosophila,* oxidative stress causes neurodegenerative phenotypes including the loss of dopaminergic neurons (Chaudhuri et al., 2007). Loss of dopaminergic neurons has been implicated as the cause of decline in locomotor ability in flies (Chaudhuri et al., 2007). In mice, upregulation of NRF2 in astrocytes provides protection to adjacent neurons from oxidative stress (Calkins et al., 2010). Such evidence is lacking in *Drosophila.* Studies regarding the effects of upregulation or down regulation of autophagy in the glia in the context of oxidative stress are lacking for all model organisms. I hypothesized that alteration of the levels of autophagy and in the activity of the NRF2/Keap1 pathway in all glia and in the SPG may affect the flies sensitivity to paraquat. In order to address the issues outlined above and test the hypothesis, I assessed whether upregulation or down regulation of autophagy and the NRF2/Keap1 pathway in all glia and/or the SPG have a protective effect on the *Drosophila* brain during acute oxidative stress. First, this was tested by examining flies in which autophagy is downregulated in all glia and a subset of glia, the SPG. The number of surviving flies was counted, their locomotor ability was tested using negative geotaxis assay and the number of dopaminergic neurons was determined after exposure to oxidative stress. Second, the impact of oxidative stress on the viability and locomotor ability was examined in flies in which upregulating or downregulating NRF2/Keap1 pathway was altered in the SPG. In these experiments acute

oxidative stress is achieved by exposure to paraquat. This exposure has been previously shown to cause a decline in survival and negative geotaxis performance (Appendix 1).

3.1.1 What is the effect of down regulation of autophagy in all glia on the sensitivity to acute oxidative stress?

In order to test the effect of down regulation of autophagy in the glia on the sensitivity to acute oxidative stress, knockdown of Atg1 and Atg18 was achieved by expressing double stranded RNA constructs under Gal4 control. The experimental genotypes Repo-Gal4>Atg1^{RNAi} and Repo-Gal4>Atg18^{RNAi} were generated by crossing with the pan-glial driver Repo-Gal4. Males from these experimental genotypes were exposed to 5% sucrose and 20 mM paraquat for 24 h at 25^0 C. The number of surviving flies was counted and their locomotor ability was evaluated using the negative geotaxis assay. Their performance was compared to parental controls carrying either the Gal4 construct or the UAS construct. Exposure to paraquat caused a significant decline in locomotor ability and survival for both experimental genotypes as well as the corresponding parental genotypes ($p \leq 0.05$) (Figure 3.1 and 3.2). Overexpression of Atg1^{RNAi} and Atg18^{RNAi} in all glia appeared to protect the flies from the deleterious effects of paraquat exposure on survival. Both experimental genotypes survived paraquat exposure at significantly higher numbers than the parental controls ($p \leq 0.05$) (Figure 3.1B and 3.2B). Only the knockdown of Atg18 in all glia seemed to protect the locomotor ability of flies from oxidative stress. The performance of Repo-Gal4>Atg18^{RNAi} flies in negative geotaxis assay was significantly better than that of the UAS-Atg18^{RNAi} control ($p \leq 0.05$) (Figure 3.1A). These data suggest that down regulation of autophagy in all glia

provides protection from the deleterious effects of paraquat exposure on survival. However, only down regulation of autophagy via the knockdown of Atg18 in all glia provides protection of locomotor ability from oxidative stress.

Down regulation of autophagy via the overexpression of $Atg8a^{RNAi}$ and upregulation of autophagy by overexpression of Atg8a cDNA were also tested in the same context. The results for these two experiments are incomplete due to missing controls. The existing data is presented in the Appendix in Figures 7.25 and 7.26.

3.1.2 What is the effect of upregulation or down regulation of autophagy in SPG on sensitivity to acute oxidative stress?

In order to test the effect of down regulation of autophagy in the SPG on the sensitivity to acute oxidative stress, Atg1 Atg18 and Atg8a were knocked down by targeting the expression double stranded RNA constructs in the the SPG using the driver Moody-Gal4. Moody-Gal4>$Atg1^{RNAi}$, Moody-Gal4>$Atg18^{RNAi}$ and Moody-Gal4>$Atg8a^{RNAi}$ males were exposed to 5% sucrose and 25 mM paraquat for 24 h at 25^0 C. The number of surviving flies was counted and the locomotor ability was tested using the negative geotaxis assay. Atg1 and Atg18 knockdown in the SPG provided protection from the deleterious effects of paraquat on negative geotaxis performance ($p>0.05$) while the Atg8a knockdown did not ($p\leq0.05$) (Figure 3.3A, 3.4A and 3.5A). The paraquat treated Moody-Gal4>$Atg1^{RNAi}$ flies had a significantly better locomotor ability compared to the treated UAS parental control ($p\leq0.05$) (Figure 3.4). The number of surviving flies for all three experimental genotypes was significantly decreased after paraquat exposure ($p\leq0.05$) (Figure 3.3B, 3.4B and 3.5B).

In order to test the effect of upregulation of autophagy in the SPG on the sensitivity to acute oxidative stress, Atg8a was overexpressed using cDNA under the control of the Moody-Gal4 driver. Moody-Gal4>Atg8a flies that were exposed to paraquat had a small but significant decline in negative geotaxis assay performance ($p \leq 0.05$) (Figure 3.6A). The negative geotaxis performance of these treated experimental flies was significantly better than the treated Gal4 parental control but not the treated UAS parental control ($p \leq 0.05$) (Figure 3.6A). A similar pattern was seen for the survival data. There was a small significant reduction in the survival for the experimental and both parental genotypes after paraquat exposure ($p \leq 0.05$) (Figure 3.6B). The number of surviving treated experimental flies was significantly greater than the number of surviving treated Gal4 parental control flies after paraquat exposure($p \leq 0.05$) (Figure 3.6B).

These data suggest that down regulation of autophagy by the knockdown of Atg1 and Atg18 in the SPG provides protection to locomotor ability from oxidative stress but it does not provide the same protection to viability. Down regulation of autophagy via $Atg8a^{RNAi}$ in the SPG does not provide protection of both locomotor ability and survival from oxidative stress. Interestingly, upregulation of autophagy by overexpression of Atg8a in the SPG protects both negative geotaxis performance and survival from oxidative stress.

3.1.3 What is the effect of upregulation and down regulation of the NRF2/Keap1 pathway in the SPG on the sensitivity to acute oxidative stress?

In order to examine the role of the NRF2/Keap1 pathway in the SPG during acute oxidative stress, I overexpressed CncC and Keap1^{RNAi} in the SPG using the SPG driver Moody-Gal4. The NRF2/Keap1 pathway was inhibited by overexpression of the repressor Keap1 in the SPG using the same Gal4 driver. Moody-Gal4>CncC, Moody-Gal4>Keap1^{RNAi} and Moody-Gal4>Keap1 males and their corresponding controls were exposed to 5% sucrose and 25 mM paraquat for 24 h. Overexpression of CncC in the SPG did not provide any protection of locomotor ability or survival from oxidative stress (Figure 3.7). In fact, overexpression of CncC in the SPG significantly reduced the performance in negative geotaxis assay in untreated flies ($p \leq 0.05$) (Figure 3.7A). Overexpression of CncC in the SPG significantly reduced the survival of paraquat-exposed flies compared to the exposed parental controls ($p \leq 0.05$) (Figure 3.7B). Flies overexpressing of Keap1^{RNAi} in the SPG did have a significant decline in negative geotaxis assay performance after paraquat treatment while a significant decline was observed for the treated parental controls in the same assay ($p \leq 0.05$) (Figure 3.8A). The negative impact of paraquat exposure on the viability of flies overexpressing Keap1^{RNAi} was not reduced ($p \leq 0.05$) (Figure 3.8B). Overexpression of Keap1 in the SPG provided protection of locomotor ability from oxidative stress, but it did not provide protection of survival under the same conditions (Figure 3.9). A significant decline in negative geotaxis performance and survival was observed only for the Gal4 parental control in this experiment ($p \leq 0.05$) (Figure 3.9).

These data suggest that overexpression of CncC in the SPG has deleterious effects on flies. Upregulation of the NRF2/Keap1 pathway via the down regulation of the Keap1 suppressor in the SPG provides some protection from oxidative stress. Interestingly, the overexpression of Keap1 in the SPG also seems to provide protection from oxidative stress.

3.2 What is the effect of acute thermal stress on survival?

Thermal stress is an alternative form of acute stress known to activate similar stress response pathways as oxidative stress (Essick & Sam, 2010). In order to expand the scope of the role of autophagy to general acute stress, the second goal of this thesis was to assess the effects of down regulation of autophagy in all glia and the SPG on viability after acute thermal stress exposure. It was hypothesized that when autophagy is downregulated in these tissues, the flies will be protected from acute thermal stress.

3.2.1 What is the effect of down regulation of autophagy in all glia and the SPG on the sensitivity to acute thermal stress?

In order to explore the effect of down regulation of autophagy in all glia and the SPG on the sensitivity to acute thermal stress, Atg1 and UAS-Atg18 were knocked down using the pan-glial driver Repo-Gal4 and the SPG driver Moody-Gal4. Experimental males and their corresponding controls were exposed to either the non-stressful temperature 29^0 C or to the stressful temperature 39^0 C. The flies were counted right after the thermal stress exposure and then after 24h after the exposure. Heat significantly reduced the survival of all genotypes tested suggesting that down regulation of autophagy

had no impact on the sensitivity to acute thermal stress (Figures 3.10-3.13; data obtained by Rachel Lee).

3.3 The effects down regulation of autophagy on lifespan and aging

Chronic exposure to oxidative stress either by metabolism or by exogenous factors and the cumulative damage it causes is one of the major causes of aging (Finkel & Holbrook, 2000). In *Drosophila*, similar stress pathways are activated during oxidative stress and in old age (Zou et al., 2000). In order to examine role of autophagy in the context of aging, the third goal of this thesis was to examine whether down regulation of autophagy in the glia or SPG changes lifespan and modifies the appearance of aging phenotypes. One such aging phenotype is the age-dependent decline in locomotor ability as seen by reduced performance in negative geotaxis assay.

3.3.1 What is the effect of down regulation of autophagy in all glia on lifespan and aging?

In order to examine the effects of down regulation of autophagy in all glia on lifespan and aging, Atg1 and Atg18 were downregulated using the pan-glial driver Repo-Gal4. The experimental and parental genotypes were aged at 29^0 C. Lifespan was measured using the longevity assay outlined in section 2.7. The age-dependent decline in locomotor ability was tested by performing the negative geotaxis assay at 3 days, 10 days 20 days and 30 days after eclosion. Kaplan-Meyer survival analysis showed that down regulation of autophagy via knockdown of Atg1 in all glia reduces lifespan, while down regulation of autophagy via knockdown of Atg18 in all glia does not have any effect on lifespan (Figures 3.14 and 3.16). Down regulation of autophagy via knockdown of both

Atg1 and Atg18 did not show change in age-dependent decline of negative geotaxis (Figures 3.15 and 3.17).

3.3.2 What is the effect of down regulation of Autophagy in the SPG on lifespan and aging?

In order to examine the effects of down regulation of autophagy in all glia on lifespan and aging, Atg1 and Atg18 were downregulated using the SPG driver Moody-Gal4. The same experimental conditions were used as outlined in section 3.3.1. Kaplan-Meyer survival analysis showed that down regulation of autophagy via knockdown of Atg1 and Atg18 in the SPG reduced lifespan (Figures 3.18 and 3.20). Down regulation of autophagy via knockdown of Atg1 and Atg18 in the SPG did change the age-dependent decline in locomotor ability (Figures 3.19 and 3.21).

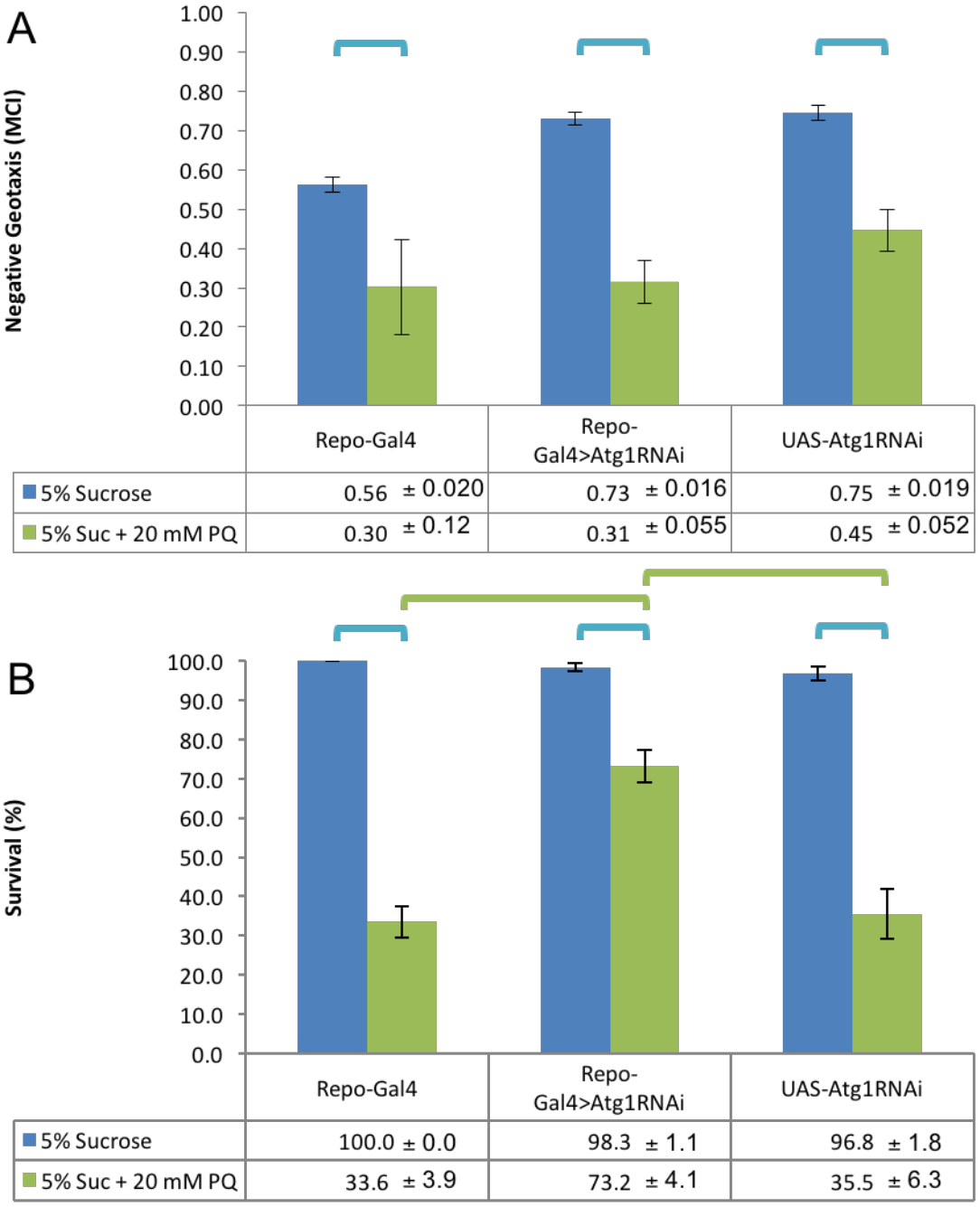

Figure 3.1: Negative Geotaxis and Survival for flies expressing Atg1^{RNAi} in the glia. The experimental and parental flies were exposed to either 5% sucrose solution or 20 mM paraquat in 5% sucrose solution for 24h. **Sample sizes: (A)** Negative Geotaxis: Repo-Gal4: 0 mM N=7 20 mM N=5; Repo-Gal4>Atg1^{RNAi} 0 mM N=5 20 mM N=11; UAS-Atg1^{RNAi} 0mM N=9 20 mM N=8 **(B)** Survival: Repo-Gal4 0mM N=7 20 mM N=46; Repo-Gal4>Atg1^{RNAi} 0 mM N=6 20 mM N=15; UAS-Atg1^{RNAi} 0 mM N=19 20 mM N=9. Bars indicate statistical significance with $p<0.05$ (ANOVA).

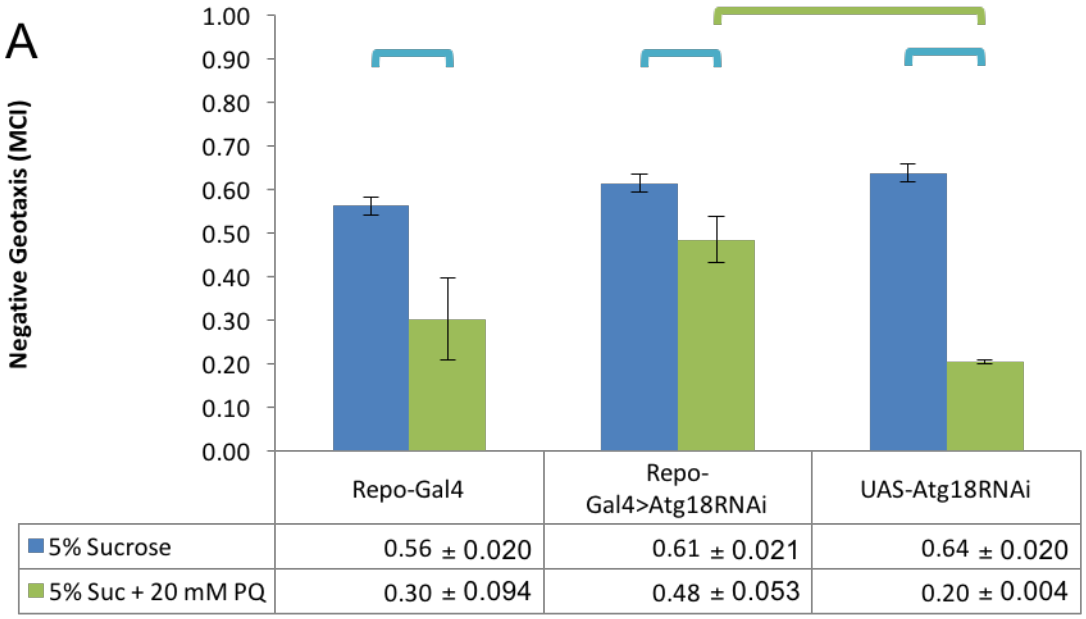

	Repo-Gal4	Repo-Gal4>Atg18RNAi	UAS-Atg18RNAi
5% Sucrose	0.56 ± 0.020	0.61 ± 0.021	0.64 ± 0.020
5% Suc + 20 mM PQ	0.30 ± 0.094	0.48 ± 0.053	0.20 ± 0.004

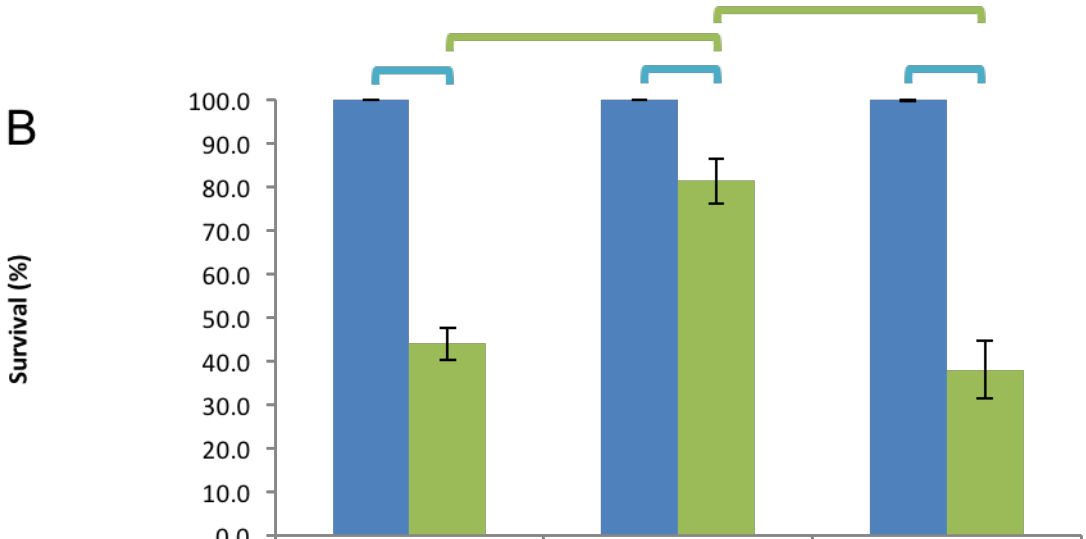

	Repo-Gal4	Repo-Gal4>Atg18RNAi	UAS-Atg18RNAi
5% Sucrose	100.0 ± 0.0	100.0 ± 0.0	100.0 ± 0.3
5% Suc + 20 mM PQ	44.0 ± 3.7	81.3 ± 5.1	38.0 ± 6.5

Figure 3.2: Negative Geotaxis and Survival for flies expressing Atg18^{RNAi} in the glia. The experimental and parental flies were exposed to either 5% sucrose solution or 20 mM paraquat in 5% sucrose solution for 24h. **Sample sizes: (A)** Negative Geotaxis: Repo-Gal4: 0 mM N=7 20 mM N=5; Repo-Gal4> Atg18^{RNAi} 0 mM N=12 20 mM N=8; UAS-Atg18^{RNAi} 0mM N=17 20 mM N=4 **(B)** Survival: Repo-Gal4 0mM N=7 20 mM N=46; Repo-Gal4>Atg18^{RNAi} 0 mM N=12 20 mM N=10; UAS-Atg18^{RNAi} 0 mM N=20 20 mM N=9. Bars indicate statistical significance with $p<0.05$ (ANOVA).

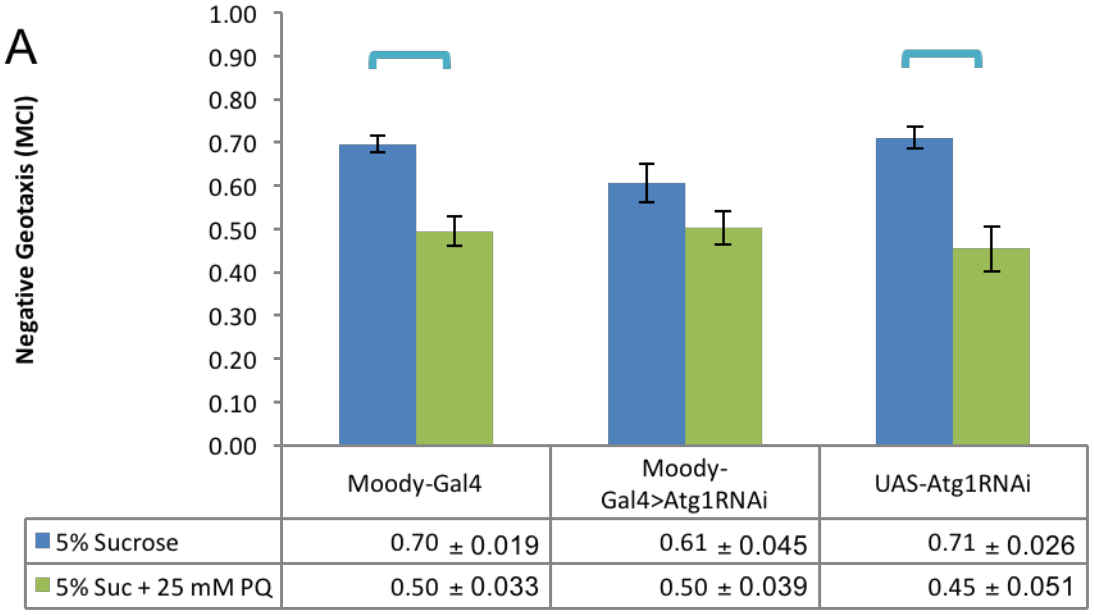

	Moody-Gal4	Moody-Gal4>Atg1RNAi	UAS-Atg1RNAi
5% Sucrose	0.70 ± 0.019	0.61 ± 0.045	0.71 ± 0.026
5% Suc + 25 mM PQ	0.50 ± 0.033	0.50 ± 0.039	0.45 ± 0.051

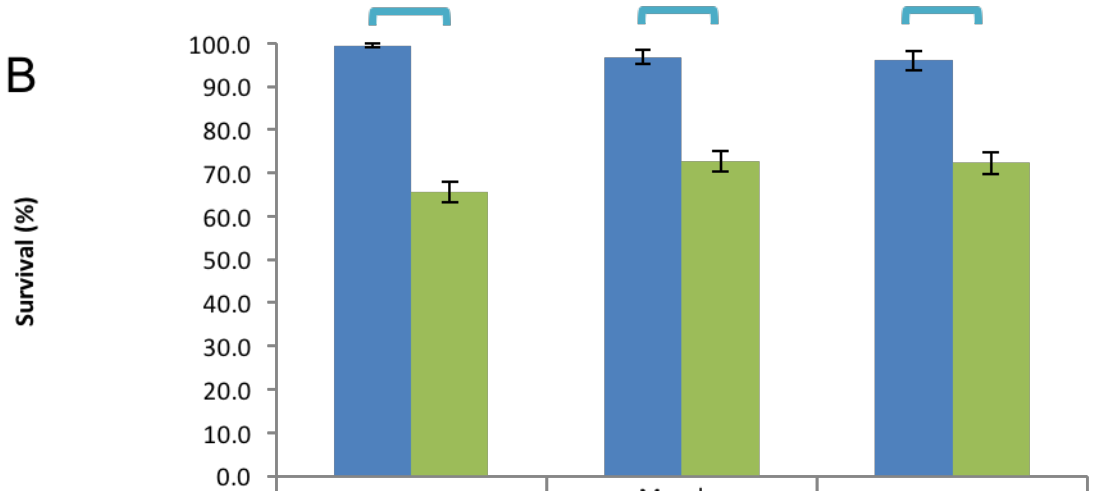

	Moody-Gal4	Moody-Gal4>Atg1RNAi	UAS-Atg1RNAi
5% Sucrose	99.5 ± 0.3	96.8 ± 1.7	96.0 ± 2.2
5% Suc+ 25 mM PQ	65.6 ± 3.7	72.7 ± 6.1	72.3 ± 3.8

Figure 3.3: Negative Geotaxis and Survival for flies expressing Atg1^{RNAi} in the SPG. The experimental and parental flies were exposed to either 5% sucrose solution or 25 mM paraquat in 5% sucrose solution for 24h. **Sample sizes: (A)** Moody-Gal4: 0 mM N=15 25 mM N=11; Moody-Gal4>Atg1^{RNAi} 0 mM N=7 25 mM N=8; UAS-Atg1^{RNAi} 0mM N=18 25 mM N=14 **(B)** Survival: Moody-Gal4 0mM N=22 25 mM N=38; Moody-Gal4>Atg1^{RNAi} 0 mM N=7 25 mM N=15; UAS-Atg1^{RNAi}0 mM N=15 20 mM N=30. Bars indicate statistical significance with $p<0.05$ (ANOVA).

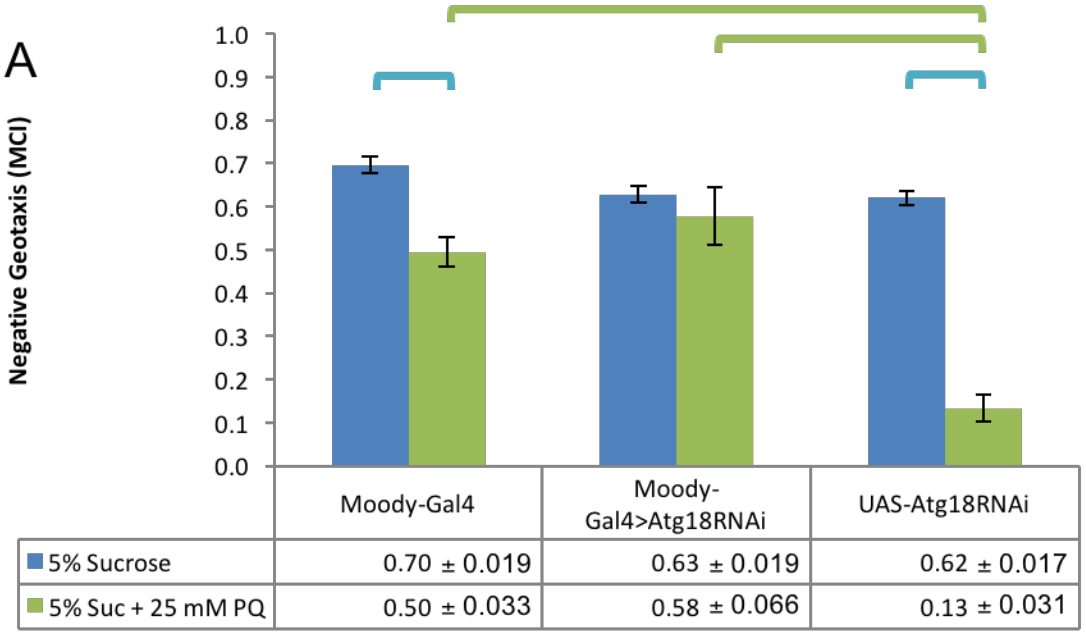

	Moody-Gal4	Moody-Gal4>Atg18RNAi	UAS-Atg18RNAi
5% Sucrose	0.70 ± 0.019	0.63 ± 0.019	0.62 ± 0.017
5% Suc + 25 mM PQ	0.50 ± 0.033	0.58 ± 0.066	0.13 ± 0.031

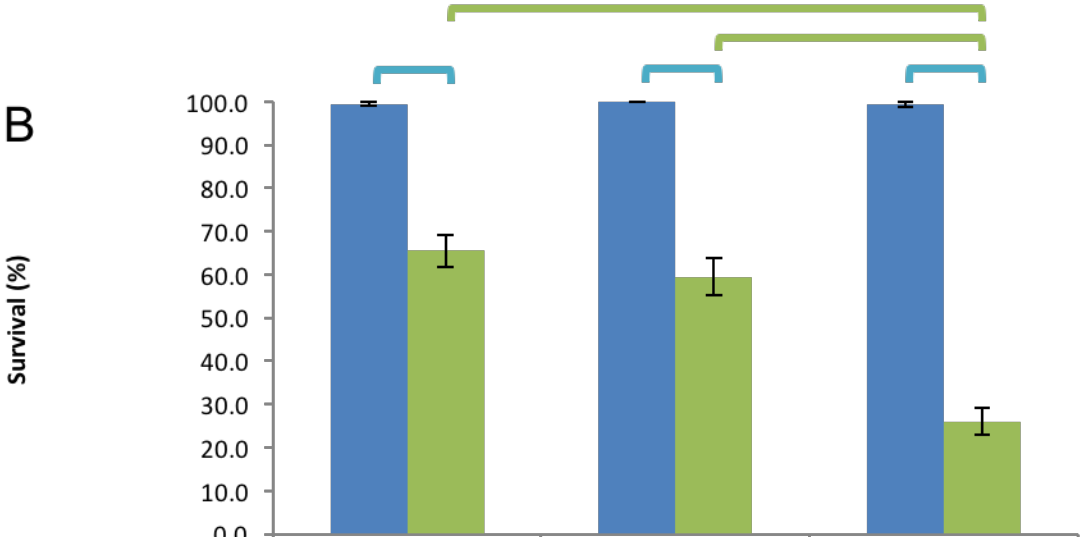

	Moody-Gal4	Moody-Gal4>Atg18RNAi	UAS-Atg18RNAi
5% Sucrose	99.5 ± 0.3	100.0 ± 0.0	99.4 ± 0.6
5% Suc + 25 mM PQ	65.6 ± 3.7	59.5 ± 4.3	26.0 ± 3.0

Figure 3.4: Negative Geotaxis and Survival for flies expressing Atg18^{RNAi} in the SPG. The experimental and parental flies were exposed to either 5% sucrose solution or 25 mM paraquat in 5% sucrose solution for 24h. **Sample sizes: (A)** Moody-Gal4: 0 mM N=15 25 mM N=11; Moody-Gal4>Atg18^{RNAi} 0 mM N=10 25 mM N=6; UAS-Atg18^{RNAi} 0mM N=17 25 mM N=8 **(B)** Survival: Moody-Gal4 0mM N=22 25 mM N=38; Moody-Gal4>Atg18^{RNAi} 0 mM N=13 25 mM N=17; UAS-Atg18^{RNAi} 0 mM N=20 20 mM N=44. Bars indicate statistical significance with $p<0.05$ (ANOVA).

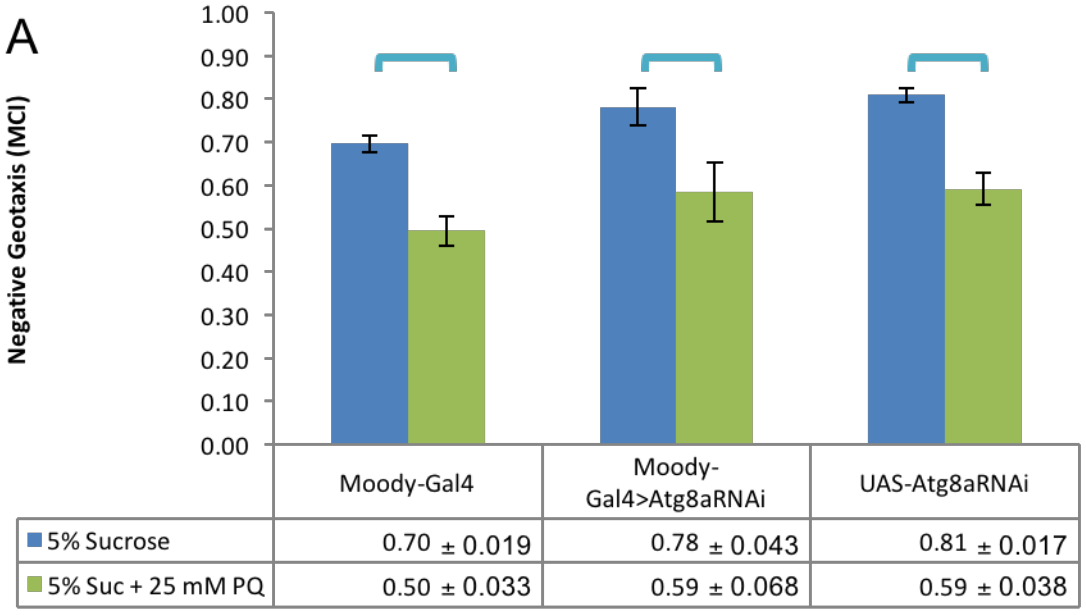

	Moody-Gal4	Moody-Gal4>Atg8aRNAi	UAS-Atg8aRNAi
5% Sucrose	0.70 ± 0.019	0.78 ± 0.043	0.81 ± 0.017
5% Suc + 25 mM PQ	0.50 ± 0.033	0.59 ± 0.068	0.59 ± 0.038

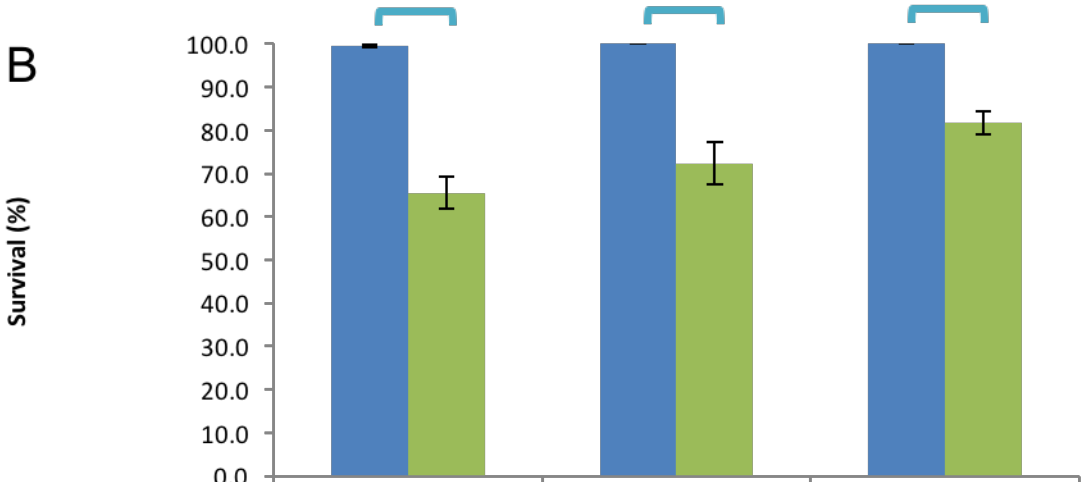

	Moody-Gal4	Moody-Gal4>Atg8aRNAi	UAS-Atg8aRNAi
5% Sucrose	99.5 ± 0.3	100.0 ± 0.0	100.0 ± 0.0
5% Suc + 25 mM PQ	65.6 ± 3.7	72.4 ± 4.9	81.7 ± 3.6

Figure 3.5: Negative Geotaxis and Survival for flies expressing Atg8a^{RNAi} in the SPG. The experimental and parental flies were exposed to either 5% sucrose solution or 25 mM paraquat in 5% sucrose solution for 24h. **Sample sizes: (A)** Moody-Gal4: 0 mM N=15 25 mM N=11; Moody-Gal4>Atg8a^{RNAi} 0 mM N=5 25 mM N=5; UAS-Atg8a^{RNAi} 0mM N=5 25 mM N=7 **(B)** Survival: Moody-Gal4 0mM N=22 25 mM N=38; Moody-Gal4>Atg8a^{RNAi} 0 mM N=6 25 mM N=12; UAS-Atg8a^{RNAi} 0 mM N=7 20 mM N=18. Bars indicate statistical significance with $p<0.05$ (ANOVA).

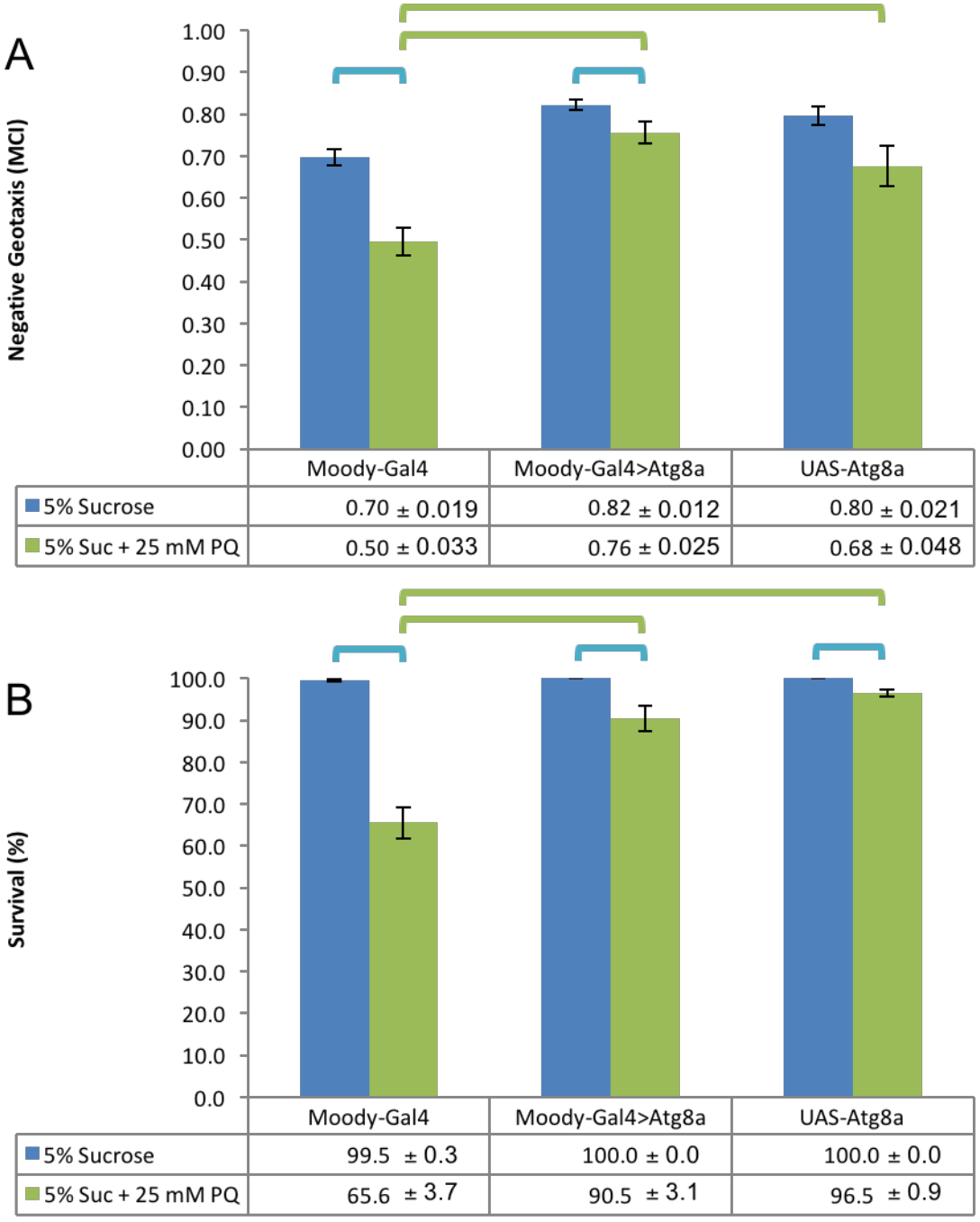

Figure 3.6: Negative Geotaxis and Survival for flies expressing Atg8a in the SPG. The experimental and parental flies were exposed to either 5% sucrose solution or 25 mM paraquat in 5% sucrose solution for 24h. **Sample sizes: (A)** Moody-Gal4 0 mM N=15 25 mM N=11; Moody-Gal4>Atg8a 0 mM N=6 25 mM N=5; UAS-Atg8a 0mM N=6 25 mM N=7 **(B)** Survival: Moody-Gal4 0mM N=22 25 mM N=38; Moody-Gal4>Atg8a 0 mM N=6 25 mM N=8; UAS-Atg8a 0 mM N=6 20 mM N=21. Bars indicate statistical significance with $p<0.05$ (ANOVA).

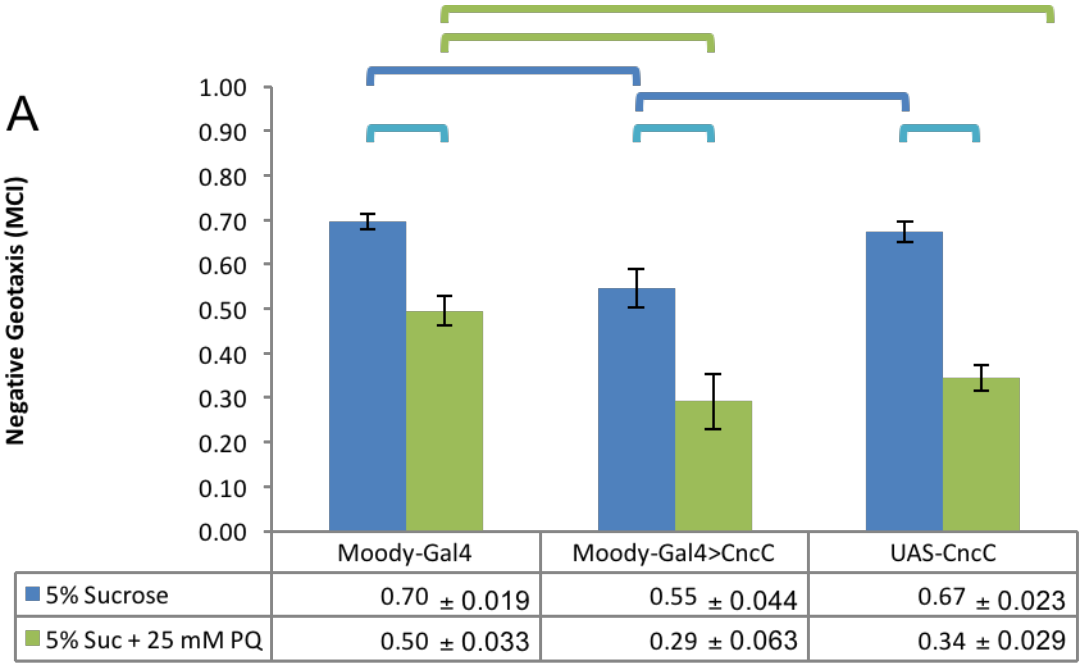

	Moody-Gal4	Moody-Gal4>CncC	UAS-CncC
5% Sucrose	0.70 ± 0.019	0.55 ± 0.044	0.67 ± 0.023
5% Suc + 25 mM PQ	0.50 ± 0.033	0.29 ± 0.063	0.34 ± 0.029

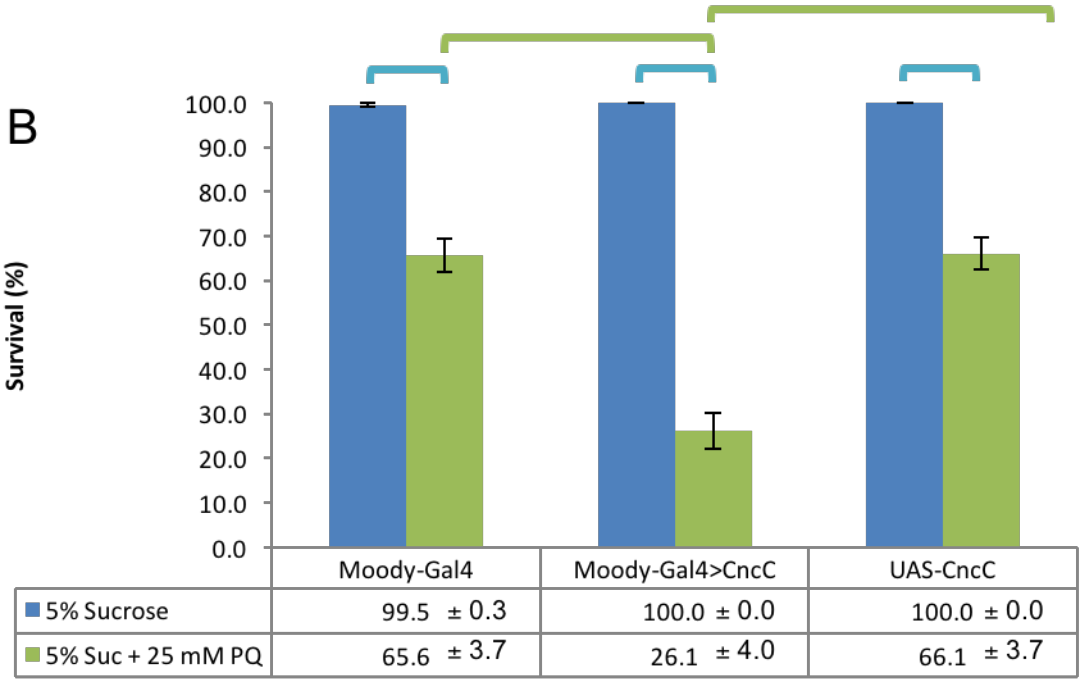

	Moody-Gal4	Moody-Gal4>CncC	UAS-CncC
5% Sucrose	99.5 ± 0.3	100.0 ± 0.0	100.0 ± 0.0
5% Suc + 25 mM PQ	65.6 ± 3.7	26.1 ± 4.0	66.1 ± 3.7

Figure 3.7: Negative Geotaxis and Survival for flies expressing CncC in the SPG. The experimental and parental flies were exposed to either 5% sucrose solution or 25 mM paraquat in 5% sucrose solution for 24h. **Sample sizes: (A)** Moody-Gal4 0 mM N=15 25 mM N=11; Moody-Gal4>CncC 0 mM N=6 25 mM N=2; UAS- CncC 0mM N=6 25 mM N=6 **(B)** Survival: Moody-Gal4 0mM N=22 25 mM N=38; Moody-Gal4>CncC 0 mM N=8 25 mM N=19; UAS-CncC 0 mM N=7 20 mM N=22. Bars indicate statistical significance with $p<0.05$ (ANOVA).

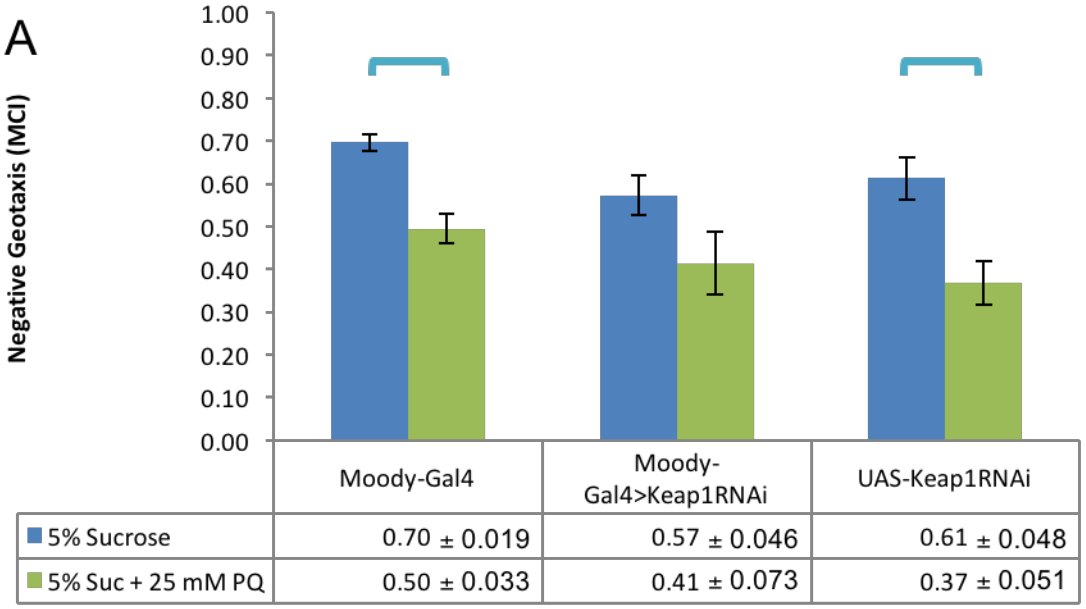

	Moody-Gal4	Moody-Gal4>Keap1RNAi	UAS-Keap1RNAi
5% Sucrose	0.70 ± 0.019	0.57 ± 0.046	0.61 ± 0.048
5% Suc + 25 mM PQ	0.50 ± 0.033	0.41 ± 0.073	0.37 ± 0.051

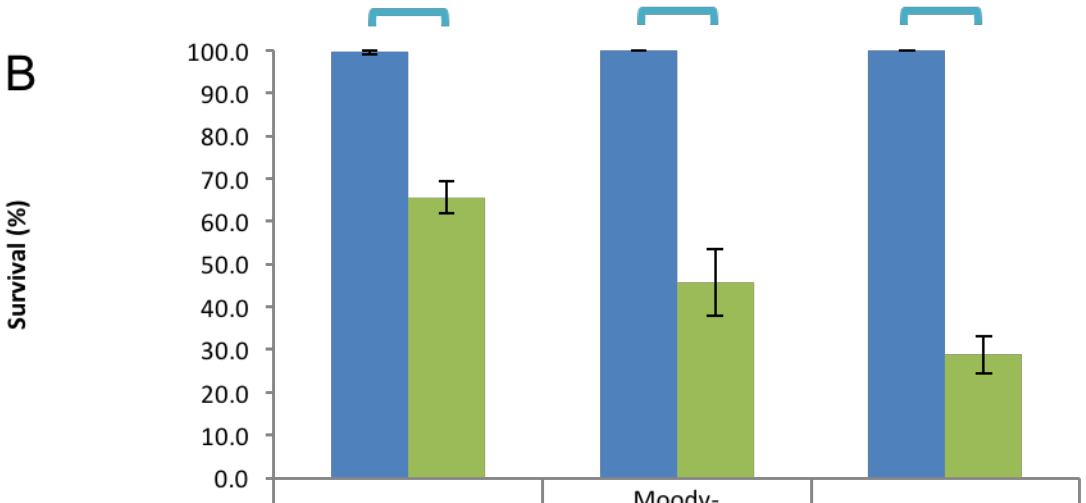

	Moody-Gal4	Moody-Gal4>Keap1RNAi	UAS-Keap1RNAi
5% Sucrose	99.5 ± 0.3	100.0 ± 0.0	100.0 ± 0.0
5% Suc + 25 mM PQ	65.6 ± 3.7	45.8 ± 7.8	28.8 ± 4.3

Figure 3.8: Negative Geotaxis and Survival for flies expressing Keap1^{RNAi} in the SPG. The experimental and parental flies were exposed to either 5% sucrose solution or 25 mM paraquat in 5% sucrose solution for 24h. **Sample sizes: (A)** Moody-Gal4 0 mM N=15 25 mM N=11; Moody-Gal4>Keap1^{RNAi} 0 mM N=6 25 mM N=4; UAS-Keap1^{RNAi} 0mM N=4 25 mM N=3 **(B)** Survival: Moody-Gal4 0mM N=22 25 mM N=38; Moody-Gal4>Keap1^{RNAi} 0 mM N=8 25 mM N=13; UAS- Keap1^{RNAi} 0 mM N=16 20 mM N=13. Bars indicate statistical significance with $p<0.05$ (ANOVA).

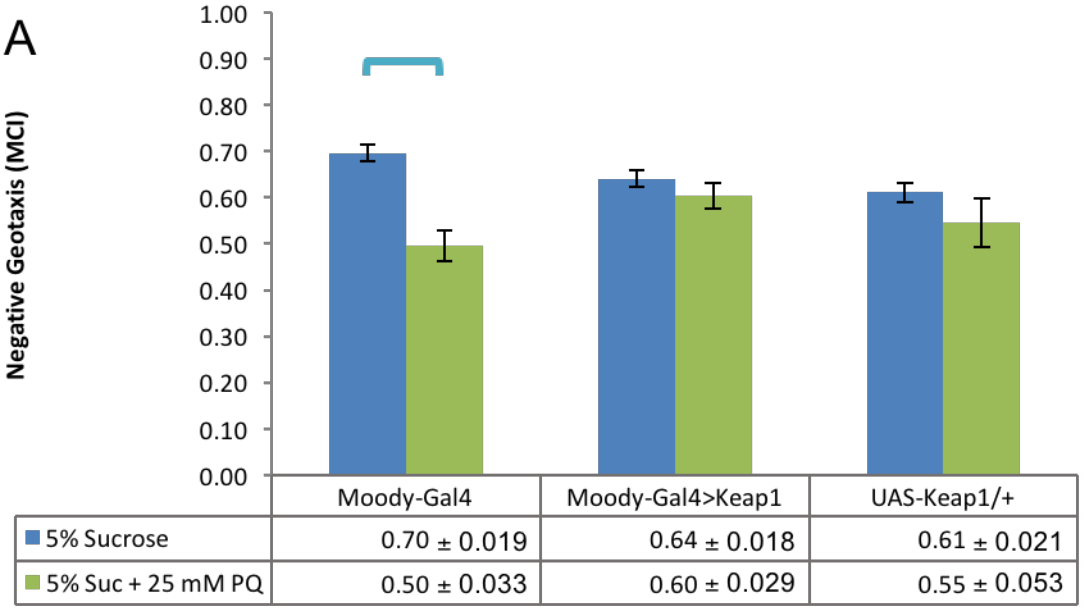

	Moody-Gal4	Moody-Gal4>Keap1	UAS-Keap1/+
5% Sucrose	0.70 ± 0.019	0.64 ± 0.018	0.61 ± 0.021
5% Suc + 25 mM PQ	0.50 ± 0.033	0.60 ± 0.029	0.55 ± 0.053

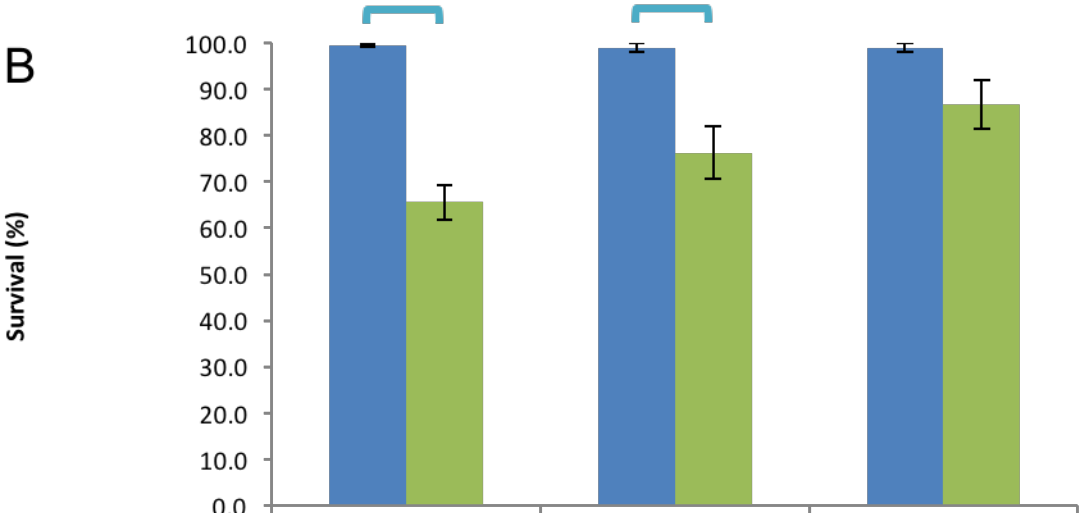

	Moody-Gal4	Moody-Gal4>Keap1	UAS-Keap1
5% Sucrose	99.5 ± 0.3	99.0 ± 1.0	99.0 ± 1.0
5% Suc + 25 mM PQ	65.6 ± 3.7	76.3 ± 5.8	86.7 ± 5.1

Figure 3.9: Negative Geotaxis and Survival for flies expressing Keap1 in the SPG. The experimental and parental flies were exposed to either 5% sucrose solution or 25 mM paraquat in 5% sucrose solution for 24h. **Sample sizes: (A)** Moody-Gal4 0 mM N=15 25 mM N=11; Moody-Gal4>Keap1 0 mM N=3 25 mM N=4; UAS-Keap1 0mM N=4 25 mM N=5 **(B)** Survival: Moody-Gal4 0mM N=22 25 mM N=38; Moody-Gal4>Keap1 0 mM N=5 25 mM N=8; UAS- Keap1 0 mM N=5 20 mM N=11. Bars indicate statistical significance with $p<0.05$ (ANOVA).

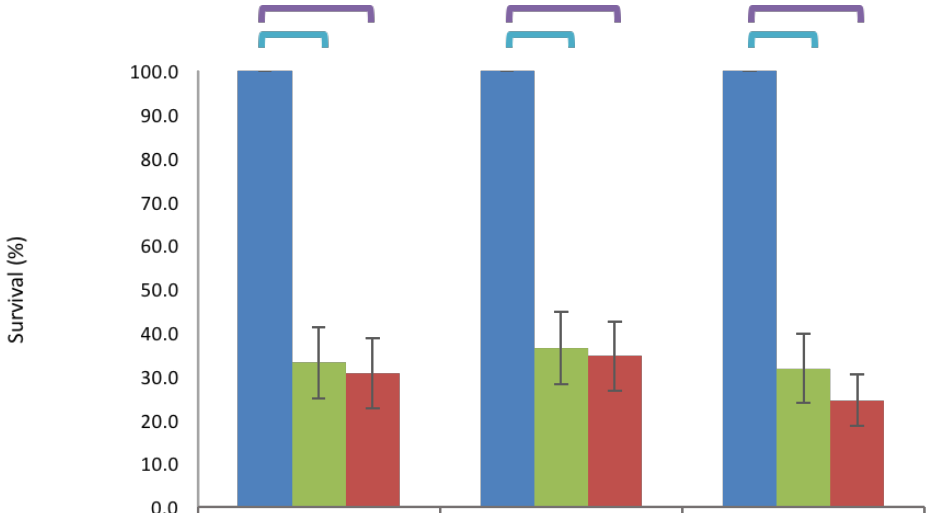

	Repo-Gal4	Repo-Gal4>Atg1RNAi	UAS-Atg1RNAi
0 h	100.0 ± 0.0	100.0 ± 0.0	100.0 ± 0.0
2h	33.1 ± 8.1	36.5 ± 8.3	31.7 ± 7.9
2h + 24h recovery	30.7 ± 8.1	34.7 ± 7.9	24.4 ± 5.9

Figure 3.10: Survival for flies expressing Atg1^{RNAi} in all glia after exposure to thermal stress . The experimental and parental flies were exposed to either a non-stressful condition (NSC) of 29^0 C or stressful condition (SC) of 37^0 C for 2h. The number of surviving flies was recounted after 24h to observe recovery (SCR). **Sample sizes:** Repo-Gal4 NSC N=5, SC and SCR N=22; Repo-Gal4>Atg1^{RNAi} NSC N=5, SC and SCR N=24; UAS-Atg1^{RNAi} NSC N=10 SC and SCR N=24. Bars indicate statistical significance with $p<0.05$ (ANOVA). Data obtained by Rachel Lee.

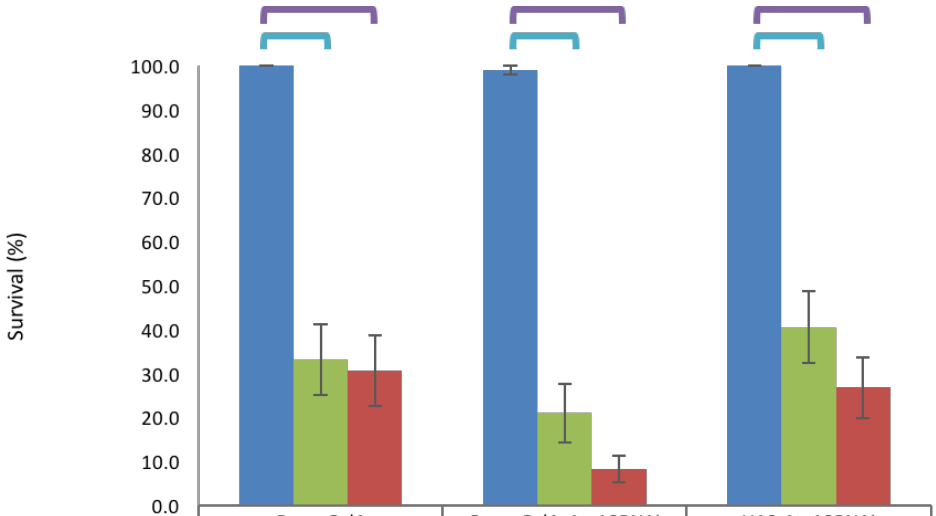

	Repo-Gal4	Repo-Gal4>Atg18RNAi	UAS-Atg18RNAi
0 h	100.0 ± 0.0	99.0 ± 1.0	100.0 ± 0.0
2h	33.1 ± 8.1	21.0 ± 6.6	40.5 ± 8.2
2h + 24h recovery	30.7 ± 8.1	8.3 ± 3.1	26.7 ± 6.9

Figure 3.11: Survival for flies expressing Atg18^{RNAi} in all glia after exposure to thermal stress . The experimental and parental flies were exposed to either a non-stressful condition (NSC) of 29^0 C or stressful condition (SC) of 37^0 C for 2h. The number of surviving flies was recounted after 24h to observe recovery (SCR). **Sample sizes:** Repo-Gal4 NSC N=5, SC and SCR N=22; Repo-Gal4>Atg18^{RNAi} NSC N=5, SC and SCR N=26; UAS-Atg18^{RNAi} NSC N=10 SC and SCR N=28. Bars indicate statistical significance with $p<0.05$ (ANOVA). Data obtained by Rachel Lee.

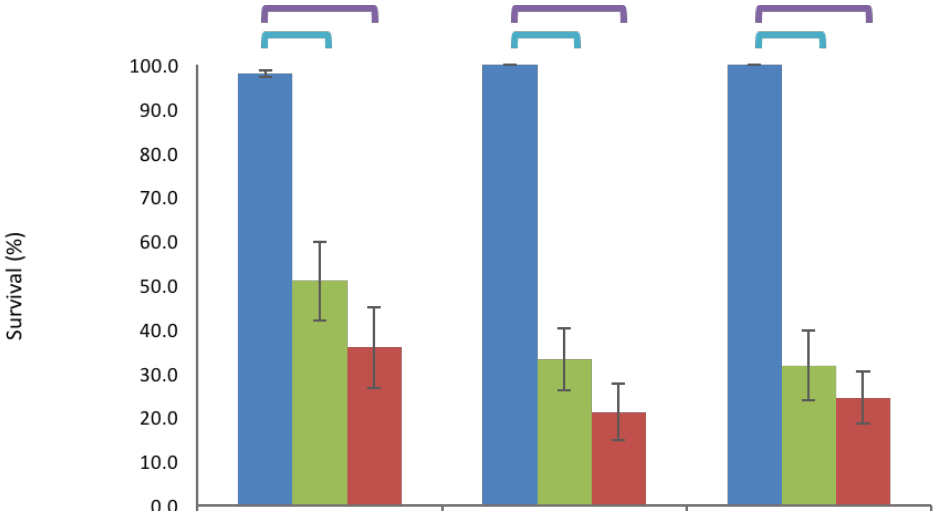

	Moody-Gal4	Moody-Gal4>Atg1RNAi	UAS-Atg1RNAi
0 h	98.0 ± 0.8	100.0 ± 0.0	100.0 ± 0.0
2h	50.9 ± 9.0	33.1 ± 7.0	31.7 ± 7.9
2h + 24h recovery	35.8 ± 9.2	21.2 ± 6.3	24.4 ± 5.9

Figure 3.12: Survival for flies expressing Atg1^{RNAi} in SPG after exposure to thermal stress . The experimental and parental flies were exposed to either a non-stressful condition (NSC) of 29^0 C or stressful condition (SC) of 37^0 C for 2h. The number of surviving flies was recounted after 24h to observe recovery (SCR). **Sample sizes:** Moody-Gal4 NSC N=10, SC and SCR N=22; Moody-Gal4>Atg1^{RNAi} NSC N=4, SC and SCR N=31; UAS-Atg1^{RNAi} NSC N=10 SC and SCR N=24. Bars indicate statistical significance with $p<0.05$ (ANOVA). Data obtained by Rachel Lee

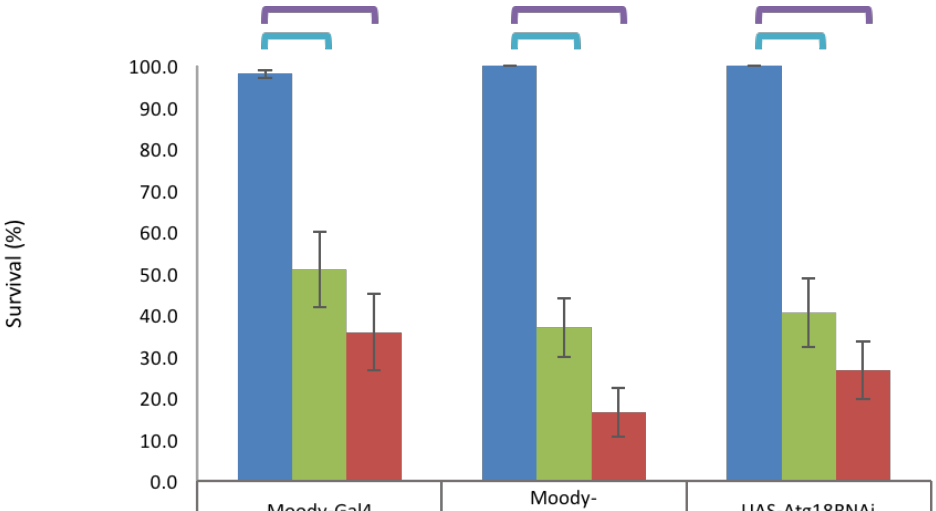

	Moody-Gal4	Moody-Gal4;>Atg18RNAi	UAS-Atg18RNAi
0 h	98.0 ± 0.8	100.0 ± 0.0	100.0 ± 0.0
2h	50.9 ± 9.0	37.0 ± 7.0	40.5 ± 8.2
2h + 24h recovery	35.8 ± 9.2	16.5 ± 5.9	26.7 ± 6.9

Figure 3.13: Survival for flies expressing Atg18^{RNAi} in SPG after exposure to thermal stress . The experimental and parental flies were exposed to either a non-stressful condition (NSC) of 29^0 C or stressful condition (SC) of 37^0 C for 2h. The number of surviving flies was recounted after 24h to observe recovery (SCR). **Sample sizes:** Moody-Gal4 NSC N=10, SC and SCR N=22; Moody-Gal4>Atg18^{RNAi} NSC N=3, SC and SCR N=30; UAS-Atg18^{RNAi} NSC N=10 SC and SCR N=28. Bars indicate statistical significance with $p<0.05$ (ANOVA). Data obtained by Rachel Lee.

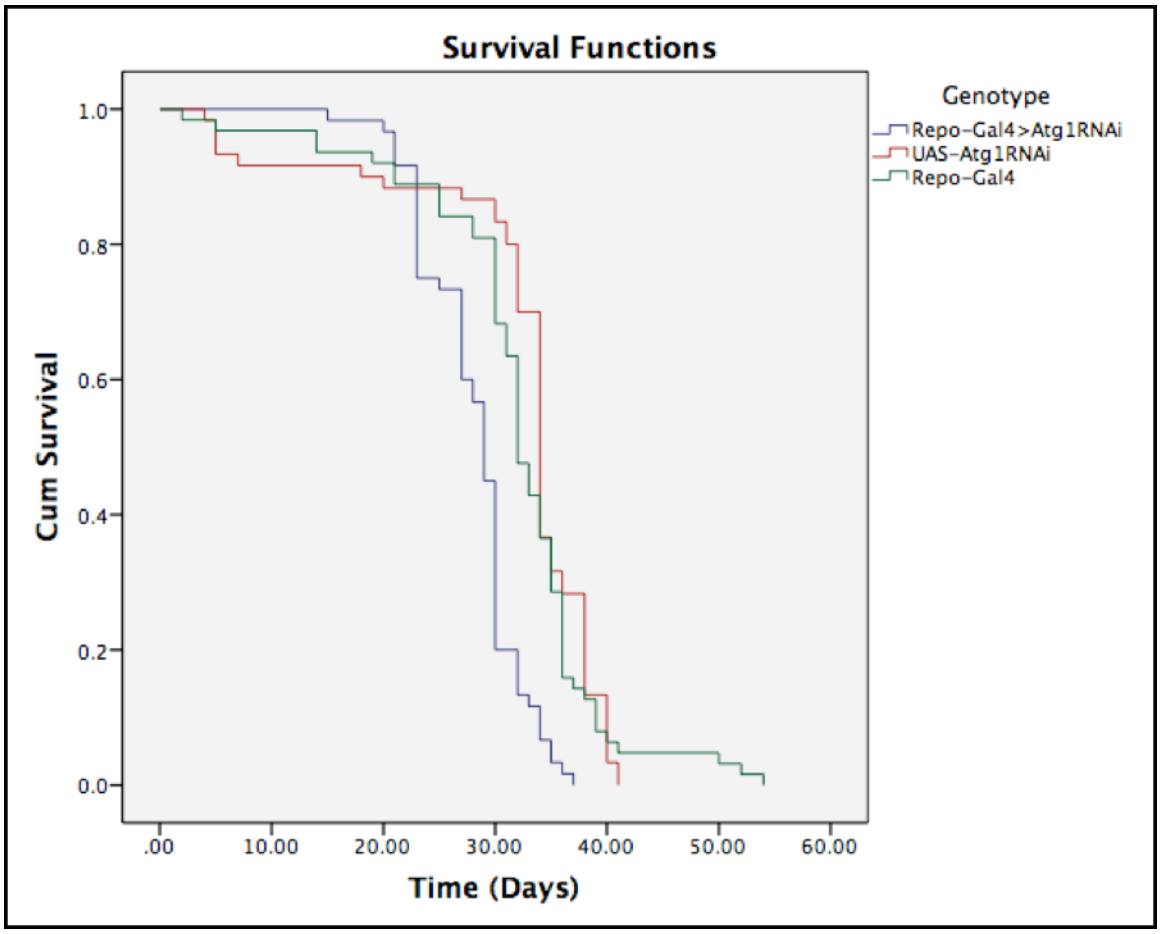

Figure 3.14: Kaplan-Meyer survival curve for flies expressing Atg1^{RNAi} in all glia. Separate samples of 60 flies for the experimental and each parental genotypes were aged at 29^{0} C and the number of living flies was recorded every day until the last surviving fly was no longer alive. The Log Rank (Mantel-Cox) significance values are: $p=1.1x10^{-11}$ for the difference between Repo-Gal4>Atg1^{RNAi} and UAS-Atg1^{RNAi}, $p=1.7x10^{-6}$ the difference between Repo-Gal4>Atg1^{RNAi} and Repo-Gal4.

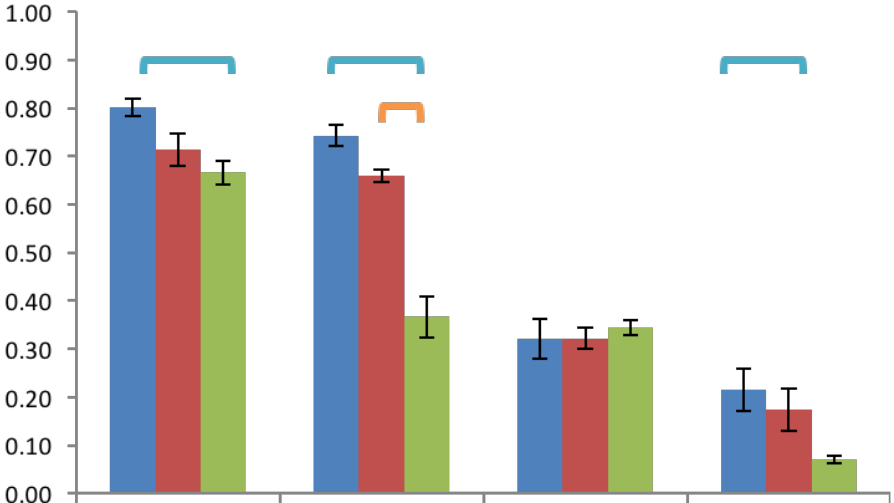

	3	10	20	30
Repo-Gal4	0.80 ± 0.02	0.74 ± 0.02	0.32 ± 0.04	0.21 ± 0.04
Repo-Gal4>Atg1RNAi	0.71 ± 0.03	0.66 ± 0.01	0.32 ± 0.02	0.17 ± 0.04
UAS-Atg1RNAi	0.67 ± 0.02	0.37 ± 0.04	0.34 ± 0.02	0.07 ± 0.01

Figure 3.15: Age-dependent negative geotaxis assay of flies expressing Atg1^{RNAi} in all glia. Flies were tested at 3 days, 10 days, 20 days and 30 days using the negative geotaxis assay. **Sample sizes**: N=5 for all days and genotypes. Bars indicate statistical significance with $p<0.05$ (ANOVA).

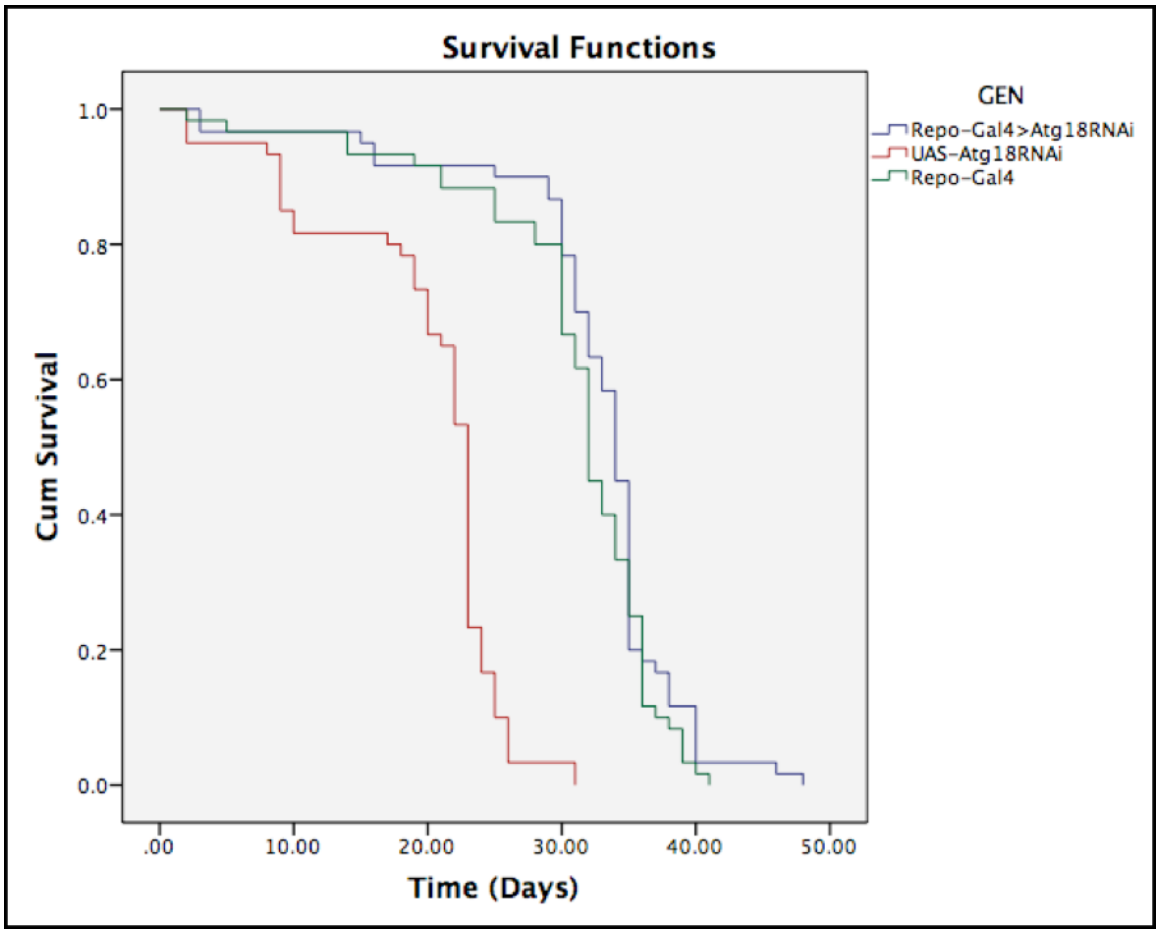

Figure 3.16: Kaplan-Meyer survival curve for flies expressing Atg18^{RNAi} in all glia. Separate samples of 60 flies for the experimental and each parental genotypes were aged at 29^0 C and the number of living flies was recorded every day until the last surviving fly was no longer alive. The Log Rank (Mantel-Cox) significance values are: $p=1x10^{-13}$ for the difference between Repo-Gal4>Atg18^{RNAi} and UAS-Atg18^{RNAi}, p=0.956 for the difference between Repo-Gal4>Atg18^{RNAi} and Repo-Gal4.

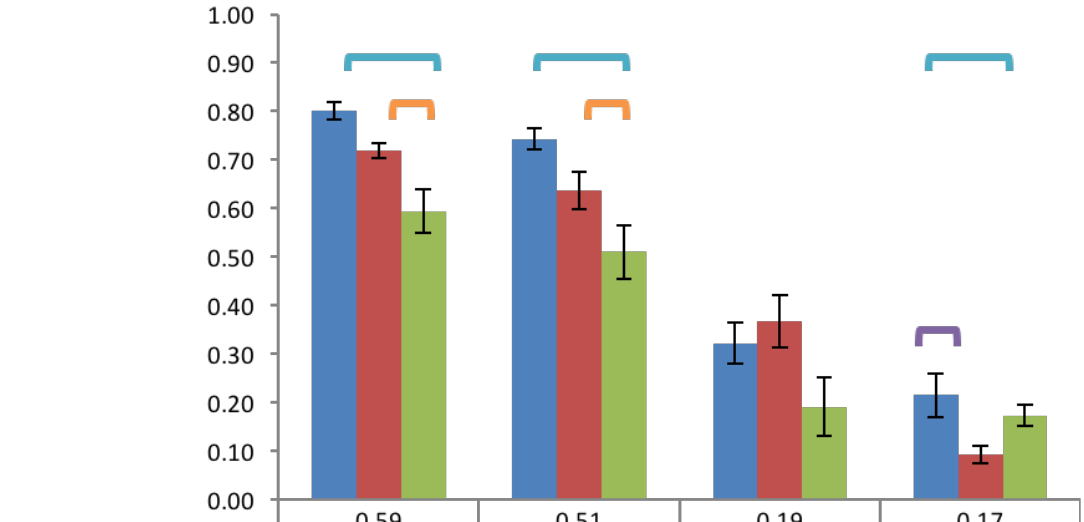

	0.59	0.51	0.19	0.17
Repo-Gal4	0.80 ± 0.02	0.74 ± 0.02	0.32 ± 0.04	0.21 ± 0.04
Repo-Gal4>Atg18RNAi	0.72 ± 0.02	0.64 ± 0.04	0.37 ± 0.05	0.09 ± 0.02
UAS-Atg18RNAi	0.59 ± 0.04	0.51 ± 0.06	0.19 ± 0.06	0.17 ± 0.02

Figure 3.17: Age-dependent negative geotaxis assay of flies expressing Atg18^{RNAi} in all glia. Flies were tested at 3 days, 10 days, 20 days and 30 days using the negative geotaxis assay. **Sample sizes**: N=5 for all days and genotypes. Bars indicate statistical significance with $p<0.05$ (ANOVA).

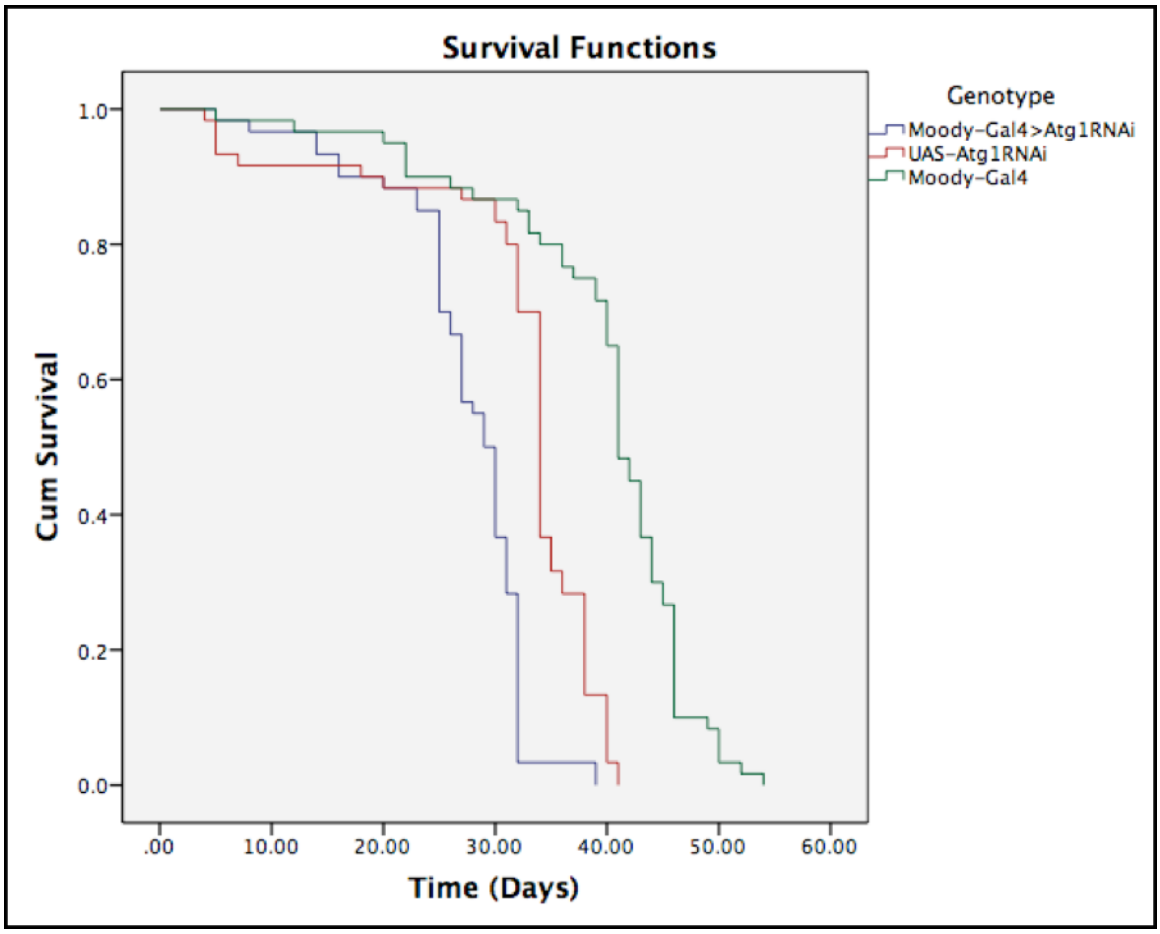

Figure 3.18: Kaplan-Meyer survival curve for flies expressing Atg1^{RNAi} in the SPG. Separate samples of 60 flies for the experimental and each parental genotypes were aged at 29^0 C and the number of living flies was recorded every day until the last surviving fly was no longer alive. The Log Rank (Mantel-Cox) significance values are: $p=8.5x10^{-12}$ for the difference between Moody-Gal4>Atg1^{RNAi} and UAS-Atg1^{RNAi}, $p=1x10^{-13}$ for the difference between Moody-Gal4>Atg1^{RNAi} and Moody-Gal4.

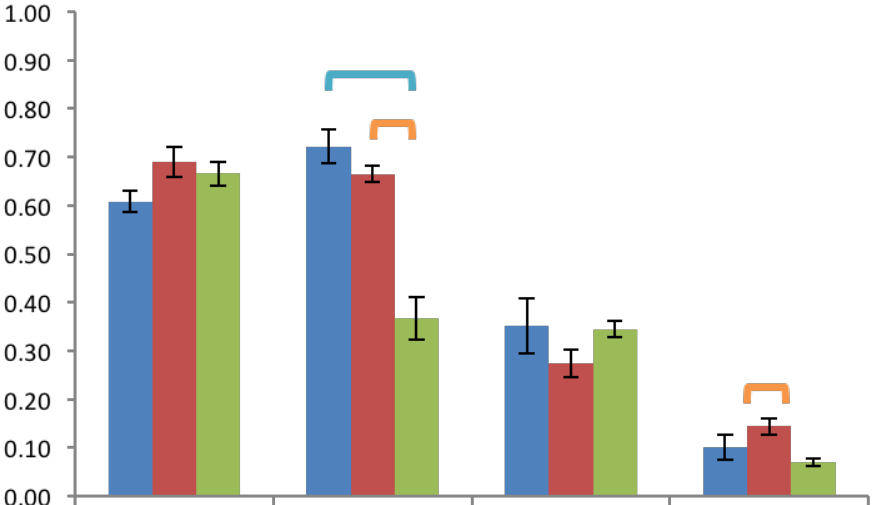

	3	10	20	30
Moody-Gal4	0.61 ± 0.02	0.72 ± 0.03	0.35 ± 0.06	0.10 ± 0.03
Moody-Gal4>Atg1RNAi	0.69 ± 0.03	0.67 ± 0.02	0.28 ± 0.03	0.14 ± 0.02
UAS-Atg1RNAi	0.67 ± 0.02	0.37 ± 0.04	0.34 ± 0.02	0.07 ± 0.01

Figure 3.19: Age-dependent negative geotaxis assay of flies expressing Atg1^{RNAi} in the SPG. Flies were tested at 3 days, 10 days, 20 days and 30 days using the negative geotaxis assay. **Sample sizes**: N=5 for all days and genotypes. Bars indicate statistical significance with $p<0.05$ (ANOVA).

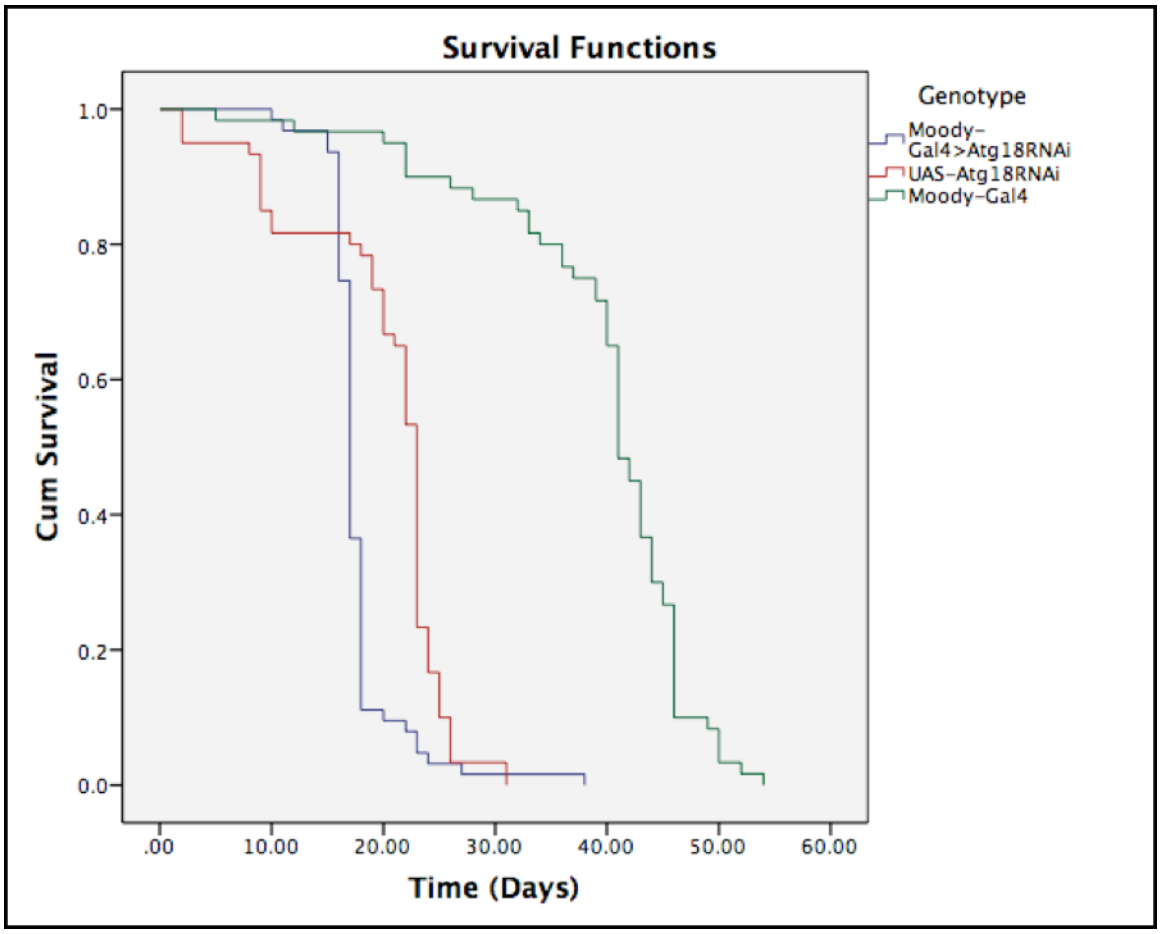

Figure 3.20: Kaplan-Meyer survival curve for flies expressing Atg18^{RNAi} in the SPG. Separate samples of 60 flies for the experimental and each parental genotypes were aged at 29^0 C and the number of living flies was recorded every day until the last surviving fly was no longer alive. The Log Rank (Mantel-Cox) significance values are: $p=1.14x10^{-6}$ for the difference between Moody-Gal4>Atg18^{RNAi} and UAS-Atg18^{RNAi}, $p=1x10^{-13}$ for the difference between Moody-Gal4>Atg18^{RNAi} and Moody-Gal4.

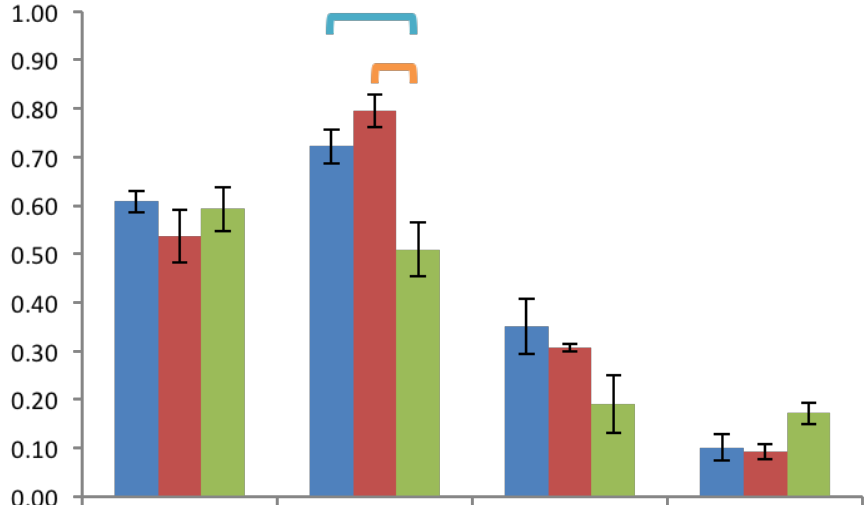

	3	10	20	30
Moody-Gal4	0.61 ± 0.02	0.72 ± 0.03	0.35 ± 0.06	0.10± 0.03
Moody-Gal4>Atg18RNAi	0.54 ± 0.05	0.80 ± 0.03	0.31 ± 0.01	0.09± 0.02
UAS-Atg18RNAi	0.59 ± 0.04	0.51 ± 0.06	0.19 ± 0.06	0.17± 0.02

Figure 3.21: Age-dependent negative geotaxis assay of flies expressing Atg18^{RNAi} in the SPG. Flies were tested at 3 days, 10 days, 20 days and 30 days using the negative geotaxis assay. **Sample sizes**: N=5 for all days and genotypes. Bars indicate statistical significance with $p<0.05$ (ANOVA).

4 Discussion

The main objective of this thesis was to explore the role of autophagy and the NRF2/Keap1 pathway in the glia during oxidative stress, thermal stress and aging in the *Drosophila melanogaster* brain.

4.1 Impact of autophagy and NRF2/Keap1 pathway down regulation and activation in the glia on sensitivity to acute oxidative stress

The first aim of this study was to explore the role of autophagy and the NRF2/Keap1 pathway in glia during acute oxidative stress on the *Drosophila* brain. I hypothesized that alteration of the levels of autophagy in all glia and the SPG has an effect on the the flie's sensitivity to oxidative stress. Figure 3.1 shows that when Atg1 is downregulated in all glia there is significant improvement in the survival after acute oxidative stress but not in negative geotaxis performance. In contrast, when Atg18 is downregulated in all glia, reduced sensitivity to oxidative stress is observed for both survival and negative geotaxis assay performance. Complete protection of survival and negative geotaxis performance, however, is not observed when autophagy is downregulated in all glia, as there is still a significant difference between the treated and untreated flies expressing $Atg1^{RNAi}$ and $Atg18^{RNAi}$ in repo cells. Down regulation of Atg1 and Atg18 in the SPG provided protection of locomotor ability from oxidative stress. A significant improvement in negative geotaxis is only observed in flies expressing $Atg18^{RNAi}$ in moody cells. Improvement and protection was not observed for survival when Atg1 or Atg18 were downregulated in the SPG. The data suggest that down regulation of autophagy via the expression of $Atg1^{RNAi}$ and $Atg18^{RNAi}$ in the glia and SPG during oxidative stress

provides some protection of survival and locomotor ability. Down regulation of Atg18 shows much better protection and improvement than down regulation of Atg1. As discussed in section *1.4.1*, Atg18 functions as an Atg8-PE recruiting protein during the elongation process of autophagosome formation (Mizushima et al., 2011). Its essential function and lack of a functionally redundant counterpart during autophagy could explain why its down regulation in all glia produces a much better protective effect compared to Atg1 (Obara, Sekito, Niimi, & Ohsumi, 2008). Atg1 functions as the main inducer of autophagy as it acts to recruit and activate downstream autophagy pathway proteins (Mizushima et al., 2011; Mizushima, 2010). Although Atg1 is essential for starvation-induced autophagy, there are redundant pathways through which autophagy can be induced, especially during stress conditions. One example is the beclin1-dependent autophagy induction, a protein that is inhibited by the anti-apoptotic factor BCL2 (Maiuri et al., 2007; Mizushima et al., 2011). This means that even through direct inhibition of Atg1 translation via the $Atg1^{RNAi}$, a functionally redundant pathway could still be activating autophagy, especially since the cells are under stressful conditions. In order to inhibit the autophagy pathway at the induction stages in future studies, both the Atg1 and its functionally redundant counterparts can be downregulated. The data in this thesis shows that targeting Atg18 provides a much more effective way of downregulating autophagy than Atg1.

Down regulation Atg8a in the SPG did not have any effect on the flies' sensitivity to oxidative stress as evident from the negative geotaxis assay and survival data (Figure 3.5). Overexpression of Atg8a in the SPG showed a small significant decline in negative

geotaxis and survival after paraquat exposure. The negative geotaxis performance and survival for the experimental flies were significantly better than the Gal4 control (Figure 3.6). This observation suggests that overexpression of Atg8a may have a protective effect. The UAS control flies had similar negative geotaxis performance and survival to the flies overexpressing Atg8a. This observation may be explained by leaky expression of the UAS promoter that could cause a ubiquitous overexpression of Atg8a in the fly. This possibility can be addressed by either a qRT-PCR, Western blot analysis, or immunostaining with an anti-Atg8a antibody in UAS-Atg8a and wild type flies. Previous studies have shown that overexpression of Atg8a in the CNS does not have any negative effects in otherwise wild type flies (Poels et al., 2012; Simonsen et al., 2008). One study showed that Atg8a overexpression in the *Drosophila* eye did not cause neuronal degeneration unless it was in a mutant background (Poels et al., 2012). In fact, pan-neuronal overexpression of Atg8a in *Drosophila* provides longer lifespan and resistance to chronic exposure to H_2O_2 compared wild type flies, while mutants lacking Atg8a expression showed reduced lifespan and greater susceptibility to chronic H_2O_2 exposure (Simonsen et al., 2008). The data presented in this thesis suggests that Atg8a has similar effect when it is overexpressed in the glia as it does when it is overexpressed in neurons.

The data discussed above provide evidence that down regulation of autophagy in the glia and SPG provides protection of the *Drosophila* from acute oxidative stress. This supports the hypothesis that alteration of the levels of autophagy affects the sensitivity to oxidative stress. In order to test this hypothesis further overexpression of Atg1 and Atg18 should be performed in the corresponding tissues.

It was also hypothesized that alteration of the levels of the NRF2/Keap1 pathway in SPG would affect the *Drosophila's* sensitivity to oxidative stress. Figure 3.7 shows that upregulation of NRF2 via direct overexpression of the CncC in the SPG does not provide any protection of survival and negative geotaxis assay performance from oxidative stress. In fact, overexpression of CncC has a deleterious effect on the flies, as the untreated and treated flies overexpressing CncC in the SPG have reduced negative geotaxis performance compared to the untreated and treated controls. The treated flies overexpressing CncC in the SPG also have reduced survival. This suggests that overexpression of the NRF2 transcription factor in the SPG has a deleterious effect in flies. This is a surprising result since the NRF2 pathway is very well known for its role in oxidative stress response as it directly regulates antioxidant genes containing the ARE promoter sequence. (Ma, 2013; Nguyen, Nioi, & Pickett, 2009; Singh et al., 2010). There are several possible explanations that could explain why NRF2 would have deleterious effects when overexpressed in the SPG. The NRF2 protein could have direct toxicity in the subperineurial cells, as they may not be able to deal with high levels of the protein. On the other hand, a more likely explanation could be that overexpression of NRF2 promotes the expression of endogenous antioxidants and it causes an overproduction of these antioxidants, causing a shift in the redox balance in the subperineurial cells. Despite the increased exogenous increase in ROS due to paraquat ingestion, the antioxidants could be overloading the cell creating a highly reduced state. Reductive stress is as deleterious as oxidative stress is as it impairs normal cell function (Finkel & Holbrook,

2000; Kohen & Nyska, 2002). This evidence suggests that maintenance or the redox balance is essential for normal cell function, especially for the SPG.

The data shown in Figure 3.8 indicates that activation of NRF2/Keap1 pathway in the SPG via inhibition of NRF2 repressor Keap1 prevents effect of paraquat exposure on negative geotaxis assay performance. However, this apparent protection could be a statistical artifact as the standard error depicted by the error bars in Figure 8 is greater then the standard error for the treated controls. The untreated flies overexpressing $Keap1^{RNAi}$ also perform significantly worse in the negative geotaxis assay compared to the Moody-Gal4/+ control. Down regulation of Keap1 in the SPG does not change the impact of paraquat exposure on survival any protection of survival.

The data depicted in Figure 3.9 shows that overexpression of Keap1 in the SPG protects flies from the deleterious effects of oxidative stress on negative geotaxis. This protection is not observed for survival. Overexpression of Keap1 in the SPG seems to have somewhat protective effects on negative geotaxis. The UAS-Keap1/+ control does not show a decline in both negative geotaxis and survival after paraquat exposure. This could be due to leaky expression of the UAS promoter in the UAS-Keap1 flies if overexpression of Keap1 in the SPG has protective effects. Keap1 is a repressor of NRF2 and it deactivates NRF2 during normal conditions (Ma, 2013; Nguyen et al., 2009; Singh et al., 2010). The reason why overexpression of Keap1 in the glia has protective effects in the SPG during oxidative stress is unclear. One possibility could be that the Keap1 protein, although in higher concentrations, might be ineffective since it goes through a conformational change during increased ROS in the cell to release NRF2 (Ma, 2013;

Nguyen et al., 2009; Singh et al., 2010). So overexpression of Keap1 may not play repressive role in NRF2 during oxidative conditions. On the other hand, it was previously discussed that the NRF2 protein could have direct toxic effects in the subperineurial cells. Overexpression of Keap1 could alleviate that toxicity by targeting NRF2 for degradation. This however is an improbable scenario and needs to be confirmed.

Our observations do not support the hypothesis that activation of NRF2 in the SPG provides protection of the brain from oxidative stress. In fact, we conclude that inhibition of NRF2 in the SPG provides protection from oxidative stress. To address these results and test the role of the NRF2/Keap1 pathway further, activation of NRF2 should be examined in repo cells. Previous data from our lab has shown that overexpression of specific antioxidants such as SOD2, a known NRF2 target, in all glia and the SPG provides protection of the brain from oxidative stress, seen as increased survival, negative geotaxis performance and the number of neurons in the PPL1 cluster (Iftekhkaruddin, 2014; Jones, Kucera, Gordon, & Boss, 1995). One study has shown activation of NRF2/Keap1 pathway, either by direct overexpression of CncC or by down regulation of Keap1 in the entire fly provides protection from oxidative stress (Sykiotis & Bohmann, 2008). Overexpression of CncC, but not overexpression of Keap1, in the eye caused aberrant eye phenotype indicating that that NRF2 overexpression may have deleterious effects in cells in the absence of oxidative stress (Sykiotis & Bohmann, 2008). In mice, overexpression of NRF2 in astrocytes provides protection from oxidative stress (Williamson et al., 2012). It is possible that overexpression of NRF2 or the subsequent

overexpression of its targets in the SPG are the cause of the deleterious effects in *Drosophila*.

4.2 The effects glial autophagy down regulation on the survival of flies during acute thermal stress

In order to see if down regulation of autophagy in glial cells had a broader protective effect in the context of stress, flies expressing $Atg1^{RNAi}$ and $Atg18^{RNAi}$ in the glia and SPG were exposed to acute thermal stress. It was hypothesized, as in case of oxidative stress, down regulation of autophagy in the glia and SPG would provide protection from acute thermal stress. Figures 3.10-3.13 show that such protective effects were not observed. This result is supported by the literature which suggests that autophagy plays an essential role in the survival and the recovery from heat shock (Nivon, Richet, Codogno, Arrigo, & Kretz-Remy, 2014). To explore the role of autophagy in the glia during thermal stress further, experiments involving the upregulation of autophagy can be done to see if that will produce protective effects on the survival. Additionally, negative geotaxis assay experiments can be performed to test the effects of upregulation and down regulation of autophagy in the glia during thermal stress on locomotor ability of the flies.

4.3 The effects of glial autophagy down regulation on the chronic exposure to stress brought on by aging

The third goal of this thesis was to determine whether down regulation of autophagy in all glia and the SPG causes an increased lifespan and a delay in the age-

dependent decline of locomotor ability. To that end, I expressing $Atg1^{RNAi}$ and $Atg18^{RNAi}$ in all glia and the SPG under the regulation of Repo-Gal4 and Moody-Gal4, and measured the lifespan and the kinetic of age dependent decline in negative geotaxis as described before.

Figures 3.14-3.21 show the results of these experiments. The Kaplan-Meyer survival curves depict that down regulation of Atg1 all glia and the SPG and down regulation of Atg18 in all SPG caused a significant decline in lifespan when compared to parental controls. Down regulation of Atg18 in the glia did not have any effect on lifespan, as it was not significantly different from the Repo-Gal4/+ control. The results of the negative geotaxis assay experiments demonstrate that down regulation of autophagy in all glia or the SPG do not have any effect on the age-dependent decline of negative geotaxis. These observations from these experiments are not sufficient to conclude that down regulation of autophagy in the glia and the SPG has any protective effects from aging. Autophagy in moderation, is a very important cellular maintenance process, especially during aging. Accumulation of cellular damage is believed to be one of the main causes of aging (Vellai, 2009). The beneficial role of autophagy as a cellular clean up mechanism, could be why down regulation of autophagy in the glia and SPG causes a decrease in lifespan. The glial cells could be aging at a faster rate than other tissues which would impair their function and cause an early death. The negative effect of down regulation of autophagy in the glia may not be observed at 30 days in the case of age-dependent negative geotaxis. In fact, the survival curves show a more rapid drop in survival after 30 days.

The negative effects of down regulation of autophagy in glial cells should be explored further. Age-dependent negative geotaxis experiments should be performed on flies older than 30 days to see if the down regulation of autophagy impairs the locomotor ability more so than the controls. Additionally, the activation of autophagy should also be studied in this context. Previous studies have shown that activating autophagy via pan-neuronal Atg8a overexpression extends the lifespan of flies (Simonsen et al., 2008). It would be interesting to see if this can be reproduced with glial expression of Atg8a as well as Atg1 and Atg18, although it should be noted that overexpression of Atg1 and Atg18 may have short term negative effects as it may induce autophagic stress or cell death (Cherra & Chu, 2008).

4.4 Conclusion and Future directions

The focus of this thesis was to explore the role of autophagy and the NRF2/Keap1 pathway in the context of glia during acute oxidative stress, acute thermal stress and aging. It can be concluded that down regulation of autophagy in the glia provides some protection survival and their locomotor ability from paraquat. Activation of the NRF2/Keap1 pathway in the SPG had deleterious effects on flies. It was proposed that NRF2 may have some direct or indirect toxicity in the SPG in *Drosophila*, however this needs to be confirmed. Down regulation of autophagy in the glia during thermal stress did not have any protective effects on survival. Additionally, down regulation of autophagy in the glia shortened the lifespan of flies and it did not have any delay in the age-dependent decline in locomotor ability. Conclusions from these results are summarized in Figure 4.1. Some experiments were already discussed in order to address these newly

raised questions. Additional future experiments that will build on this thesis include looking at the effect of down regulation of autophagy in repo cells and activation of the NRF2/Keap1 pathway in both moody and repo cells on the dopaminergic neuron numbers and integrity. Also, the effects of upregulation of autophagy can be studied further in the context of glia during oxidative stress, thermal stress and aging via the overexpression of Atg1, Atg18 and Atg8a in moody and repo cells. Additionally, the role of the NRF2/Keap1 pathway can also be explored in the context of glia during thermal stress, as well as during aging. The role of the NRF2/Keap1 pathway can be further studied in the glia by the analysis of ARE-GFP and ARE-RFP fusions. The literature suggests that autophagy positively regulates the NRF2/Keap1 pathway via P62 (Jain et al., 2010). Therefore, the abovementioned ARE fusions can be analyzed in flies in which autophagy is upregulated or downregulated in the glia. Furthermore, the interaction between the NRF2/Keap1 pathway and autophagy can be studied in the context of glia during oxidative stress by creating co-expression stocks containing UAS-Atg1^{RNAi}, UAS-Atg18^{RNAi} or other autophagy components along with components of the NRF2/Keap1 pathway. Finally, MAPK, JNK and p38 stress markers can be measured using Western blotting when autophagy and the NRF2/Keap1 pathway are being upregulated and downregulated in the glia. These experiments will greatly improve our knowledge and answer questions regarding the role of autophagy and the NRF2/Keap1 pathway and their interaction in glia during stressful conditions.

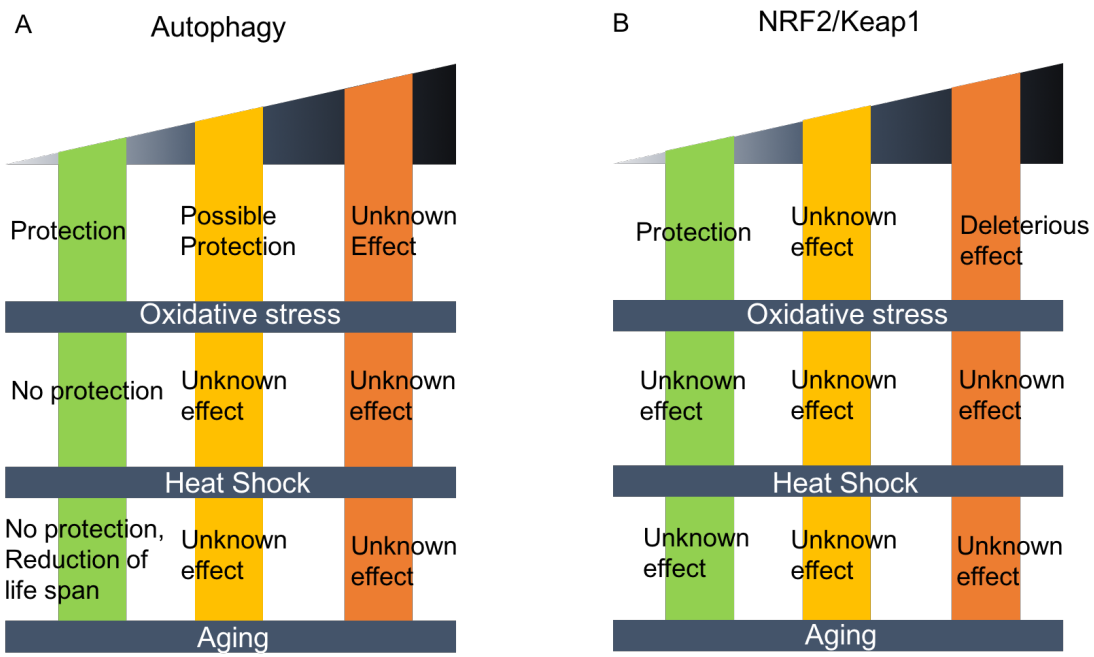

Figure 4.1 The effect of different levels of autophagy and the NRF2/Keap1 pathway on *Drosophila* in the context of oxidative stress, heat shock and aging.

5 References

Andersen, J. K. (2004). Oxidative stress in neurodegeneration: cause or consequence?

Barone, M. C., & Bohmann, D. (2013). Assessing neurodegenerative phenotypes in Drosophila dopaminergic neurons by climbing assays and whole brain immunostaining. *Journal of Visualized Experiments : JoVE*, (74), e50339. http://doi.org/10.3791/50339

Barone, M. C., Sykiotis, G. P., & Bohmann, D. (2011). Genetic activation of Nrf2 signaling is sufficient to ameliorate neurodegenerative phenotypes in a Drosophila model of Parkinson's disease. *Disease Models & Mechanisms*, *4*(5), 701–707. http://doi.org/10.1242/dmm.007575

Beal, M. F. (1995). Aging, energy, and oxidative stress in neurodegenerative diseases. *Annals of Neurology*, *38*(3), 357–66. http://doi.org/10.1002/ana.410380304

Blackstone, N. W. (1995). A units-of-evolution perspective on the endosymbiont theory of the origin of the mitochondrion. *Evolution*, *49*(5), 785–797. Retrieved from http://go.galegroup.com.libaccess.lib.mcmaster.ca/ps/i.do?id=GALE%7CA17951645&sid=googleScholar&v=2.1&it=r&linkaccess=fulltext&issn=00143820&p=AONE&sw=w

Botella, J. A., Bayersdorfer, F., Gmeiner, F., & Schneuwly, S. (2009). Modelling Parkinson's disease in Drosophila. *Neuromolecular Medicine*, *11*(4), 268–80. http://doi.org/10.1007/s12017-009-8098-6

Butterfield, A. D., Castegna, A., Lauderback, C., & Drake, J. (2002). Evidence that amyloid beta-peptide-induced lipid peroxidation and its sequelae in Alzheimer's disease brain contribute to neuronal death1. *Neurobiology of Aging*, *23*(5), 655–664. http://doi.org/10.1016/S0197-4580(01)00340-2

Calkins, M. J., Jakel, R. J., Johnson, D. A., Chan, K., Kan, Y. W., & Johnson, J. A. (2005). Protection from mitochondrial complex II inhibition in vitro and in vivo by Nrf2-mediated transcription. *Proceedings of the National Academy of Sciences of the United States of America*, *102*(1), 244–9. http://doi.org/10.1073/pnas.0408487101

Calkins, M. J., Vargas, M. R., Johnson, D. A., & Johnson, J. A. (2010). Astrocyte-specific overexpression of Nrf2 protects striatal neurons from mitochondrial complex II inhibition. *Toxicological Sciences : An Official Journal of the Society of Toxicology*, *115*(2), 557–68. http://doi.org/10.1093/toxsci/kfq072

Chaudhuri, A., Bowling, K., Funderburk, C., Lawal, H., Inamdar, A., Wang, Z., & O'Donnell, J. M. (2007). Interaction of genetic and environmental factors in a Drosophila parkinsonism model. *The Journal of Neuroscience : The Official Journal of the Society for Neuroscience*, *27*(10), 2457–67. http://doi.org/10.1523/JNEUROSCI.4239-06.2007

Cherra, S. J. 3rd, & Chu, C. T. (2008). Autophagy in neuroprotection and neurodegeneration: a question of balance. Retrieved from http://www.futuremedicine.com/doi/abs/10.2217/14796708.3.3.309

Dexter, D. T., Carter, C. J., Wells, F. R., Javoy-Agid, F., Agid, Y., Lees, A., … Marsden, C. D. (1989). Basal Lipid Peroxidation in Substantia Nigra Is Increased in Parkinson's Disease. *Journal of Neurochemistry*, *52*(2), 381–389. http://doi.org/10.1111/j.1471-4159.1989.tb09133.x

Edwards, T. N., & Meinertzhagen, I. A. (2010). The functional organisation of glia in the adult brain of Drosophila and other insects. *Progress in Neurobiology*, *90*(4), 471–497. http://doi.org/10.1016/j.pneurobio.2010.01.001

Essick, E. E., & Sam, F. (2010). Oxidative stress and autophagy in cardiac disease, neurological disorders, aging and cancer. *Oxidative Medicine and Cellular Longevity*, *3*(3), 168–77. http://doi.org/10.4161/oxim.3.3.12106

Feany, M. B., & Bender, W. W. (2000). A Drosophila model of Parkinson's disease. *Nature*, *404*(6776), 394–8. http://doi.org/10.1038/35006074

Feng, Y., He, D., Yao, Z., & Klionsky, D. J. (2014). The machinery of macroautophagy. *Cell Research*, *24*(1), 24–41. http://doi.org/10.1038/cr.2013.168

Feng, Y., Yao, Z., & Klionsky, D. J. (2015). How to control self-digestion: transcriptional, post-transcriptional, and post-translational regulation of autophagy. *Trends in Cell Biology*, *25*(6), 354–363. http://doi.org/10.1016/j.tcb.2015.02.002

Finkel, T., & Holbrook, N. J. (2000). Oxidants, oxidative stress and the biology of ageing. *Nature*, *408*(6809), 239–247. http://doi.org/10.1038/35041687

Friggi-Grelin, F., Coulom, H., Meller, M., Gomez, D., Hirsh, J., & Birman, S. (2003). Targeted gene expression in Drosophila dopaminergic cells using regulatory sequences from tyrosine hydroxylase. *Journal of Neurobiology*, *54*(4), 618–27. http://doi.org/10.1002/neu.10185

Gabbita, S. P., Aksenov, M. Y., Lovell, M. A., & Markesbery, W. R. (2002). Decrease in Peptide Methionine Sulfoxide Reductase in Alzheimer's Disease Brain. *Journal of Neurochemistry*, *73*(4), 1660–1666. http://doi.org/10.1046/j.1471-4159.1999.0731660.x

Gao, Y., Chu, S.-F., Li, J.-P., Zuo, W., Wen, Z.-L., He, W.-B., … Chen, N.-H. (2015). Do glial cells play an anti-oxidative role in Huntington's disease? *Free Radical Research*. Retrieved from http://www.tandfonline.com/doi/abs/10.3109/10715762.2014.936432#.VbfsQ7cSPJY

Geng, J., & Klionsky, D. J. (2008). The Atg8 and Atg12 ubiquitin-like conjugation systems in macroautophagy. "Protein modifications: beyond the usual suspects" review series. *EMBO Reports*, *9*(9), 859–64. http://doi.org/10.1038/embor.2008.163

Harman, D. (1956). Aging: A Theory Based on Free Radical and Radiation Chemistry. *Journal of Gerontology*, *11*(3), 298–300. http://doi.org/10.1093/geronj/11.3.298

Harman, D. (1992). Free radical theory of aging. *Mutation Research/DNAging*, *275*(3-6), 257–266. http://doi.org/10.1016/0921-8734(92)90030-S

Harman, D. (2002). Aging: A Theory Based on Free Radical and Radiation Chemistry. *Sci. Aging Knowl. Environ.*, *2002*(37), cp14–. Retrieved from http://sageke.sciencemag.org/cgi/content/abstract/2002/37/cp14

Hensley, K., Maidt, M. L., Yu, Z., Sang, H., Markesbery, W. R., & Floyd, R. A. (1998). Electrochemical Analysis of Protein Nitrotyrosine and Dityrosine in the Alzheimer Brain Indicates Region-Specific Accumulation. *J. Neurosci.*, *18*(20), 8126–8132. Retrieved from http://www.jneurosci.org/content/18/20/8126.short

Hirsch, E. C., Breidert, T., Rousselet, E., Hunot, S., Hartmann, A., & Michel, P. P. (2006). The Role of Glial Reaction and Inflammation in Parkinson's Disease. *Annals of the New York Academy of Sciences*, *991*(1), 214–228. http://doi.org/10.1111/j.1749-6632.2003.tb07478.x

Hirth, F. (2010). Drosophila melanogaster in the study of human neurodegeneration. *CNS & Neurological Disorders Drug Targets*, *9*(4), 504–23. Retrieved from http://www.pubmedcentral.nih.gov/articlerender.fcgi?artid=2992341&tool=pmcentrez&rendertype=abstract

Iftekhkaruddin, N. (2014). *Up-regulation of antioxidants in the glia protects Drosoplila from oxidative stress*. McMaster University.

Jain, A., Lamark, T., Sjøttem, E., Larsen, K. B., Awuh, J. A., Øvervatn, A., … Johansen, T. (2010). p62/SQSTM1 is a target gene for transcription factor NRF2 and creates a positive feedback loop by inducing antioxidant response element-driven gene transcription. *The Journal of Biological Chemistry*, *285*(29), 22576–91. http://doi.org/10.1074/jbc.M110.118976

Jaiswal, M., Sandoval, H., Zhang, K., Bayat, V., & Bellen, H. J. J. (2012). Probing mechanisms that underlie human neurodegenerative diseases in Drosophila. *Annual Review of Genetics*, *46*, 371–96. http://doi.org/10.1146/annurev-genet-110711-155456

Jones, P. L., Kucera, G., Gordon, H., & Boss, J. M. (1995). Cloning and characterization of the murine manganous superoxide dismutase-encoding gene. *Gene*, *153*(2), 155–161. http://doi.org/10.1016/0378-1119(94)00666-G

Kiffin, R., Bandyopadhyay, U., & Cuervo, A. M. (2006). Oxidative Stress and Autophagy. Retrieved from http://online.liebertpub.com/doi/abs/10.1089/ars.2006.8.152

Klivenyi, P., St. Clair, D., Wermer, M., Yen, H.-C., Oberley, T., Yang, L., & Beal, M. F. (1998). Manganese Superoxide Dismutase Overexpression Attenuates MPTP

Toxicity. *Neurobiology of Disease*, *5*(4), 253–258. http://doi.org/10.1006/nbdi.1998.0191

Kohen, R., & Nyska, A. (2002). Oxidation of Biological Systems: Oxidative Stress Phenomena, Antioxidants, Redox Reactions, and Methods for Their Quantification. *Toxicologic Pathology*, *30*(6), 620–650. http://doi.org/10.1080/01926230290166724

Komatsu, M., Kurokawa, H., Waguri, S., Taguchi, K., Kobayashi, A., Ichimura, Y., … Yamamoto, M. (2010). The selective autophagy substrate p62 activates the stress responsive transcription factor Nrf2 through inactivation of Keap1. *Nature Cell Biology*, *12*(3), 213–23. http://doi.org/10.1038/ncb2021

Komatsu, M., Waguri, S., Chiba, T., Murata, S., Iwata, J., Tanida, I., … Tanaka, K. (2006). Loss of autophagy in the central nervous system causes neurodegeneration in mice. *Nature*, *441*(7095), 880–4. http://doi.org/10.1038/nature04723

Lau, A., Wang, X.-J., Zhao, F., Villeneuve, N. F., Wu, T., Jiang, T., … Zhang, D. D. (2010). A noncanonical mechanism of Nrf2 activation by autophagy deficiency: direct interaction between Keap1 and p62. *Molecular and Cellular Biology*, *30*(13), 3275–85. http://doi.org/10.1128/MCB.00248-10

Lin, M. T., & Beal, M. F. (2006). Mitochondrial dysfunction and oxidative stress in neurodegenerative diseases. *Nature*, *443*(7113), 787–95. http://doi.org/10.1038/nature05292

Ma, Q. (2013, January). Role of Nrf2 in Oxidative Stress and Toxicity. Retrieved from http://www.annualreviews.org/doi/abs/10.1146/annurev-pharmtox-011112-140320

Magwere, T., West, M., Riyahi, K., Murphy, M. P., Smith, R. A. J., & Partridge, L. (2006). The effects of exogenous antioxidants on lifespan and oxidative stress resistance in Drosophila melanogaster. *Mechanisms of Ageing and Development*, *127*(4), 356–70. http://doi.org/10.1016/j.mad.2005.12.009

Maiuri, M. C., Zalckvar, E., Kimchi, A., & Kroemer, G. (2007). Self-eating and self-killing: crosstalk between autophagy and apoptosis. *Nature Reviews. Molecular Cell Biology*, *8*(9), 741–52. http://doi.org/10.1038/nrm2239

Maragakis, N. J., & Rothstein, J. D. (2006). Mechanisms of Disease: astrocytes in neurodegenerative disease. *Nature Clinical Practice. Neurology*, *2*(12), 679–89. http://doi.org/10.1038/ncpneuro0355

Mariño, G., Madeo, F., & Kroemer, G. (2011). Autophagy for tissue homeostasis and neuroprotection. *Current Opinion in Cell Biology*, *23*(2), 198–206. http://doi.org/10.1016/j.ceb.2010.10.001

Martindale, J. L., & Holbrook, N. J. (2002). Cellular response to oxidative stress: Signaling for suicide and survival. *Journal of Cellular Physiology*, *192*(1), 1–15. http://doi.org/10.1002/jcp.10119

Martinez-Vicente, M., & Cuervo, A. M. (2007). Autophagy and neurodegeneration: when

the cleaning crew goes on strike. *Lancet Neurology*, *6*(4), 352–61. http://doi.org/10.1016/S1474-4422(07)70076-5

Mates, J. M., Pérez-Gómez, C., & De Castro, I. N. (1999). Antioxidant enzymes and human diseases. *Clinical Biochemistry*, *32*(8), 595–603. http://doi.org/10.1016/S0009-9120(99)00075-2

McCormack, A. L., Thiruchelvam, M., Manning-Bog, A. B., Thiffault, C., Langston, J. W., Cory-Slechta, D. A., & Di Monte, D. A. (2002). Environmental Risk Factors and Parkinson's Disease: Selective Degeneration of Nigral Dopaminergic Neurons Caused by the Herbicide Paraquat. *Neurobiology of Disease*, *10*(2), 119–127. http://doi.org/10.1006/nbdi.2002.0507

Mittler, R. (2002). Oxidative stress, antioxidants and stress tolerance. *Trends in Plant Science*, *7*(9), 405–410. http://doi.org/10.1016/S1360-1385(02)02312-9

Miwa, S., & Brand, M. D. (2003). Mitochondrial matrix reactive oxygen species production is very sensitive to mild uncoupling. *Biochemical Society Transactions*, *31*(Pt 6), 1300–1301. http://doi.org/10.1042/

Mizushima, N. (2007). Autophagy: process and function. *Genes & Development*, *21*(22), 2861–2873. http://doi.org/10.1101/gad.1599207

Mizushima, N. (2010). The role of the Atg1/ULK1 complex in autophagy regulation. *Current Opinion in Cell Biology*, *22*(2), 132–9. http://doi.org/10.1016/j.ceb.2009.12.004

Mizushima, N., Levine, B., Cuervo, A. M., & Klionsky, D. J. (2008). Autophagy fights disease through cellular self-digestion. *Nature*, *451*(7182), 1069–1075. http://doi.org/10.1038/nature06639

Mizushima, N., Yoshimori, T., & Ohsumi, Y. (2011). The role of Atg proteins in autophagosome formation. *Annual Review of Cell and Developmental Biology*, *27*, 107–32. http://doi.org/10.1146/annurev-cellbio-092910-154005

Nair, U., Cao, Y., Xie, Z., & Klionsky, D. J. (2010). Roles of the lipid-binding motifs of Atg18 and Atg21 in the cytoplasm to vacuole targeting pathway and autophagy. *The Journal of Biological Chemistry*, *285*(15), 11476–88. http://doi.org/10.1074/jbc.M109.080374

Nezis, I. P., Simonsen, A., Sagona, A. P., Finley, K., Gaumer, S., Contamine, D., … Brech, A. (2008). Ref(2)P, the Drosophila melanogaster homologue of mammalian p62, is required for the formation of protein aggregates in adult brain. *The Journal of Cell Biology*, *180*(6), 1065–71. http://doi.org/10.1083/jcb.200711108

Nguyen, T., Nioi, P., & Pickett, C. B. (2009). The Nrf2-Antioxidant Response Element Signaling Pathway and Its Activation by Oxidative Stress. *Journal of Biological Chemistry*, *284*(20), 13291–13295. http://doi.org/10.1074/jbc.R900010200

Nguyen, T., Sherratt, P. J., & Pickett, C. B. (2003). Regulatory mechanisms controlling

gene expression mediated by the antioxidant response element. *Annual Review of Pharmacology and Toxicology*, *43*(1), 233–60. http://doi.org/10.1146/annurev.pharmtox.43.100901.140229

Nisticò, R., Mehdawy, B., Piccirilli, S., & Mercuri, N. (2011). Paraquat-and Rotenone-Induced Models of Parkinson's Disease. *International Journal of Immunopathology and Pharmacology*, *24*(2), 313–322. http://doi.org/10.1177/039463201102400205

Nivon, M., Richet, E., Codogno, P., Arrigo, A.-P., & Kretz-Remy, C. (2014). Autophagy activation by NFκB is essential for cell survival after heat shock. *Autophagy*, *5*(6), 766–783. http://doi.org/10.4161/auto.8788

Obara, K., Sekito, T., Niimi, K., & Ohsumi, Y. (2008). The Atg18-Atg2 complex is recruited to autophagic membranes via phosphatidylinositol 3-phosphate and exerts an essential function. *The Journal of Biological Chemistry*, *283*(35), 23972–80. http://doi.org/10.1074/jbc.M803180200

Orr, W. C., & Sohal, R. S. (1992). The effects of catalase gene overexpression on life span and resistance to oxidative stress in transgenic Drosophila melanogaster. *Archives of Biochemistry and Biophysics*, *297*(1), 35–41. http://doi.org/10.1016/0003-9861(92)90637-C

Orr, W. C., & Sohal, R. S. (1993). Effects of Cu-Zn Superoxide Dismutase Overexpression on Life Span and Resistance to Oxidative Stress in Transgenic Drosophila melanogaster. *Archives of Biochemistry and Biophysics*, *301*(1), 34–40. http://doi.org/10.1006/abbi.1993.1111

Orr, W. C., & Sohal, R. S. (1994). Extension of life-span by overexpression of superoxide dismutase and catalase in Drosophila melanogaster. *Science*, *263*(5150), 1128–1130. http://doi.org/10.1126/science.8108730

Pankiv, S., Clausen, T. H., Lamark, T., Brech, A., Bruun, J.-A., Outzen, H., … Johansen, T. (2007). p62/SQSTM1 binds directly to Atg8/LC3 to facilitate degradation of ubiquitinated protein aggregates by autophagy. *The Journal of Biological Chemistry*, *282*(33), 24131–45. http://doi.org/10.1074/jbc.M702824200

Papadeas, S. T., Kraig, S. E., O'Banion, C., Lepore, A. C., & Maragakis, N. J. (2011). Astrocytes carrying the superoxide dismutase 1 (SOD1G93A) mutation induce wild-type motor neuron degeneration in vivo. *Proceedings of the National Academy of Sciences of the United States of America*, *108*(43), 17803–8. http://doi.org/10.1073/pnas.1103141108

Pappolla, M. A., Omar, R. A., Kim, K. S., & Robakis, N. K. (1992). Immunohistochemical evidence of oxidative [corrected] stress in Alzheimer's disease. *The American Journal of Pathology*, *140*(3), 621–8. Retrieved from http://www.pubmedcentral.nih.gov/articlerender.fcgi?artid=1886174&tool=pmcentrez&rendertype=abstract

Perry, T. L., Godin, D. V., & Hansen, S. (1982). Parkinson's disease: A disorder due to

nigral glutathione deficiency? *Neuroscience Letters*, *33*(3), 305–310. http://doi.org/10.1016/0304-3940(82)90390-1

Pietrocola, F., Izzo, V., Niso-Santano, M., Vacchelli, E., Galluzzi, L., Maiuri, M. C., & Kroemer, G. (2013). Regulation of autophagy by stress-responsive transcription factors. *Seminars in Cancer Biology*, *23*(5), 310–22. http://doi.org/10.1016/j.semcancer.2013.05.008

Poels, J., Spasić, M. R., Gistelinck, M., Mutert, J., Schellens, A., Callaerts, P., & Norga, K. K. (2012). Autophagy and phagocytosis-like cell cannibalism exert opposing effects on cellular survival during metabolic stress. *Cell Death and Differentiation*, *19*(10), 1590–601. http://doi.org/10.1038/cdd.2012.37

Polson, H. E. J., de Lartigue, J., Rigden, D. J., Reedijk, M., Urbé, S., Clague, M. J., & Tooze, S. A. (2010). Mammalian Atg18 (WIPI2) localizes to omegasome-anchored phagophores and positively regulates LC3 lipidation. *Autophagy*, *6*(4), 506–22. http://doi.org/10.4161/auto.6.4.11863

Rajasekaran, N. S., Connell, P., Christians, E. S., Yan, L.-J., Taylor, R. P., Orosz, A., … Benjamin, I. J. (2007). Human alpha B-crystallin mutation causes oxido-reductive stress and protein aggregation cardiomyopathy in mice. *Cell*, *130*(3), 427–39. http://doi.org/10.1016/j.cell.2007.06.044

Ravikumar, B. (2002). Aggregate-prone proteins with polyglutamine and polyalanine expansions are degraded by autophagy. *Human Molecular Genetics*, *11*(9), 1107–1117. http://doi.org/10.1093/hmg/11.9.1107

Riley, B. E., Kaiser, S. E., Shaler, T. A., Ng, A. C. Y., Hara, T., Hipp, M. S., … Kopito, R. R. (2010). Ubiquitin accumulation in autophagy-deficient mice is dependent on the Nrf2-mediated stress response pathway: a potential role for protein aggregation in autophagic substrate selection. *The Journal of Cell Biology*, *191*(3), 537–52. http://doi.org/10.1083/jcb.201005012

Rojo, A. I. (2010). Nrf2 regulates microglial dynamics and neuroinflammation in experimental Parkinson's disease. *Glia*, *58*(5), 588–598. Retrieved from http://resolver.scholarsportal.info/resolve/08941491/v58i0005/588_nrmdaniepd.xml

Runchel, C., Matsuzawa, A., & Ichijo, H. (2011). Mitogen-activated protein kinases in mammalian oxidative stress responses. *Antioxidants & Redox Signaling*, *15*(1), 205–18. http://doi.org/10.1089/ars.2010.3733

Scherz-Shouval, R., & Elazar, Z. (2007). ROS, mitochondria and the regulation of autophagy. *Trends in Cell Biology*, *17*(9), 422–7. http://doi.org/10.1016/j.tcb.2007.07.009

Scherz-Shouval, R., & Elazar, Z. (2011). Regulation of autophagy by ROS: physiology and pathology. *Trends in Biochemical Sciences*, *36*(1), 30–8. http://doi.org/10.1016/j.tibs.2010.07.007

Scherz-Shouval, R., Shvets, E., Fass, E., Shorer, H., Gil, L., & Elazar, Z. (2007). Reactive oxygen species are essential for autophagy and specifically regulate the activity of Atg4. *The EMBO Journal*, *26*(7), 1749–60. http://doi.org/10.1038/sj.emboj.7601623

Seet, R. C. S., Lee, C.-Y. J., Lim, E. C. H., Tan, J. J. H., Quek, A. M. L., Chong, W.-L., … Chan, Y.-H. (2010). Oxidative damage in Parkinson disease: Measurement using accurate biomarkers. *Free Radical Biology and Medicine*, *48*(4), 560–566. http://doi.org/10.1016/j.freeradbiomed.2009.11.026

Shih, A. Y., Imbeault, S., Barakauskas, V., Erb, H., Jiang, L., Li, P., & Murphy, T. H. (2005). Induction of the Nrf2-driven antioxidant response confers neuroprotection during mitochondrial stress in vivo. *The Journal of Biological Chemistry*, *280*(24), 22925–36. http://doi.org/10.1074/jbc.M414635200

Shih, A. Y., Johnson, D. A., Wong, G., Kraft, A. D., Jiang, L., Erb, H., … Murphy, T. H. (2003). Coordinate Regulation of Glutathione Biosynthesis and Release by Nrf2-Expressing Glia Potently Protects Neurons from Oxidative Stress. *J. Neurosci.*, *23*(8), 3394–3406. Retrieved from http://www.jneurosci.org/content/23/8/3394.short

Shimizu, K., Ohtaki, K., Matsubara, K., Aoyama, K., Uezono, T., Saito, O., … Shiono, H. (2001). Carrier-mediated processes in blood–brain barrier penetration and neural uptake of paraquat. *Brain Research*, *906*(1-2), 135–142. http://doi.org/10.1016/S0006-8993(01)02577-X

Simonian, N. A., & Coyle, J. T. (1996). Oxidative stress in neurodegenerative diseases. *Annual Review of Pharmacology and Toxicology*, *36*, 83–106. http://doi.org/10.1146/annurev.pa.36.040196.000503

Simonsen, A., Cumming, R. C., Brech, A., Isakson, P., Schubert, D. R., & Finley, K. D. (2008). Promoting basal levels of autophagy in the nervous system enhances longevity and oxidant resistance in adult Drosophila. *Autophagy*, *4*(2), 176–184. Retrieved from http://www.landesbioscience.com/journals/auto/abstract.php?id=5269

Singh, S., Vrishni, S., Singh, B. K., Rahman, I., & Kakkar, P. (2010). Nrf2-ARE stress response mechanism: A control point in oxidative stress-mediated dysfunctions and chronic inflammatory diseases. *Free Radical Research*, *44*(11), 1267–1288. http://doi.org/10.3109/10715762.2010.507670

Smith, L. L., Rose, M. S., & Wyatt, I. (1978). The pathology and biochemistry of paraquat. *Ciba Foundation Symposium*, (65), 321–41. Retrieved from http://www.ncbi.nlm.nih.gov/pubmed/38952

Sohal, R. S., Arnold, L., & Orr, W. C. (1990). Effect of age on superoxide dismutase, catalase, glutathione reductase, inorganic peroxides, TBA-reactive material, GSH/GSSG, NADPH/NADP+ and NADH/NAD+ in Drosophila melanogaster. *Mechanisms of Ageing and Development*, *56*(3), 223–235.

http://doi.org/10.1016/0047-6374(90)90084-S

Stork, T., Bernardos, R., & Freeman, M. R. (2012). Analysis of Glial Cell Development and Function in Drosophila. *Cold Spring Harbor Protocols*, *2012*(1), pdb.top067587. http://doi.org/10.1101/pdb.top067587

Sykiotis, G. P., & Bohmann, D. (2008). Keap1/Nrf2 Signaling Regulates Oxidative Stress Tolerance and Lifespan in Drosophila. *Developmental Cell*, *14*(1), 76–85. http://doi.org/10.1016/j.devcel.2007.12.002

Tamura, N., Oku, M., Ito, M., Noda, N. N., Inagaki, F., & Sakai, Y. (2013). Atg18 phosphoregulation controls organellar dynamics by modulating its phosphoinositide-binding activity. *The Journal of Cell Biology*, *202*(4), 685–98. http://doi.org/10.1083/jcb.201302067

Tang, H.-W., Liao, H.-M., Peng, W.-H., Lin, H.-R., Chen, C.-H., & Chen, G.-C. (2013). Atg9 interacts with dTRAF2/TRAF6 to regulate oxidative stress-induced JNK activation and autophagy induction. *Developmental Cell*, *27*(5), 489–503. http://doi.org/10.1016/j.devcel.2013.10.017

Tanner, C. M., Kamel, F., Ross, G. W., Hoppin, J. A., Goldman, S. M., Korell, M., … Langston, J. W. (2011). Rotenone, paraquat, and Parkinson's disease. *Environmental Health Perspectives*, *119*(6), 866–72. http://doi.org/10.1289/ehp.1002839

Terman, A., & Brunk, U. T. (2004). Lipofuscin. *The International Journal of Biochemistry & Cell Biology*, *36*(8), 1400–4. http://doi.org/10.1016/j.biocel.2003.08.009

Terman, A., Dalen, H., & Brunk, U. T. (1999). Ceroid/lipofuscin-loaded human fibroblasts show decreased survival time and diminished autophagocytosis during amino acid starvation☆. *Experimental Gerontology*, *34*(8), 943–957. http://doi.org/10.1016/S0531-5565(99)00070-4

Tompkins, M. M., Basgall, E. J., Zamrini, E., & Hill, W. D. (1997). Apoptotic-like changes in Lewy-body-associated disorders and normal aging in substantia nigral neurons. *The American Journal of Pathology*, *150*(1), 119–31. Retrieved from http://www.pubmedcentral.nih.gov/articlerender.fcgi?artid=1858540&tool=pmcentrez&rendertype=abstract

Turrens, J. F. (1997). Superoxide Production by the Mitochondrial Respiratory Chain. *Bioscience Reports*, *17*(1), 3–8. http://doi.org/10.1023/A:1027374931887

Turrens, J. F. (2003). Mitochondrial formation of reactive oxygen species. *The Journal of Physiology*, *552*(Pt 2), 335–44. http://doi.org/10.1113/jphysiol.2003.049478

Valori, C., Brambilla, L., & Rossi, D. (2014). *Pathological Potential of Neuroglia*. (V. Parpura & A. Verkhratsky, Eds.). New York, NY: Springer New York. http://doi.org/10.1007/978-1-4939-0974-2

Vanduyn, N., Settivari, R., Wong, G., & Nass, R. (2010). SKN-1/Nrf2 inhibits dopamine

neuron degeneration in a Caenorhabditis elegans model of methylmercury toxicity. *Toxicological Sciences : An Official Journal of the Society of Toxicology*, *118*(2), 613–24. http://doi.org/10.1093/toxsci/kfq285

Vargas, M. R., Johnson, D. A., Sirkis, D. W., Messing, A., & Johnson, J. A. (2008). Nrf2 activation in astrocytes protects against neurodegeneration in mouse models of familial amyotrophic lateral sclerosis. *The Journal of Neuroscience : The Official Journal of the Society for Neuroscience*, *28*(50), 13574–81. http://doi.org/10.1523/JNEUROSCI.4099-08.2008

Vellai, T. (2009). Autophagy genes and ageing. *Cell Death and Differentiation*, *16*(1), 94–102. http://doi.org/10.1038/cdd.2008.126

Wang, B., Liu, Q., Shan, H., Xia, C., & Liu, Z. (2015). Nrf2 inducer and cncC overexpression attenuates neurodegeneration due to α-synuclein in Drosophila. *Biochemistry and Cell Biology = Biochimie et Biologie Cellulaire*, *93*(4), 351–8. http://doi.org/10.1139/bcb-2015-0015

Wang, X., Martindale, J., Liu, Y., & Holbrook, N. (1998, July). The cellular response to oxidative stress: influences of mitogen-activated protein kinase signalling pathways on cell survival. Retrieved from http://www.biochemj.org/bj/333/bj3330291.htm

Webb, J. L., Ravikumar, B., Atkins, J., Skepper, J. N., & Rubinsztein, D. C. (2003). Alpha-Synuclein is degraded by both autophagy and the proteasome. *The Journal of Biological Chemistry*, *278*(27), 25009–13. http://doi.org/10.1074/jbc.M300227200

White, K. E., Humphrey, D. M., & Hirth, F. (2010). The dopaminergic system in the aging brain of Drosophila. *Frontiers in Neuroscience*, *4*, 205. http://doi.org/10.3389/fnins.2010.00205

Whitworth, A. J., Theodore, D. A., Greene, J. C., Benes, H., Wes, P. D., & Pallanck, L. J. (2005). Increased glutathione S-transferase activity rescues dopaminergic neuron loss in a Drosophila model of Parkinson's disease. *Proceedings of the National Academy of Sciences of the United States of America*, *102*(22), 8024–9. http://doi.org/10.1073/pnas.0501078102

Whitworth, A. J., Wes, P. D., & Pallanck, L. J. (2006). Drosophila models pioneer a new approach to drug discovery for Parkinson's disease. *Drug Discovery Today*, *11*(3-4), 119–26. http://doi.org/10.1016/S1359-6446(05)03693-7

Williamson, T. P., Johnson, D. A., & Johnson, J. A. (2012). Activation of the Nrf2-ARE pathway by siRNA knockdown of Keap1 reduces oxidative stress and provides partial protection from MPTP-mediated neurotoxicity. *NeuroToxicology*, *33*(3), 272–279. http://doi.org/10.1016/j.neuro.2012.01.015

Winslow, A. R., & Rubinsztein, D. C. (2008). Autophagy in neurodegeneration and development. *Biochimica et Biophysica Acta*, *1782*(12), 723–729. http://doi.org/10.1016/j.bbadis.2008.06.010

Wu, H., Wang, M. C., & Bohmann, D. (2009). JNK protects Drosophila from oxidative stress by trancriptionally activating autophagy. *Mechanisms of Development*, *126*(8-9), 624–37. http://doi.org/10.1016/j.mod.2009.06.1082

Xie, Z., Nair, U., & Klionsky, D. J. (2008). Atg8 controls phagophore expansion during autophagosome formation. *Molecular Biology of the Cell*, *19*(8), 3290–8. http://doi.org/10.1091/mbc.E07-12-1292

Yamanaka, K., Chun, S. J., Boillee, S., Fujimori-Tonou, N., Yamashita, H., Gutmann, D. H., … Cleveland, D. W. (2008). Astrocytes as determinants of disease progression in inherited amyotrophic lateral sclerosis. *Nature Neuroscience*, *11*(3), 251–3. http://doi.org/10.1038/nn2047

Zemlan, F. P., Thienhaus, O. J., & Bosmann, H. B. (1989). Superoxide dismutase activity in Alzheimer's disease: possible mechanism for paired helical filament formation. *Brain Research*, *476*(1), 160–162. http://doi.org/10.1016/0006-8993(89)91550-3

Zhang, D. D. (2006). Mechanistic studies of the Nrf2-Keap1 signaling pathway. *Drug Metabolism Reviews*, *38*(4), 769–89. http://doi.org/10.1080/03602530600971974

Zhang, J., Graham, D., Montine, T., & Ho, Y.-S. (2000). Enhanced N-Methyl-4-Phenyl-1,2,3,6-Tetrahydropyridine Toxicity in Mice Deficient in CuZn-Superoxide Dismutase or Glutathione Peroxidase. *Journal of Neuropathology & Experimental Neurology*, *59*(1), 53–61. Retrieved from http://gateway.tx.ovid.com.libaccess.lib.mcmaster.ca/sp-3.17.0a/ovidweb.cgi?QS2=434f4e1a73d37e8cbd1f8b492ba53676aadeb5685a2b4152716a134dfde1d14a1a4c5e2ce5cecdd4b10dbddbce8f2c0fe11a46e6709ccd766a86f2fb95879621685af469f9baf34f0ade2ed6c08c8d234b687c01f1e9b29

Zou, S., Meadows, S., Sharp, L., Jan, L. Y., & Jan, Y. N. (2000). Genome-wide study of aging and oxidative stress response in Drosophila melanogaster. *Proceedings of the National Academy of Sciences of the United States of America*, *97*(25), 13726–31. http://doi.org/10.1073/pnas.260496697

6 Appendix 1: Data from pilot experiments

6.1 Pilot experiments on parental genotypes in order to determine the optimal concentration of paraquat.

In the initial steps of this project, pilot experiments were performed on the parental genotypes in order to determine the optimal concentration of paraquat to be used for the rest of the experiments. Concentrations of 15 mM, 20 mM and 25 mM paraquat in 5% sucrose solution were used. The results from these experiments are outlined in Figures 6.1-6.6. A general trend for this data that can be concluded is that exposure to 20 mM paraquat or more in 5% solution seems to cause a significant decline in both survival and negative geotaxis performance, however there are some exceptions. It was determined that the experiments with Moody-Gal4 will be performed using 25 mM paraquat. Given that the NP2276-Gal4 and Repo-Gal4 parental genotypes were very sensitive to 25 mM paraquat, it was determined use 20 mM paraquat for the Repo-Gal4 experiments.

6.2 Pilot experiment to determine the effect of CO_2 anesthesia on the negative geotaxis assay

A pilot experiment was performed in order to determine the amount of time that flies require to fully recover after CO_2 anesthesia. This pilot experiment was performed on w^{1118} flies that have been exposed to either 0 min, 2 min or 5 min of CO_2 anesthesia. The flies were tested 10 min, 20 min, 30 min, 40 min, 50 min, 60 min, and 90 min after CO_2 exposure. This data is outlined in Figure 6.7. The data shows that the differences between different times after exposure are not significant for any of the times of exposure,

although a trend of increasing negative geotaxis performance is evident for flies exposed to 5 min of CO_2 anesthesia between 10 min after exposure and 60 min after exposure. There are significant differences between 0 min exposure and 2 min exposure, 0 min exposure and 5 min exposure as well as 2 min exposure and 5 min exposure for flies that were tested 10 min after exposure. A similar result is evident for flies tested after 50 and 60 min after exposure, where there is significant difference between 0 min of exposure and 2 min of exposure as well as 0 min of exposure and 5 min of exposure, but no significant difference is seen between 2 min and 5 min of exposure. An interesting result to note from this experiment is that the flies that were not exposed to any CO_2 anesthesia seem to have a lower negative geotaxis performance than flies that have been exposed to CO_2 anesthesia.

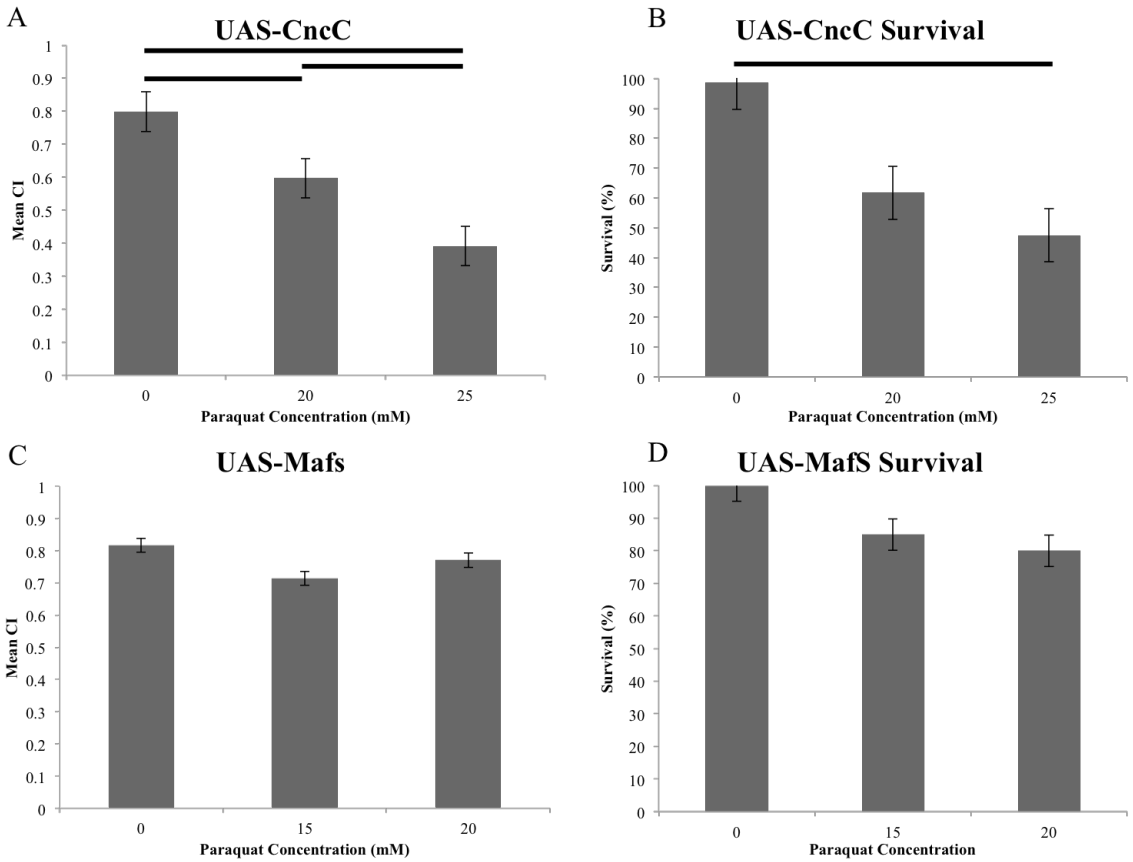

Figure 6.1 Pilot negative geotaxis and survival assay for parental genotypes UAS-CncC and UAS-MafS. 24h exposure to 15 mM 20 mM or 25 mM in 5% sucrose; negative geotaxis: (A, C) N=3 for all genotypes and treatments; survival: (B) UAS-CncC N=4 for all treatments; (D) UAS-MafS 0 mM N=2; 15 mM and 20 mM N=3. Statistics: (A) 0 mM vs. 20 mM p=0.004; 0 mM vs. 25 mM p=8.9 x 10^{-5}; 20 mM vs. 25 mM p=0.004; (B) 0 mM vs. 25 mM p=0.033.

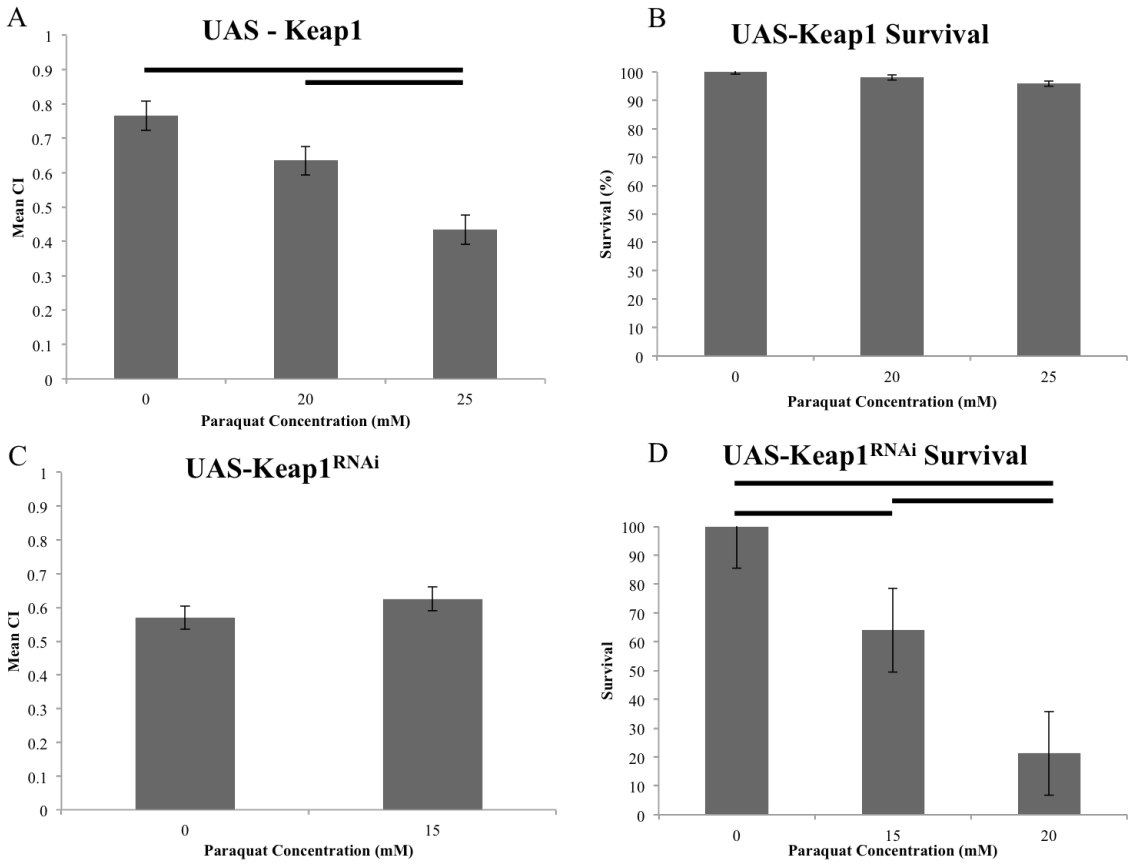

Figure 6.2: Pilot negative geotaxis and survival assay for parental genotypes UAS-Keap1 and UAS-Keap1^{RNAi}. 24h exposure to 15 mM 20 mM or 25 mM in 5% sucrose; negative geotaxis: (A) UAS-Keap1 N=6 for all treatments; (C) UAS-Keap1^{RNAi} N=2 for all treatments; survival: (B) UAS-Keap1 0 mM and 20 mM N=5; 25 mM N=6; (D) UAS-Keap1^{RNAi} N=2 for all treatments. Statistics: (A) 0 mM vs. 25 mM p=0.001; 20 mM vs. 25 mM p=0.028; (D) 0 mM vs. 15 mM p=0.011; 0 mM vs. 20 mM p=0.001; 15 mM vs. 20 mM p=0.007.

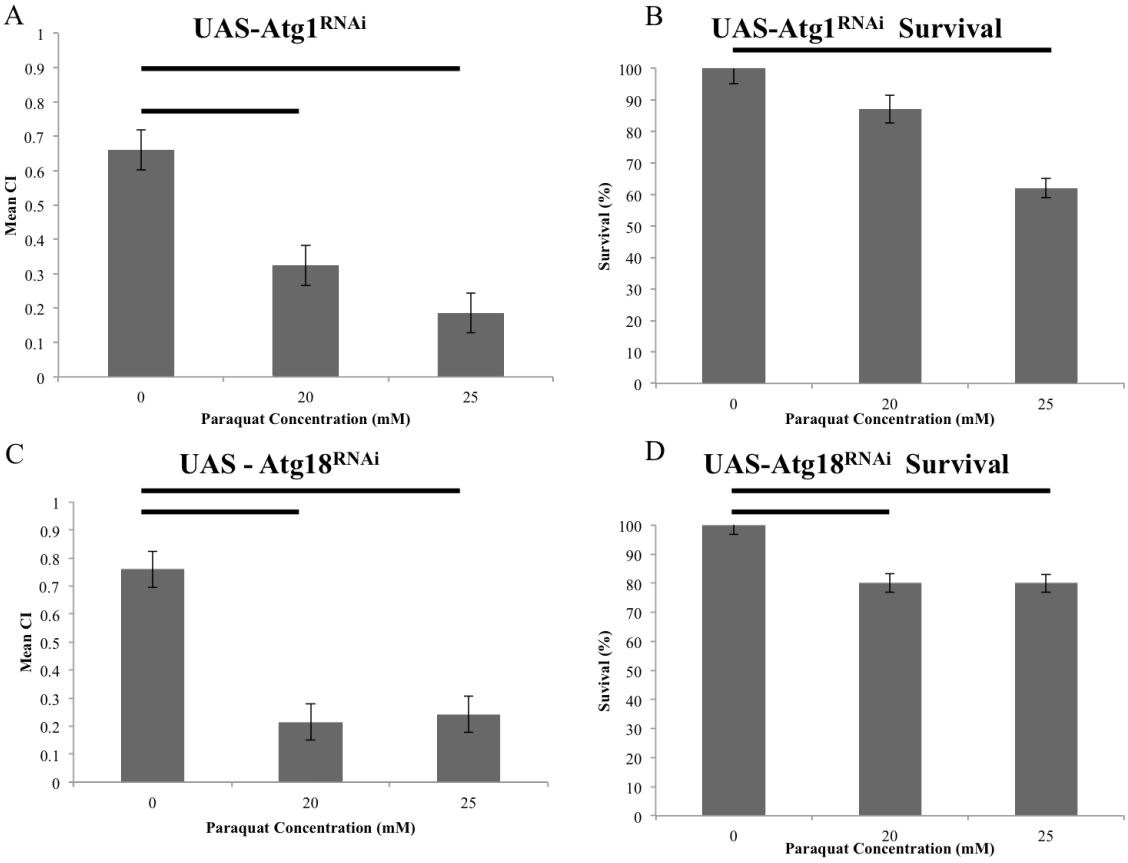

Figure 6.3: Pilot negative geotaxis and survival assay for parental genotypes UAS-Atg1^{RNAi} and UAS-Atg18^{RNAi}. 24h exposure to 15 mM 20 mM or 25 mM in 5% sucrose; negative geotaxis: (A, C) N=6 for all genotypes and treatments; survival: (B, D) N=5 for all genotypes and treatments. Statistics: (A) 0 mM vs. 20 mM p=0.003; 0 mM vs. 25 mM p=1.26 x 10^{-4}; (B) 0 mM vs. 25 mM p=0.015; (C) 0 mM vs. 20 mM p=2.0 x 10^{-7}; 0 mM vs. 25 mM p=4 x 10^{-7}; (D) 0 mM vs. 20 mM p=0.005; 0 mM vs. 25 mM p=0.005.

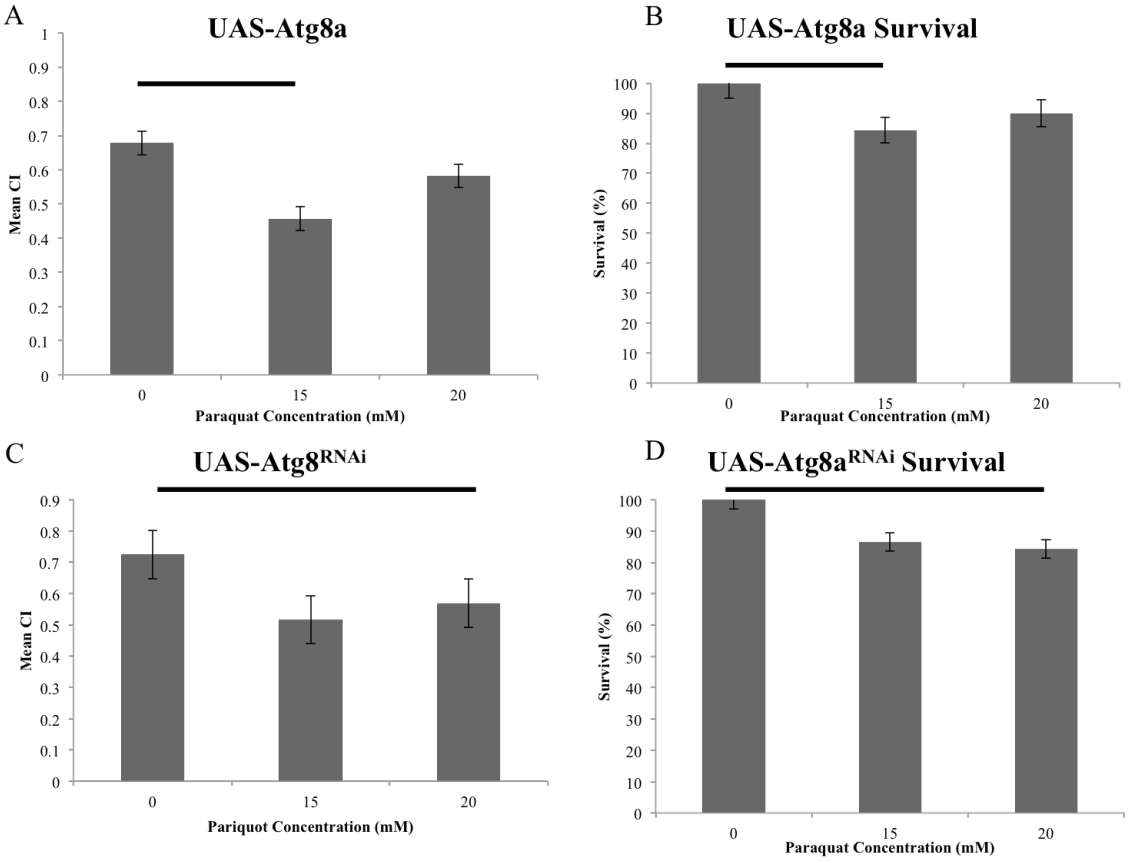

Figure 6.4: Pilot negative geotaxis and survival assay for parental genotypes UAS-Atg8a and UAS-Atg8a^{RNAi}. 24h exposure to 15 mM 20 mM or 25 mM in 5% sucrose; negative geotaxis: (A) UAS-Atg8a N=6 for all treatments; (C) UAS-Atg8a^{RNAi} 0 mM and 15 mM N=4; 20mM N=2; survival: (B) UAS-Atg8a 0 mM N=6 ; 15 mM and 20 mM N=7; (D) UAS-Atg8a^{RNAi} 0mM N=3; 15 mM and 20mM N=4. Statistics: (A) 0 mM vs. 15 mM p=0.017; (B) 0 mM vs. 15 mM p=0.042; (C) 0 mM vs. 20 mM p=0.013; (D) 0 mM vs. 20 mM p=0.043.

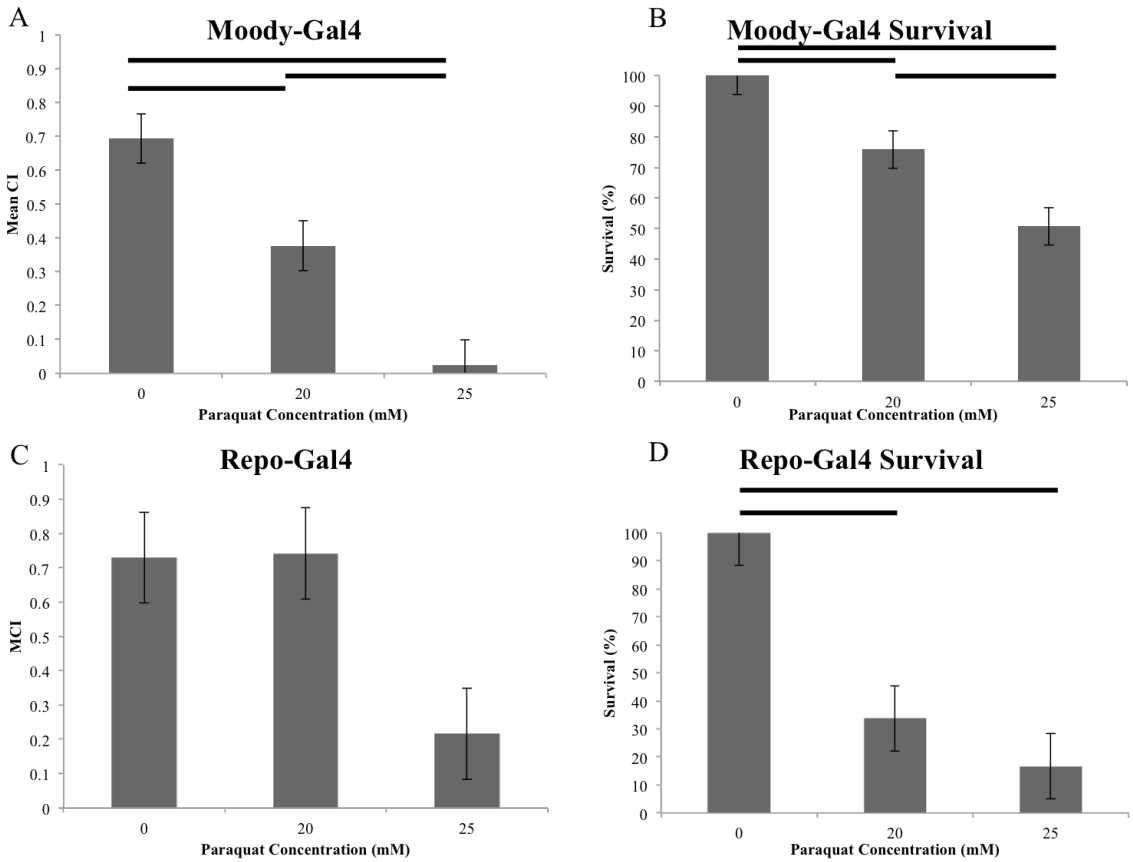

Figure 6.5: Pilot negative geotaxis and survival assay for parental genotypes Moody-Gal4 and Repo-Gal4. 24h exposure to 15 mM 20 mM or 25 mM in 5% sucrose; negative geotaxis: (A) Moody-Gal4 0 mM N=6; 20 mM N=5; 25 mM N=2; (C) Repo-Gal4 0 mM N=2; 20 mM and 25 mM N=1; survival: (B) Moody-Gal4 0 mM and 20 mM N=6; 25 mM N=7; (D) Repo-Gal4 0 mM N=3; 20 mM and 25 mM N=4. Statistics: (A) 0 mM vs. 20 mM p=0.001; 0 mM vs. 25 mM p=2.6 x 10^{-5}; 20 mM vs. 25 mM p=0.005 (B) 0 mM vs. 20 mM p=0.007; 0 mM vs. 25 mM p=3.0 x 10^{-4}; 20 mM vs. 25 mM p=0.047; (D) 0 mM vs. 20 mM p=0.002; 0 mM vs. 25 mM p=4.3 x 10^{-4}.

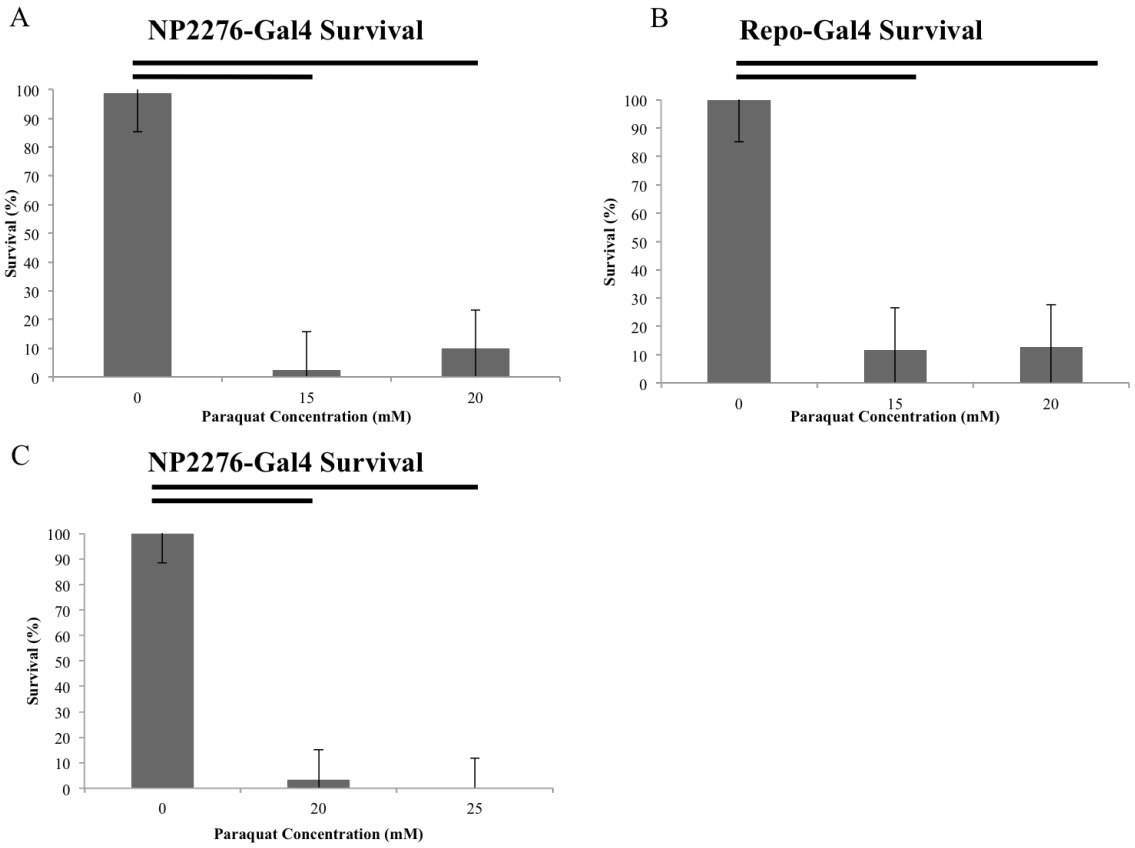

Figure 6.6: Pilot survival assay for parental genotypes NP2276-Gal4 and Repo-Gal4. 24h exposure to 15 mM 20 mM or 25 mM in 5% sucrose; survival: (A) NP2276-Gal4 N=4 for all treatments; (B) Repo-Gal4 0 mM N=2; 15 mM and 20 mM N=3; (C) NP2276-Gal4 0 mM and 20 mM N=3; 25 mM N=4. Statistics: (A) 0 mM vs. 15 mM $p=1.8 \times 10^{-7}$; 0 mM vs. 20 mM $p=3.5 \times 10^{-7}$; (B) 0 mM vs. 15 mM p=0.001; 0 mM vs. 20 mM p=0.001; (C) 0 mM vs. 20 mM $P=1.0 \times 10^{-7}$; 0 mM vs. 25 mM $p=1.0 \times 10^{-7}$.

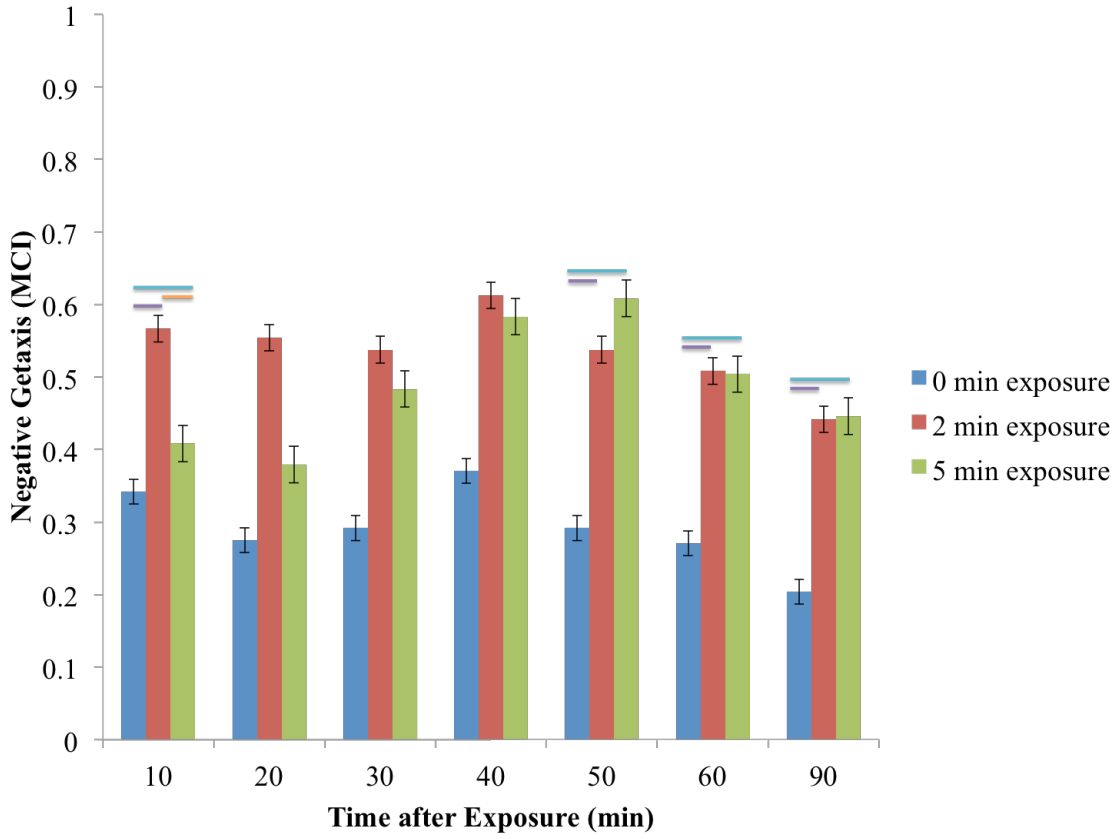

Figure 6.7: Negative geotaxis recovery time of w^{1118} flies after CO_2 anesthesia. w1118 flies were exposed to CO2 anesthesia for 0 min, 2 min and 5 min. The flies were tested via the negative geotaxis assay 10 min, 20 min, 30 min, 40 min, 50 min, 60 min and 90 min after exposure. N=2 per exposure per time after exposure. Statistics: 10 min after exposure: 0 min vs. 2 min p=0.001; 0 min vs. 5 min p=0.044; 2 min vs. 5 min p=0.004; 50 min after exposure: 0 min vs. 2 min p=0.003; 0 min vs. 5 min p=0.003; 60 min after exposure: 0 min vs. 2 min p=0.003; 0 min vs. 5 min p=0.003.

7 Appendix 2: Data from excluded experiments, incomplete experiments, and/or experiments performed using alternative methods

7.1 Data from excluded experiments using methods form section 2

7.1.1 What is the effect of down regulation of Autophagy in the SPG during acute oxidative stress on dopaminergic neurons?

In order to test whether the down regulation of autophagy in the SPG has an effect on the number of dopaminergic neurons in flies exposed to paraquat, I downregulated Atg1 and Atg18 in the SPG using the Moody-Gal4 driver. I performed immunostaining of the dopaminergic neurons using anti-TH antibody on the experimental genotypes Moody-Gal4>Atg1^{RNAi} and Moody-Gal4>Atg18^{RNAi}, as well as their corresponding parental controls. Down regulation of Atg1 in the SPG did not provide any protection of the dopaminergic neurons from paraquat exposure (Figure 3.10). The PPL2 cluster had a significantly reduced number of dopaminergic neurons in paraquat treated Moody-Gal4>Atg1^{RNAi} flies (Figure 3.10). This reduction in dopaminergic neuros in the PPL2 cluster was not observed in the parental controls (Figure 3.10). The Gal4 parental control had a significantly reduced number of dopaminergic neurons in the PPM1 cluster due to paraquat exposure, which was not observed in both experimental genotypes (Figures 3.10 and 3.11). Down regulation of Atg18 in the SPG provided protection to the number of dopaminergic neurons in the PPL1 cluster after paraquat exposure. The number of dopaminergic neurons in the PPL1 cluster in the treated experimental flies was significantly greater than the number of dopaminergic neurons in the PPL1 cluster in the treated UAS parental control (Figure 3.11).

Qualitative analysis of the dopaminergic neuron morphology indicated that differences in size and shape were not observed for all genotypes except for the UAS-Atg1^{RNAi} parental control. The exposed UAS-Atg1^{RNAi} flies had smaller dopaminergic neurons compared to the untreated flies (measurements not taken) (Figures 3.16-3.19). The dopaminergic neurons in the treated UAS-Atg1^{RNAi} flies also had more rounded morphology compared to the untreated flies (Figures 3.16-3.19).

These data suggest that down regulation of autophagy in the SPG provides some protection of dopaminergic neurons during oxidative stress.

7.1.2 Down regulation of autophagy in the SPG using the NP2276-Gal4 driver

The fly line UAS-Atg1^{RNAi} was chosen for cross with the NP2276-Gal4 driver in order to test the role of autophagy in SPG cells during acute oxidative stress. The male progeny from the crosses of these lines with NP2276-Gal4 were exposed to 5% sucrose and 25 mM paraquat in 5% sucrose for 24 h and then tested with the survival and negative geotaxis assays. The results from these experiments are outlined in Figure 7.1.

The data outlined in Figure 7.1 shows that there is a significant decline in negative geotaxis performance in the paraquat treated NP2276-Gal4;UAS-Atg1^{RNAi} flies as well as a significant decline in the negative geotaxis performance in the treated and untreated controls NP2276-Gal4/+ and UAS-Atg1^{RNAi}/+. The treated flies for all of the genotypes were not different from each other. For the survival data, a similar significant decline is observed for all three genotypes as well.

7.2 Data from incomplete experiments using methods from section 2

7.2.1 Down regulation and upregulation of autophagy using the UAS-Atg8a and UAS-Atg8aRNAi in all glia

The fly lines UAS-Atg8a and UAS-Atg8aRNAi were chosen for cross with the Repo-Gal4 driver in order to test the role of autophagy in glial cells during acute oxidative stress. The male progeny from the crosses of these lines with Repo-Gal4 were exposed to 5% sucrose and 20 mM paraquat in 5% sucrose and 25 mM paraquat in 5% sucrose for 24 h and then tested with the survival and negative geotaxis assays. The results from these experiments are outlined in Figures 7.2 and 7.3

The data outlined in Figure 7.2 shows that there is a significant decline in negative geotaxis performance in the paraquat treated UAS-Atg8a;Repo-Gal4 flies with both 20 mM and 25 mM paraquat. There is a significant decline in the negative geotaxis performance in the Repo-Gal4/+ treated with 20 mM paraquat, but this is not seen in the other parental control UAS-Atg8a/+ treated with 25 mM paraquat. For the survival data, significant decline is observed for all three genotypes treated with either both 20 and 25 mM paraquat. The UAS-Atg8a parental control has significantly better survival than the other two genotypes. The 25 mM paraquat treated UAS-Atg8a;Repo-Gal4 has significantly better survival than the 25mM paraquat treated Repo-Gal4/+.

The data outlined in Figure 7.3 shows that there is a significant decline in negative geotaxis performance in the paraquat treated Repo-Gal4/UAS-Atg8a^{RNAi} and UAS-Atg8a^{RNAi}/+ flies with 25 mM paraquat. There is a significant decline in the negative geotaxis performance in the Repo-Gal4/+ treated with 20 mM paraquat. The treated

UAS-Atg8a^{RNAi}/+ have significantly better negative geotaxis than the treated Repo-Gal4/UAS-Atg8a^{RNAi}. For the survival data, significant decline is observed for all three genotypes treated with either both 20 and 25 mM paraquat. The Repo-Gal4/+ decline in survival is significantly lower than the other two genotypes.

7.3 Data from experiments using alternative methods outlined in section 7.4

7.3.1 Upregulation or down regulation of different components of the NRF2 pathway in the SPG using the Moody-Gal4 driver

In order to test the NRF2/Keap1 pathway and its role in neuroprotection when it is activated the *Drosophila* SPG during oxidative stress, the fly lines UAS-CncC, UAS-Keap1, UAS-Keap1^{RNAi}, and UAS-MafS were chosen. These lines were crossed with the SPG driver Moody-Gal4 in order to overexpress the NRF2/Keap1 pathway genes CncC, Keap1 and MafS, or suppress the gene Keap1 via RNAi exclusively in the SPG. The male progeny of these crosses, as well as crosses producing parental control flies (the UAS and Gal4 stocks crossed with w^{1118}) were exposed to 5% sucrose solution, 15 mM paraquat in 5% sucrose solution and/or 20 mM paraquat in 5% sucrose solution for 24 hours and then tested using the survival and negative geotaxis assays. This data is outlined in Figures 7.4-7.7. It was hypothesized that direct and indirect (through repression of Keap1) upregulation of CncC as well as upregulation of MafS in the SPG will provide protection from oxidative stress caused by paraquat exposure. Therefore, it was predicted that the paraquat exposed progeny from the crosses Moody-Gal4 x UAS-CncC, Moody-Gal4 x UAS-Keap1^{RNAi} and Moody-Gal4 x UAS-MafS will show similar survival and negative geotaxis performance as the non-exposed experimental flies, while the exposed parental

crosses' progeny will show a significant decline in both survival and negative geotaxis performance compared to non-exposed parental cross progeny as well as both exposed and non-exposed experimental progeny. This expected result was not present in any of these experiments. In addition, it was hypothesized that down regulation of CncC in the glia via upregulation of Keap1 will significantly decrease the flies' tolerance to oxidative stress caused by paraquat. It was predicted that the exposed progeny of the Moody-Gal4 x UAS-Keap1 cross will show significantly worse survival and negative geotaxis performance compared to non-treated progeny from this cross. Also it was predicted that this decline will much more drastic than the decline between exposed and non-exposed parental crosses' progeny. Once again, this expected result was not observed. Some noteworthy results from this set of data include the very drastic decline in both survival and negative geotaxis performance of the exposed Moody-Gal4 x UAS-MafS progeny compared to the parental crosses' progeny. Similar, although not as drastic, was the decline in both survival and negative geotaxis performance of the exposed Moody-Gal4 x UAS-CncC progeny compared to the parental crosses' progeny. These results show an opposite effect than what was originally hypothesized. One possible reason for the unexpected results with CncC could be the potential toxicity of overexpression of this protein during development.

7.3.2 Upregulation or down regulation of different components of the Autophagy pathway in the SPG using the Moody-Gal4 driver

The fly lines UAS-Atg1^{RNAi}, UAS-Atg18 ^{RNAi}, UAS-Atg8a and UAS-Atg8a^{RNAi} were chosen for crosses with the Moody-Gal4 driver. The male progeny from the crosses of

these lines with Moody-Gal4 were exposed to 5% sucrose and 20 mM paraquat in 5% sucrose for 24 h and then tested with the survival and negative geotaxis assays. The results from these experiments are outlined in Figures 7.8-7.11. It was hypothesized that when Atg1, Atg18 and Atg8a genes are downregulated in the SPG, they will provide protection from oxidative stress when the flies are exposed to paraquat. Therefore, it was predicted that the paraquat exposed progeny of the Moody-Gal4 x UAS-Atg1^{RNAi}, Moody-Gal4 x UAS-Atg18^{RNAi} and Moody-Gal4 x UAS-Atg8a^{RNAi} crosses will have similar survival and negative geotaxis performance as non-treated progeny from the same crosses, while treated parental crosses progeny will have significantly worse survival and negative geotaxis performance than non-treated parental crosses progeny. On the contrary, it was hypothesized that the upregulation of the Atg8a gene, will cause a decline in the resistance to oxidative stress of the exposed flies and therefore it was predicted that paraquat exposed progeny of the Moody-Gal4 x UAS-Atg8a cross will show lower survival and negative geotaxis performance than non-treated progeny from the same cross as well as significantly lower survival and negative geotaxis performance than treated and non-treated parental crosses progeny. The data shows that only the Moody-Gal4 x UAS-Atg1^{RNAi} progeny show the predicted trend in survival and negative geotaxis performance. There is a significant difference between the treated experimental flies compared to the treated parental flies, meanwhile significant difference between the treated and non-treated experimental flies is not seen for both survival and negative geotaxis performance. Down regulation of the other autophagy genes in the SPG did not show the similar rescue observed in Moody-Gal4 x UAS-Atg1^{RNAi} progeny for both

survival and negative geotaxis performance when the flies are exposed to paraquat. Upregulation of Atg8a did decrease the survival of the flies treated to paraquat compared to non-treated flies, however this is not lower than the parental flies and therefore these results were inconclusive as well.

7.3.3 Upregulation of different components of the Autophagy pathway using the drivers NP2276-Gal4, NP2693-Gal4 and Elav-Gal4

Since the predicted rescue was observed for the Moody-Gal4 x UAS-Atg1^{RNAi} flies, we decided to see whether down regulation of the Atg1 gene using different Gal4 drivers will produce a similar effect. We chose NP2276-Gal4 (SPG driver), NP2693-Gal4 (PNG driver), and elav-Gal4 (pan-neural driver). The same conditions were used for the NP2276-Gal4 x UAS-Atg1^{RNAi}, NP2693-Gal4 x UAS-Atg1^{RNAi} and elav-Gal4 x UAS-Atg1^{RNAi} crosses as for the Moody-Gal4 x UAS-Atg1^{RNAi}. The data from these experiments is shown in Figure 7.12-7.14. The data shows that the effect seen for the Moody-Gal4 x UAS-Atg1^{RNAi} cross is not seen for the NP2276-Gal4 x UAS-Atg1^{RNAi}, NP2693-Gal4 x UAS-Atg1^{RNAi} and elav-Gal4 x UAS-Atg1^{RNAi} crosses.

7.3.4 Developmental Lethality Experiments

As previously mentioned, one of the possible reasons that causes the opposite effect than the expected rescue of the of survival and negative geotaxis performance when CncC is overexpressed in the SPG could be that this protein may have toxic effects during development. One way to test if overexpression of a protein has toxic effects is through the developmental lethality assay. We performed developmental lethality assay for Moody-Gal4 x UAS-CncC, Moody-Gal4 x UAS-Keap1^{RNAi} and NP2276-Gal4 x

UAS-CncC crosses. This data is shown in Figure 7.15. The data shows that there is 12.4% difference between Moody-Gal4/UAS-CncC compared to the internal control UAS-CncC/Cyo. A much drastic difference of about 62% is seen between NP2276-Gal4/UAS-CncC and UAS-CncC/Cyo. However, for the Moody-Gal4 x UAS-Keap1^{RNAi} cross, the Moody-Gal4/UAS-Keap1^{RNAi} flies are 6.7% above the internal control Moody-Gal4/Cyo suggesting that developmental lethality is not present in this case. This data suggests that developmental lethality is observed when CncC is directly overexpressed in the SPG and that overexpression of CncC could have potentially toxic effects during development.

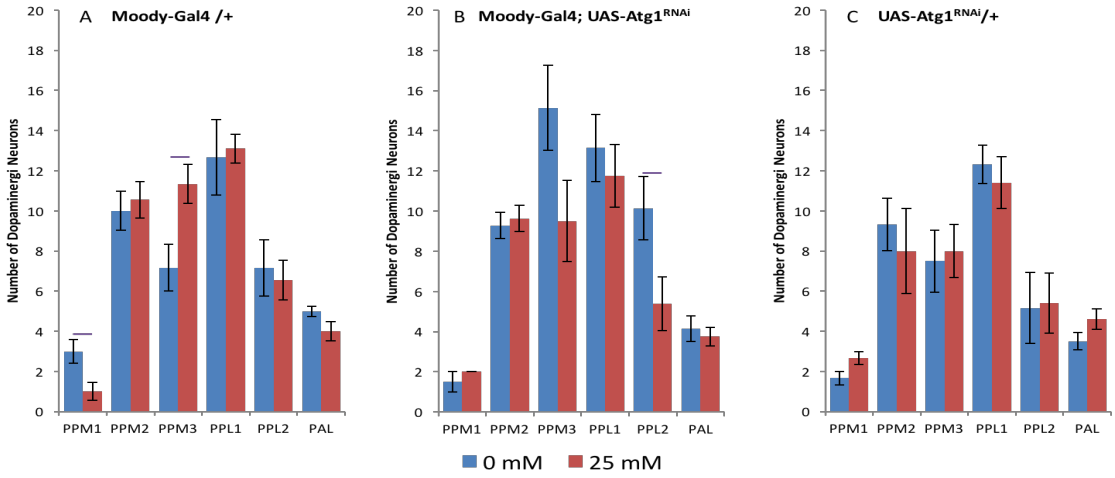

Figure 7.1: Dopaminergic neuron quantification for flies expressing Atg1^{RNAi} in the SPG: The experimental and parental flies were exposed to either 5% sucrose solution or 25 mM paraquat in 5% sucrose solution for 24h. The brains these exposed flies were dissected out and they were immunostained with anti-TH antibody. **Sample sizes: (A) Moody-Gal4/+:** PPM1 0 mM N=3, 25 mM N=5; PPM2, PPM3, PPL1, PPL2 and PAM 0 mM N=6, 25 mM N=9; **(B) Moody-Gal4;UAS-Atg1^{RNAi}:** PPM1 0 mM N=4, 25 mM N=4; PPM2, PPM3, PPL1, PPL2 and PAM 0 mM N=7, 25 mM N=8; **(C) UAS-Atg1RNAi/+**: PPM1 0 mM N=3, 25 mM N=3; PPM2, PPM3, PPL1, PPL2 and PAM 0 mM N=6, 25 mM N=5. The lines above bars and their varying thickness depict statistical significance and the level of statistical significance. Each increase of thickness implies a 10-fold increase in significance.

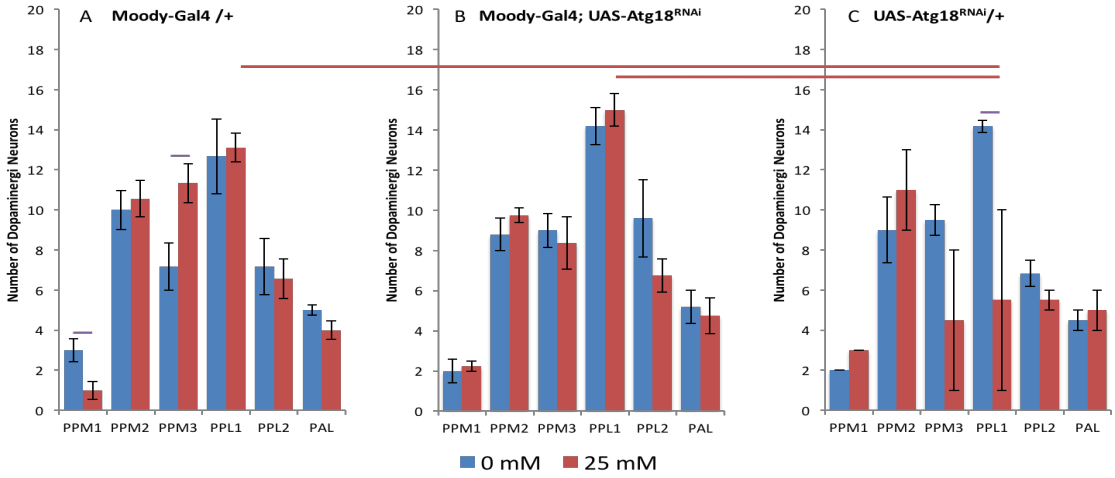

Figure 7.2: Dopaminergic neuron quantification for flies expressing Atg18^{RNAi} in the SPG: The experimental and parental flies were exposed to either 5% sucrose solution or 25 mM paraquat in 5% sucrose solution for 24h. The brains these exposed flies were dissected out and they were immunostained with anti-TH antibody. **Figure 7.3: Dopaminergic neuron quantification for flies expressing Atg1^{RNAi} in the SPG:** The experimental and parental flies were exposed to either 5% sucrose solution or 25 mM paraquat in 5% sucrose solution for 24h. The brains these exposed flies were dissected out and they were immunostained with anti-TH antibody. **Sample sizes: (A) Moody-Gal4/+:** PPM1 0 mM N=3, 25 mM N=5; PPM2, PPM3, PPL1, PPL2 and PAM 0 mM N=6, 25 mM N=9; **(B) Moody-Gal4;UAS-Atg1^{RNAi}:** PPM1 0 mM N=4, 25 mM N=4; PPM2, PPM3, PPL1, PPL2 and PAM 0 mM N=7, 25 mM N=8; **(C) UAS-Atg1RNAi/+**: PPM1 0 mM N=3, 25 mM N=3; PPM2, PPM3, PPL1, PPL2 and PAM 0 mM N=6, 25 mM N=5.The lines above bars and their varying thickness depict statistical significance and the level of statistical significance. Each increase of thickness implies a 10-fold increase in significance.

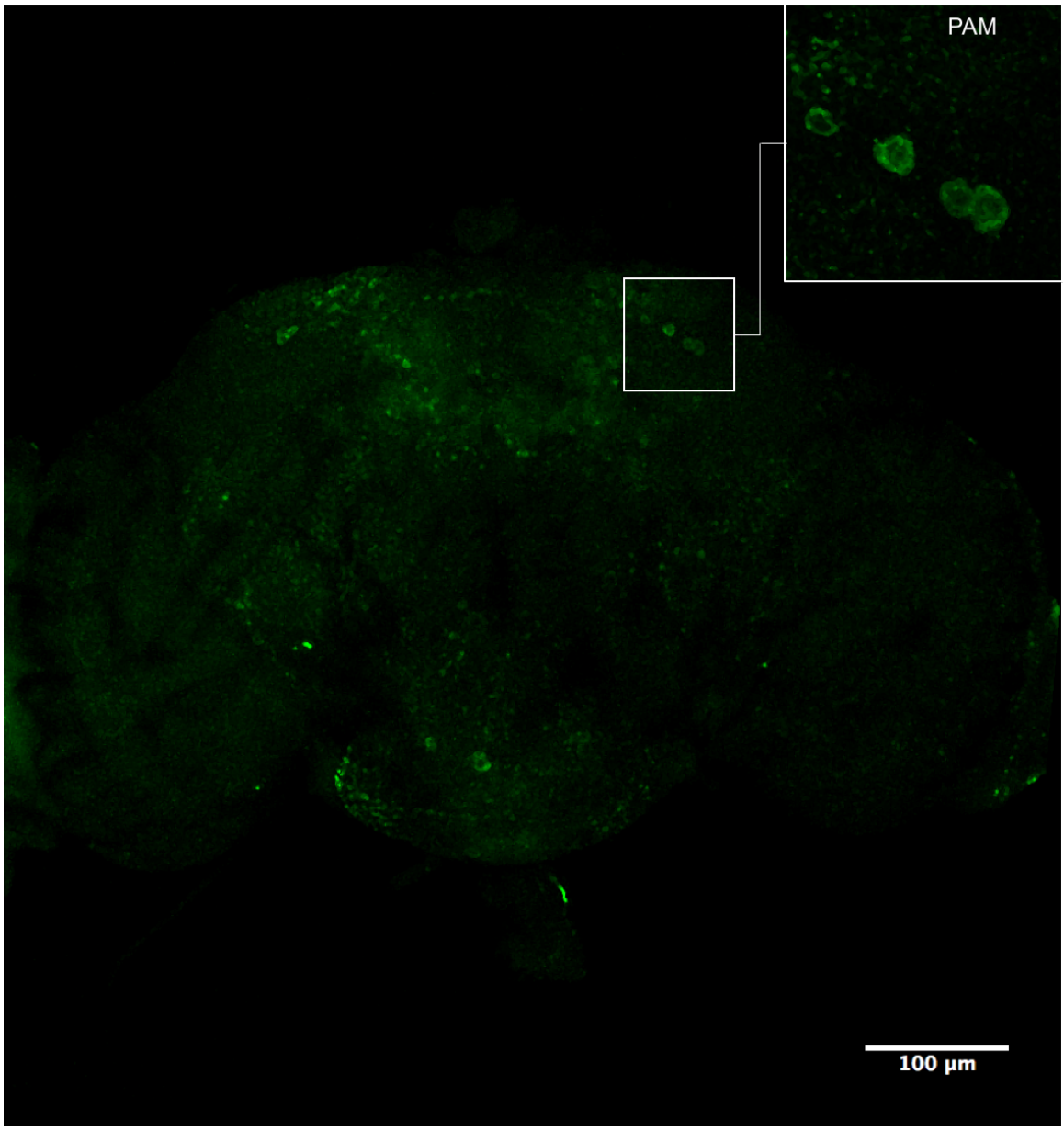

Figure 7.4: Immunostaining of the dopaminergic neurons in the anterior brain region of untreated Moody-Gal4;UAS-Atg1^{RNAi} fly. Representative confocal image of adult fly brains labeled using an anti-TH antibody. The box depicts the dopaminergic neuron cluster PAM. Image magnified 20x , z-stack projection of 46 steps within 22.16 µm section. The zoomed in box is magnified 63x, z-stack projection of 20 steps within 9 µm section.

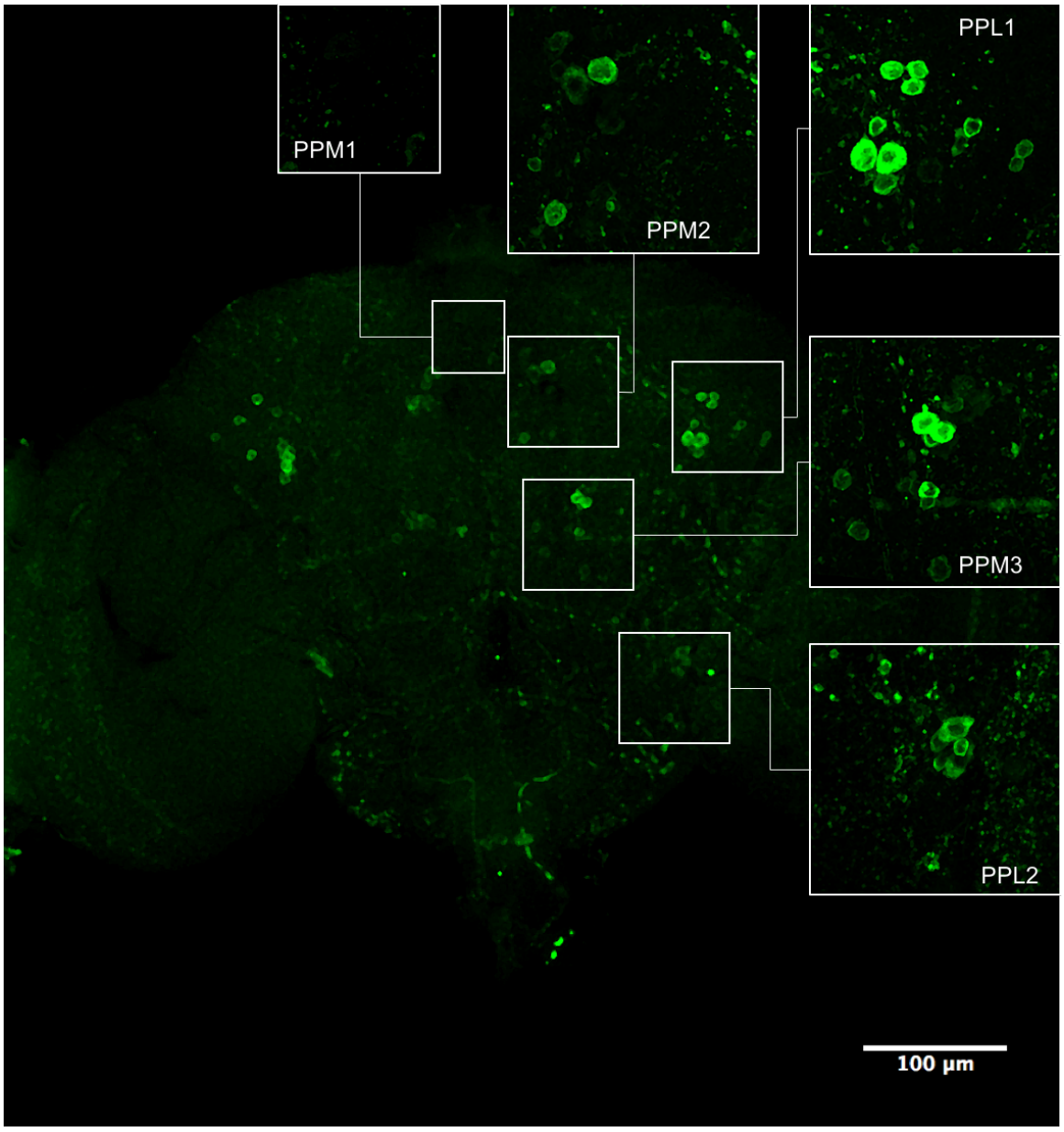

Figure 7.5: Immunostaining of the dopaminergic neurons in the posterior brain region of untreated Moody-Gal4;UAS-Atg1^{RNAi} fly. Representative confocal image of adult fly brains labeled using an anti-TH antibody. The boxes depict the dopaminergic neuron clusters PPM1, PPM2, PPM3, PPL1 and PPL2. Image magnified 20x, z-stack projection of 81 steps within 40.15 µm section. The zoomed in boxes for the PPM1, PPM2 PPM3 and PPL1 are magnified 63x, z-stack projection of 35 steps within 17.1 µm section. The box for the PPL2 cluster is magnified 63x, z-stack projection of 21 steps within 9.59 µm section.

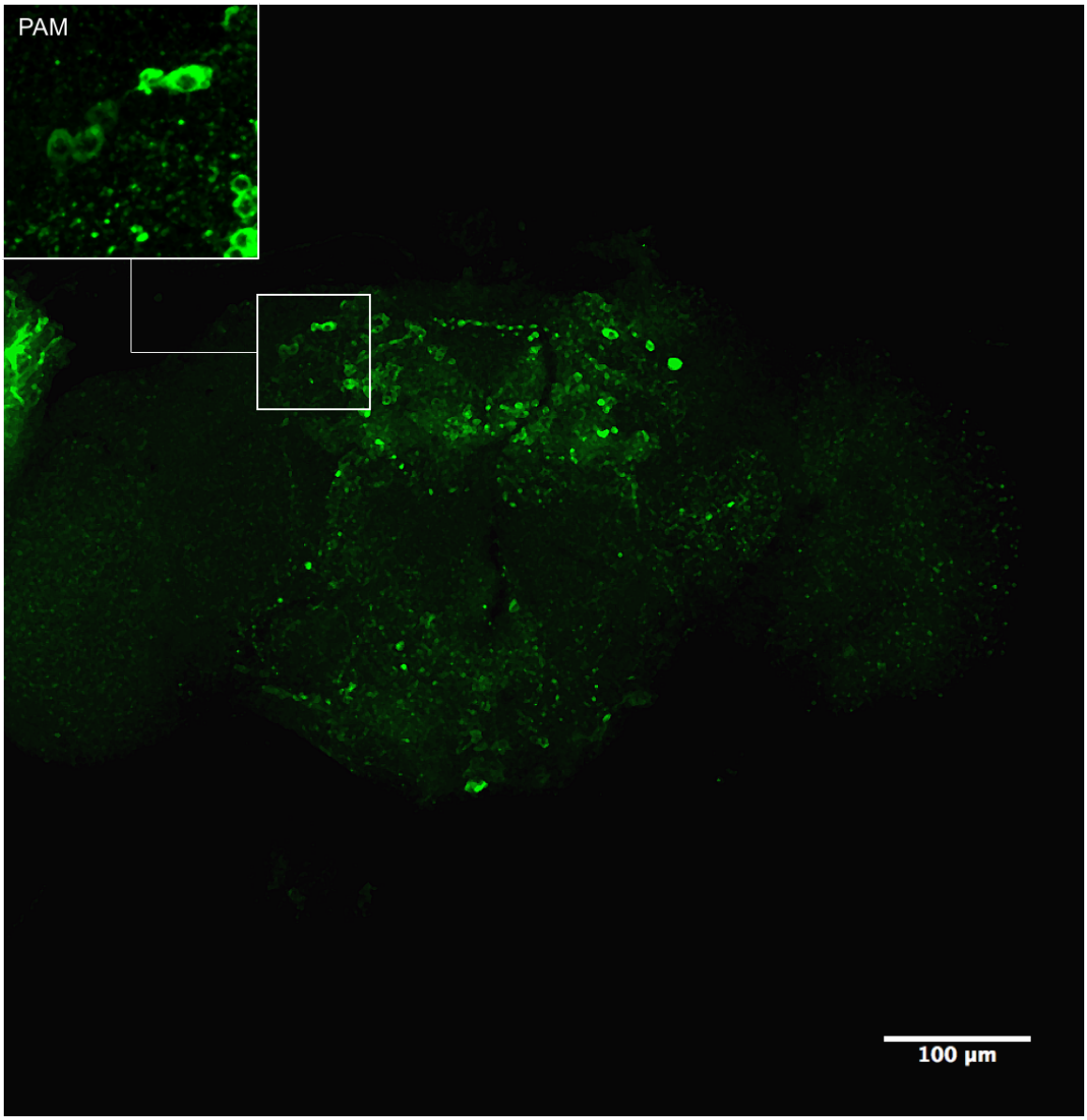

Figure 7.6: Immunostaining of the dopaminergic neurons in the anterior brain region of Moody-Gal4;UAS-Atg1^{RNAi} fly treated with 25 mM paraquat. Representative confocal image of adult fly brains labeled using an anti-TH antibody. The box depicts the dopaminergic neuron cluster PAM. Image is magnified 20x , z-stack projection of 64 steps within 21.72 µm section. The zoomed in box is magnified 63x, z-stack projection of 51 steps within 25.18 µm section.

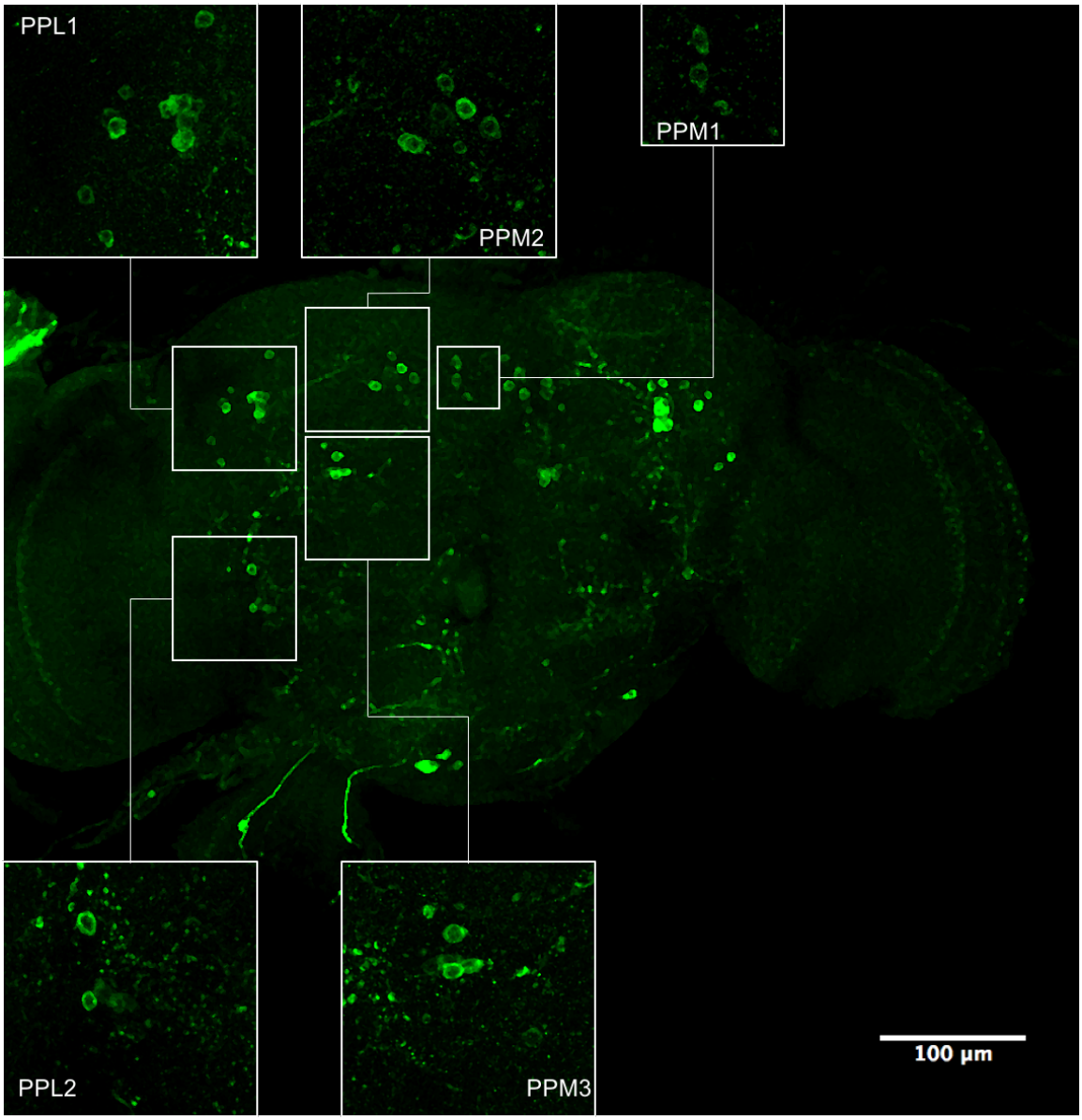

Figure 7.7: Immunostaining of the dopaminergic neurons in the posterior brain region of Moody-Gal4;UAS-Atg1^{RNAi} fly treated with 25 mM paraquat. Representative confocal image of adult fly brains labeled using an anti-TH antibody. The boxes depict the dopaminergic neuron clusters PPM1, PPM2, PPM3, PPL1 and PPL2. Image magnified 20x, z-stack projection of 73 steps within 36.22 µm section. The zoomed in boxes for the PPM1, PPM2 PPM3 and PPL1 are magnified 63x, z-stack projection of 81 steps within 40.29 µm section. The box for the PPL2 cluster is magnified 63x, z-stack projection of 83 steps within 41.56 µm section.

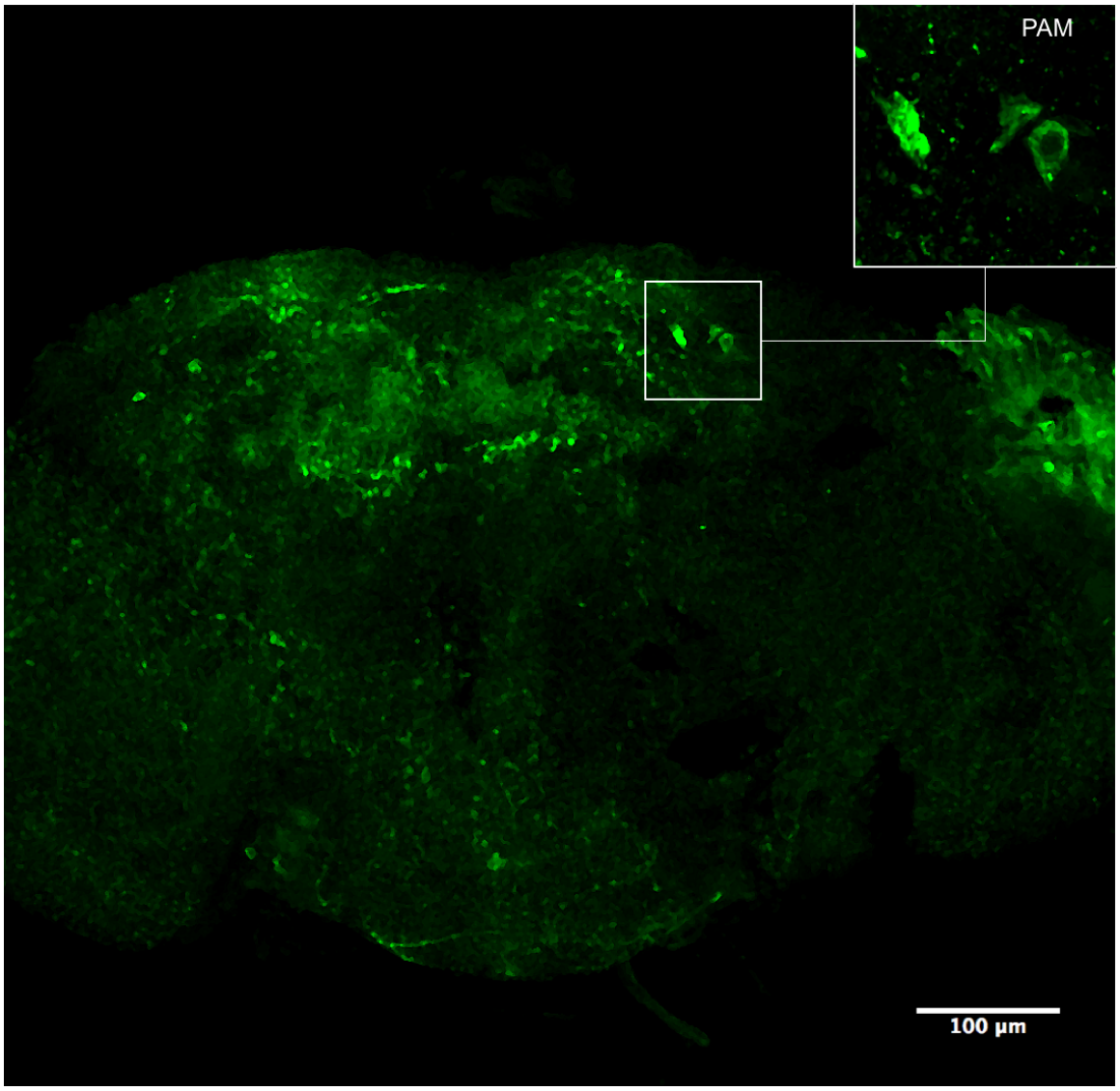

Figure 7.8: Immunostaining of the dopaminergic neurons in the anterior brain region of untreated UAS-Atg1^{RNAi}/+ fly. Representative confocal image of adult fly brains labeled using an anti-TH antibody. The box depicts the dopaminergic neuron cluster PAM. Image magnified 20x , z-stack projection of 45 steps within 22.16 µm section. The zoomed in box is magnified 63x, z-stack projection of 30 steps within 14.6 µm section.

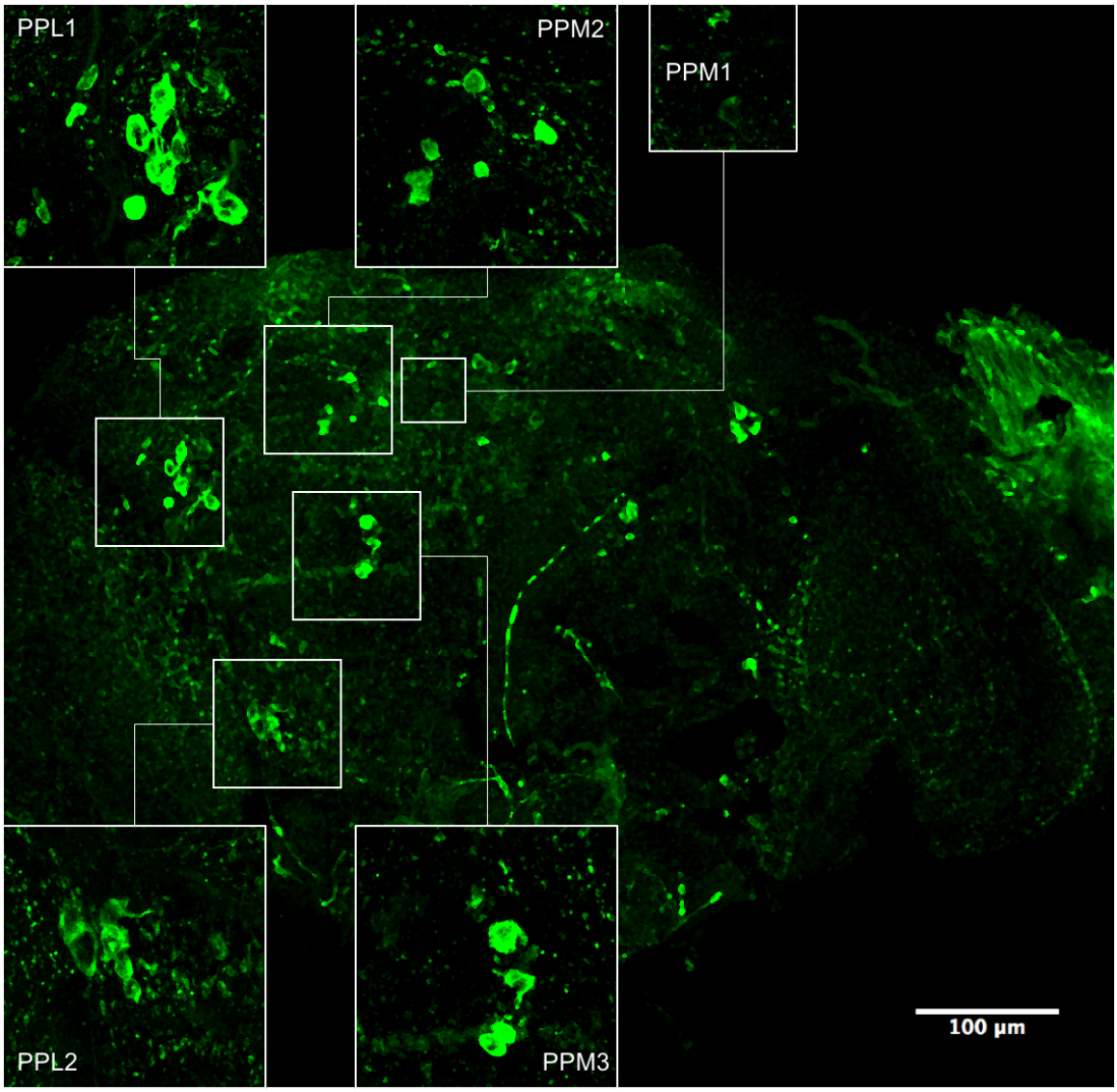

Figure 7.9: Immunostaining of the dopaminergic neurons in the posterior brain region of untreated UAS-Atg1^{RNAi}/+ fly. Representative confocal image of adult fly brains labeled using an anti-TH antibody. The boxes depict the dopaminergic neuron clusters PPM1, PPM2, PPM3, PPL1 and PPL2. Image magnified 20x, z-stack projection of 44 steps within 21.65 µm section. The zoomed in boxes for the PPM1, PPM2 PPM3 and PPL1 are magnified 63x, z-stack projection of 27 steps within 13.09 µm section. The box for the PPL2 cluster is magnified 63x, z-stack projection of 26 steps within 12.59 µm section.

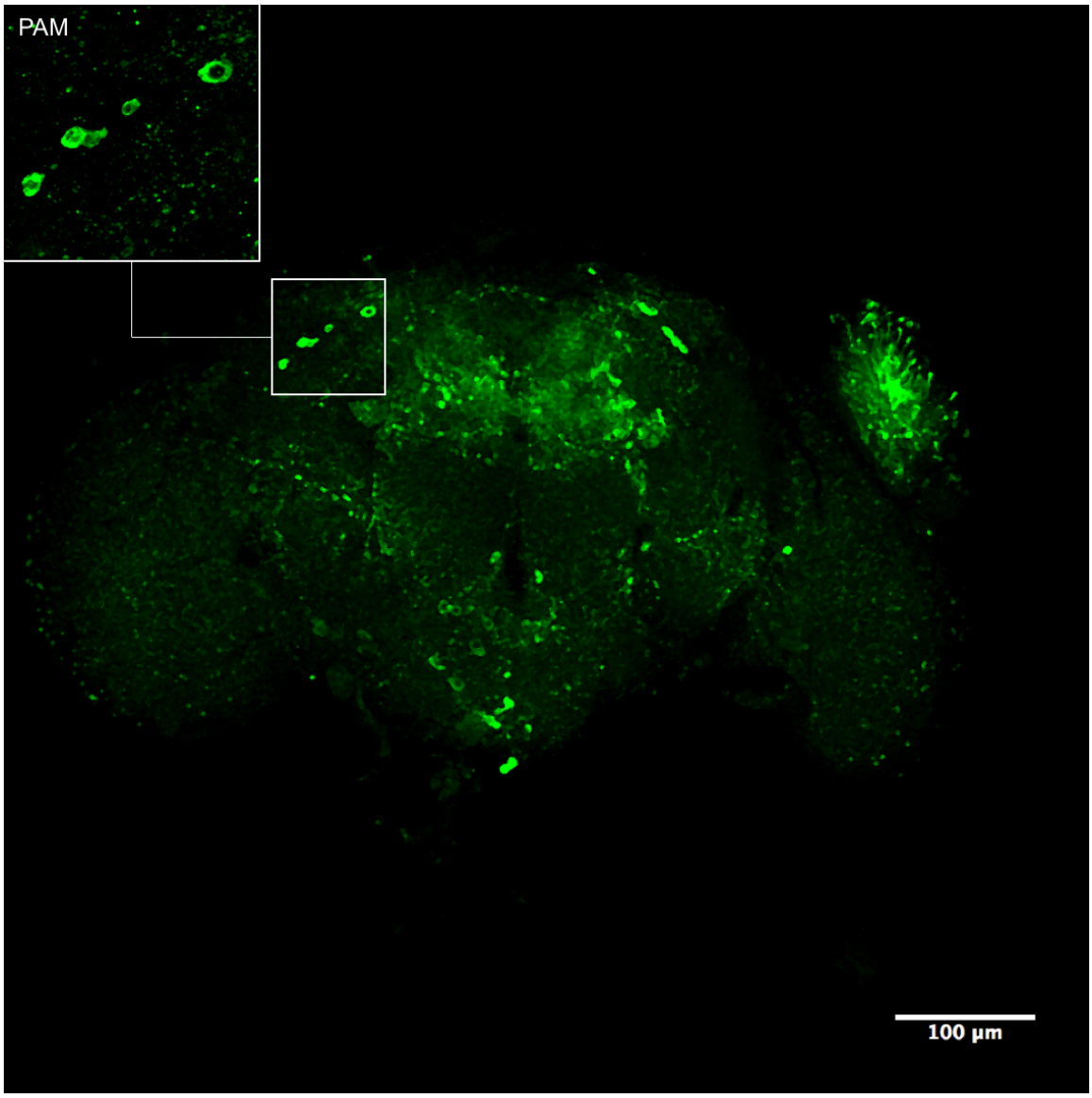

Figure 7.10: Immunostaining of the dopaminergic neurons in the anterior brain region of UAS-Atg1^{RNAi}/+ fly treated with 25 mM paraquat. Representative confocal image of adult fly brains labeled using an anti-TH antibody. The box depicts the dopaminergic neuron cluster PAM. Image magnified 20x , z-stack projection of 50 steps within 24.67 µm section. The zoomed in box is magnified 63x, z-stack projection of 50 steps within 24.97 µm section.

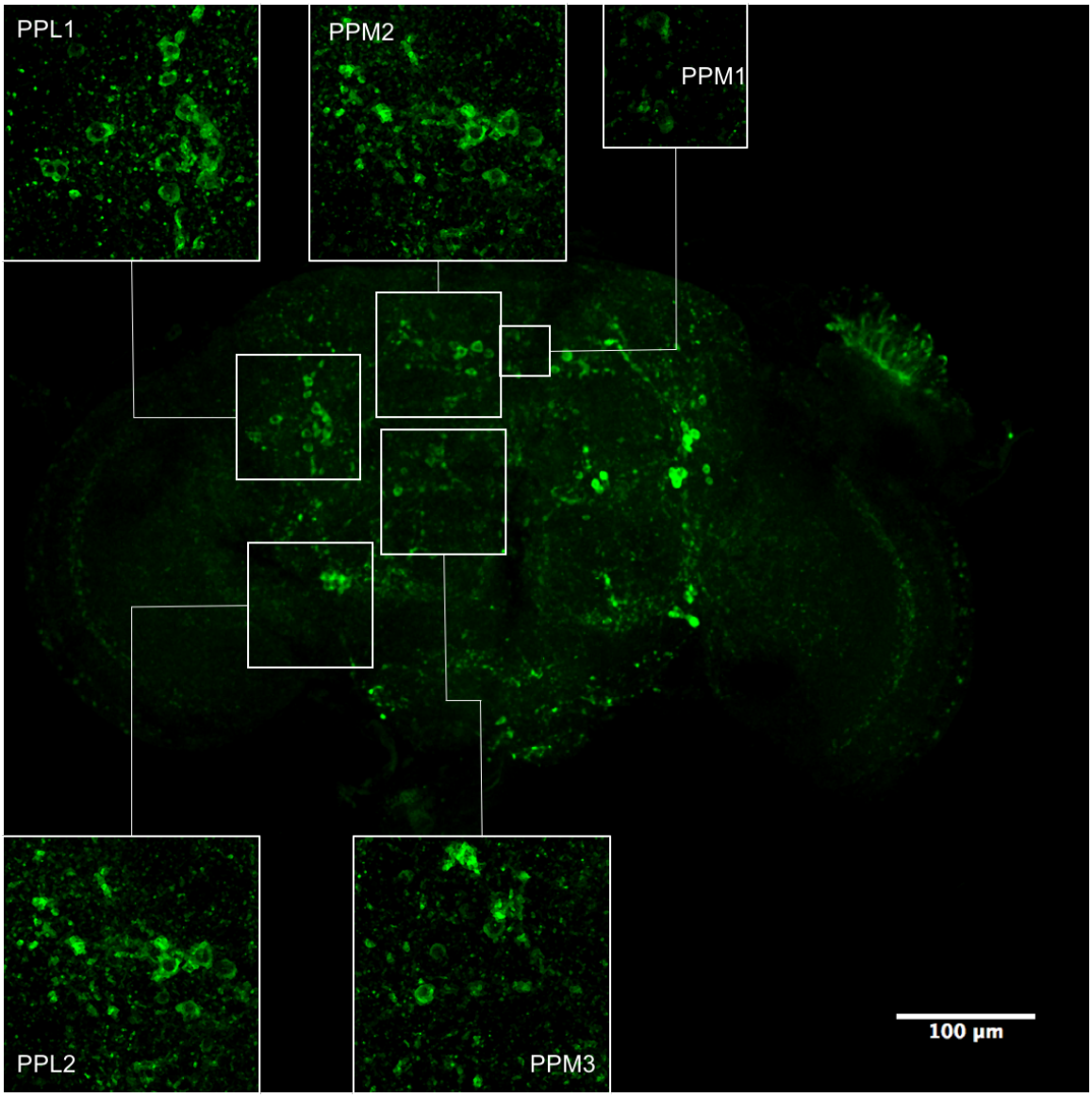

Figure 7.11: Immunostaining of the dopaminergic neurons in the posterior brain region of UAS-Atg1^{RNAi}/+ fly treated with 25 mM paraquat. Representative confocal image of adult fly brains labeled using an anti-TH antibody. The boxes depict the dopaminergic neuron clusters PPM1, PPM2, PPM3, PPL1 and PPL2. Image magnified 20x, z-stack projection of 61 steps within 30.22 µm section. The zoomed in boxes for the PPM1, PPM2 PPM3 and PPL1 are magnified 63x, z-stack projection of 75 steps within 37.29 µm section. The box for the PPL2 cluster is magnified 63x, z-stack projection of 65 steps within 32.23 µm section.

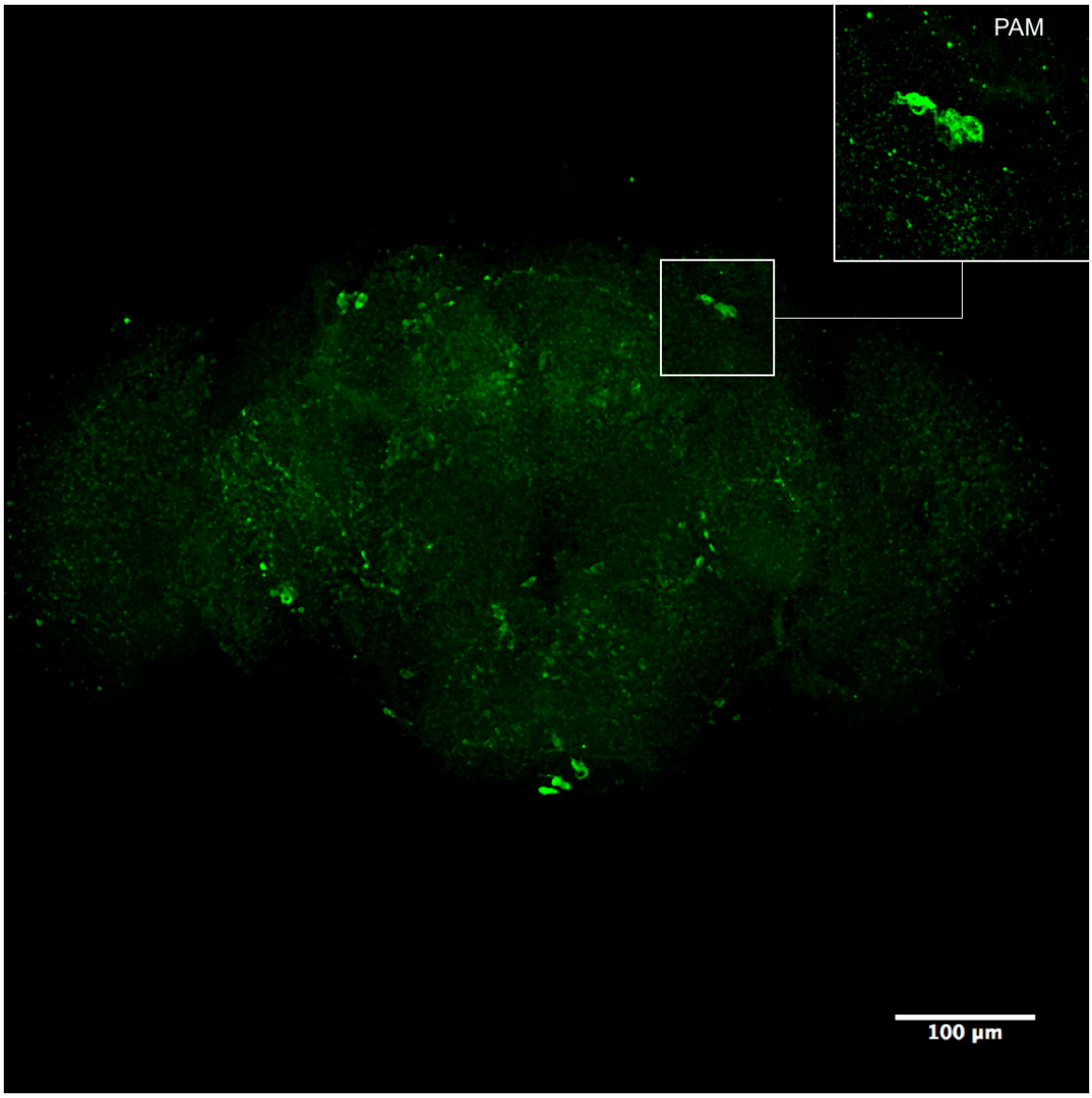

Figure 7.12: Immunostaining of the dopaminergic neurons in the anterior brain region of untreated Moody-Gal4/+ fly. Representative confocal image of adult fly brains labeled using an anti-TH antibody. The box depicts the dopaminergic neuron cluster PAM. Image magnified 20x , z-stack projection of 56 steps within 27.7 µm section. The zoomed in box is magnified 63x, z-stack projection of 29 steps within 14.1 µm section.

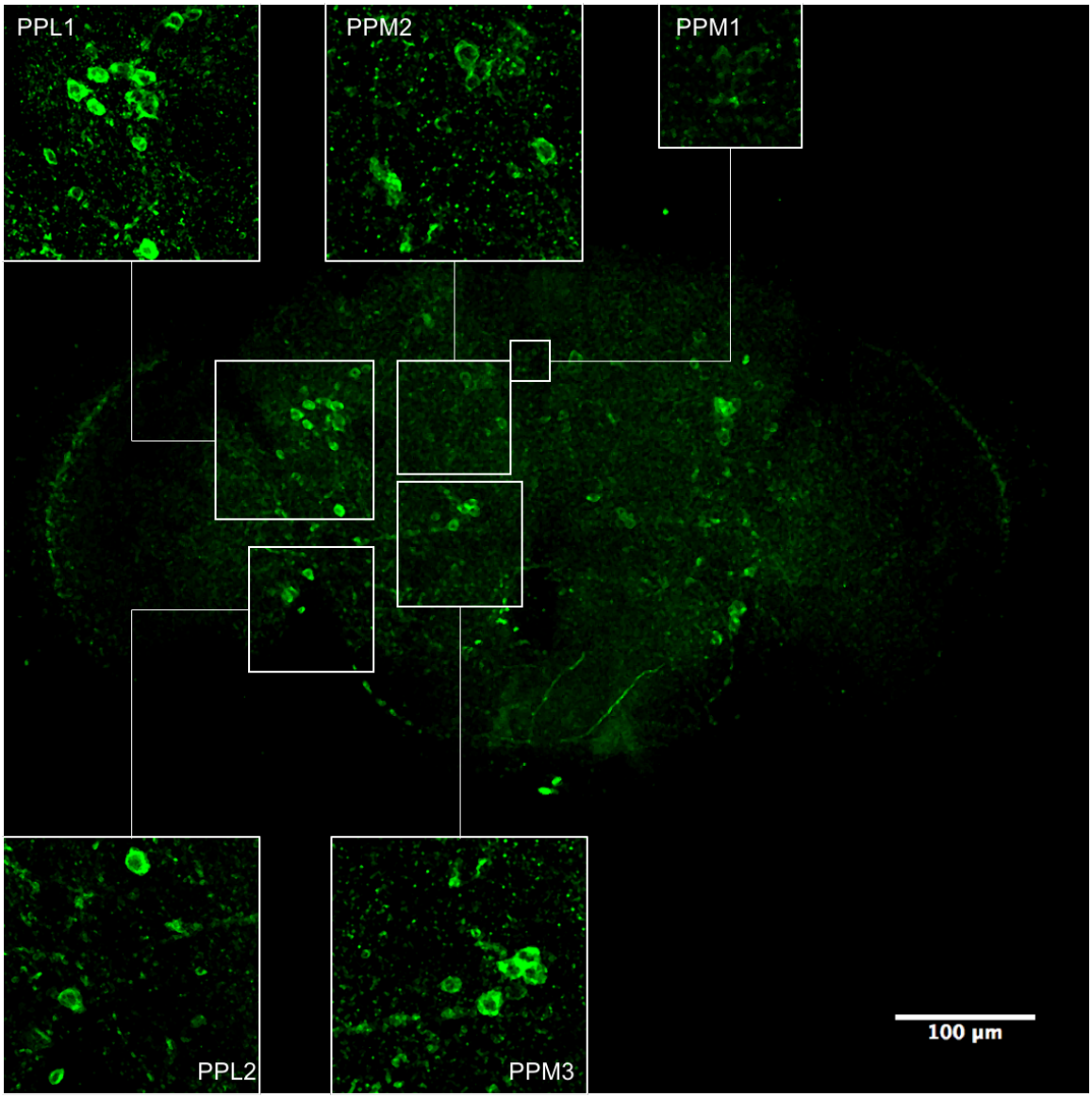

Figure 7.13: Immunostaining of the dopaminergic neurons in the posterior brain region of untreated Moody-Gal4/+ fly. Representative confocal image of adult fly brains labeled using an anti-TH antibody. The boxes depict the dopaminergic neuron clusters PPM1, PPM2, PPM3, PPL1 and PPL2. Image magnified 20x, z-stack projection of 46 steps within 22.66 µm section. The zoomed in boxes for the PPM1, PPM2 PPM3 and PPL1 are magnified 63x, z-stack projection of 47 steps within 23.16 µm section. The box for the PPL2 cluster is magnified 63x, z-stack projection of 34 steps within 16.61 µm section.

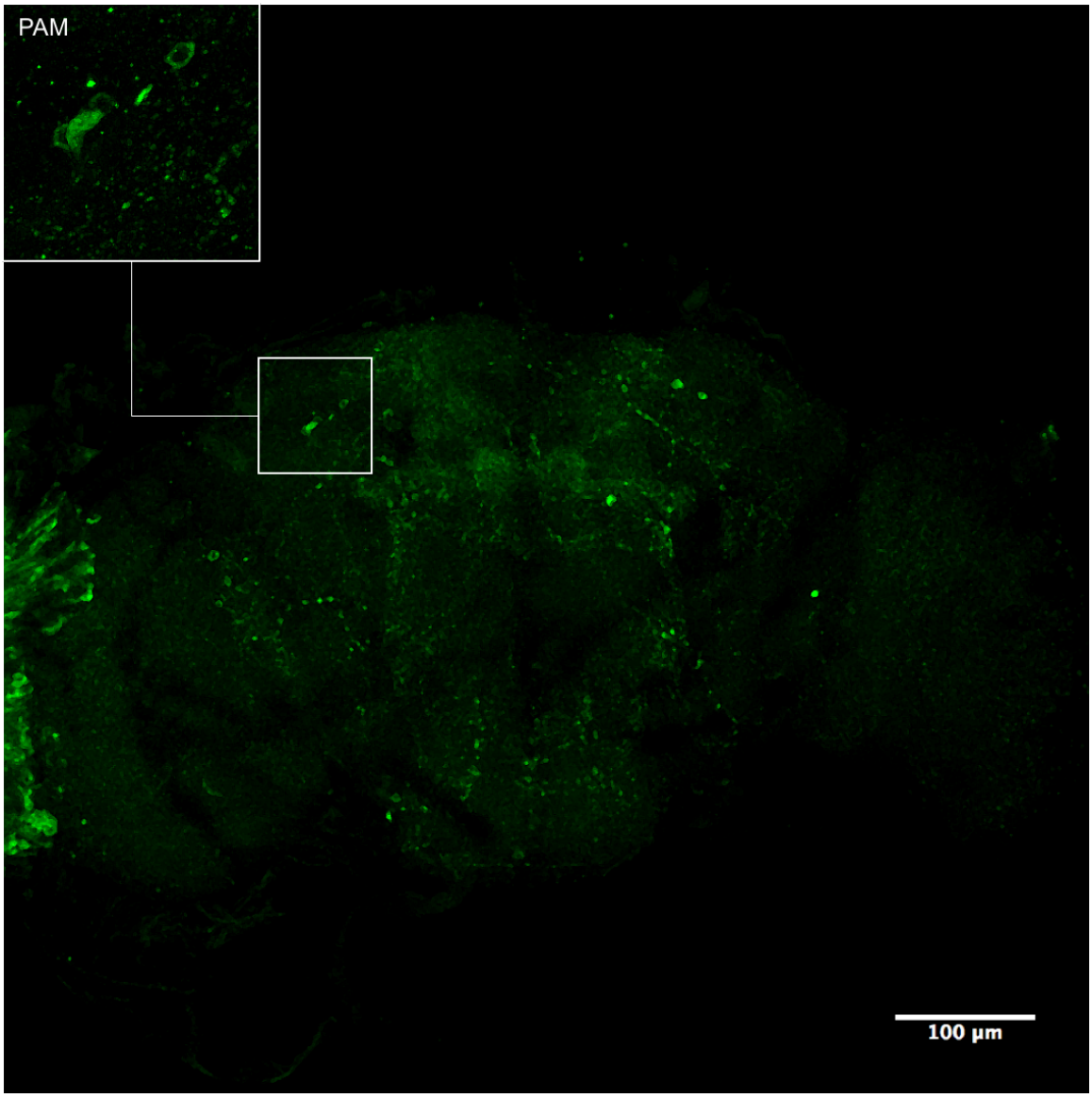

Figure 7.14: Immunostaining of the dopaminergic neurons in the anterior brain region Moody-Gal4/+ fly treated with 25 mM paraquat. Representative confocal image of adult fly brains labeled using an anti-TH antibody. The box depicts the dopaminergic neuron cluster PAM. Image magnified 20x , z-stack projection of 50 steps within 24.68 µm section. The zoomed in box is magnified 63x, z-stack projection of 37 steps within 18.13 µm section.

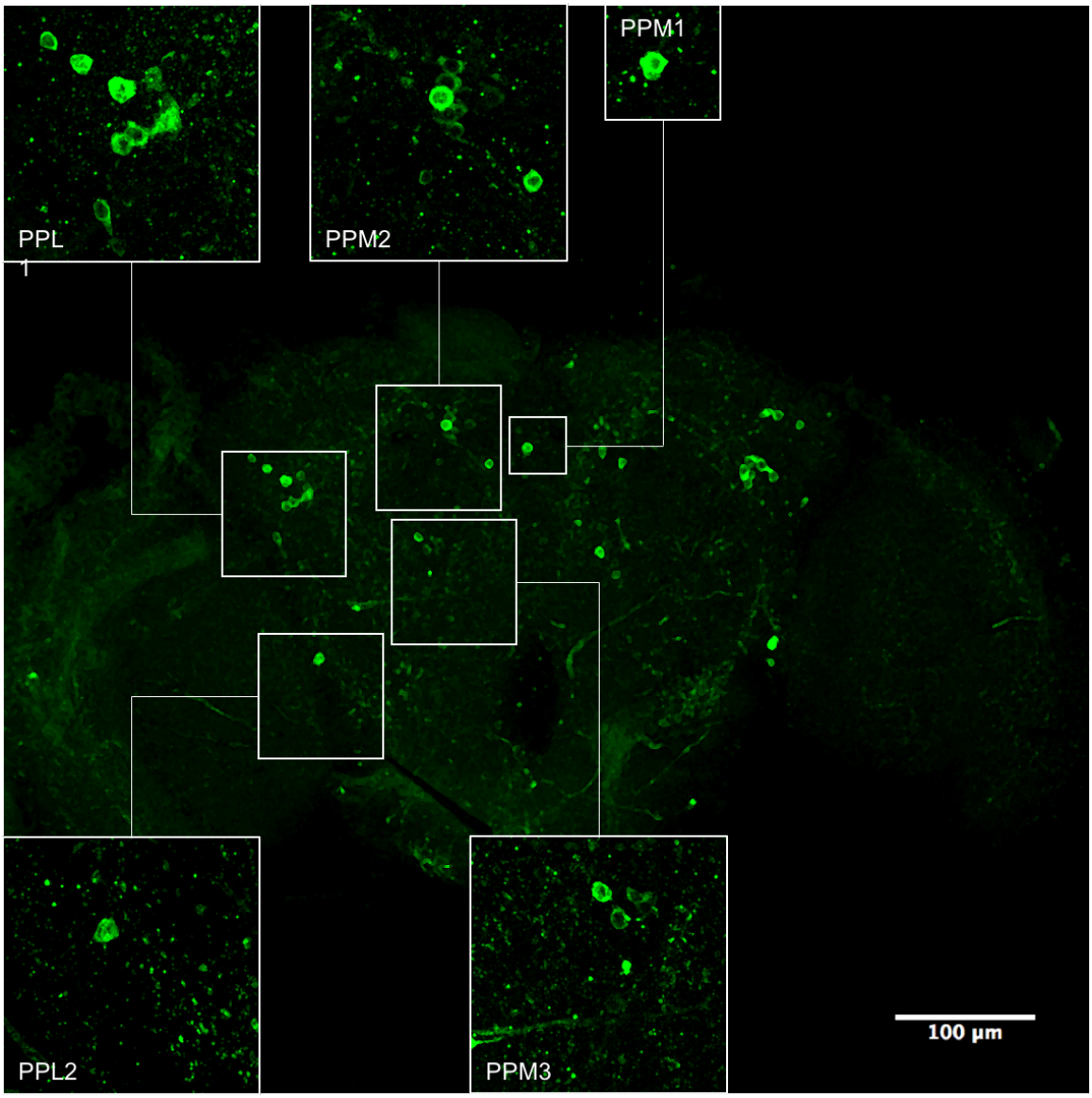

Figure 7.15: Immunostaining of the dopaminergic neurons in the posterior brain region of Moody-Gal4/+ fly treated with 25 mM paraquat. Representative confocal image of adult fly brains labeled using an anti-TH antibody. The boxes depict the dopaminergic neuron clusters PPM1, PPM2, PPM3, PPL1 and PPL2. Image magnified 20x, z-stack projection of 58 steps within 28.7 µm section. The zoomed in boxes for the PPM1, PPM2 PPM3 and PPL1 are magnified 63x, z-stack projection of 64 steps within 31.72 µm section. The box for the PPL2 cluster is magnified 63x, z-stack projection of 64 steps within 31.73 µm section.

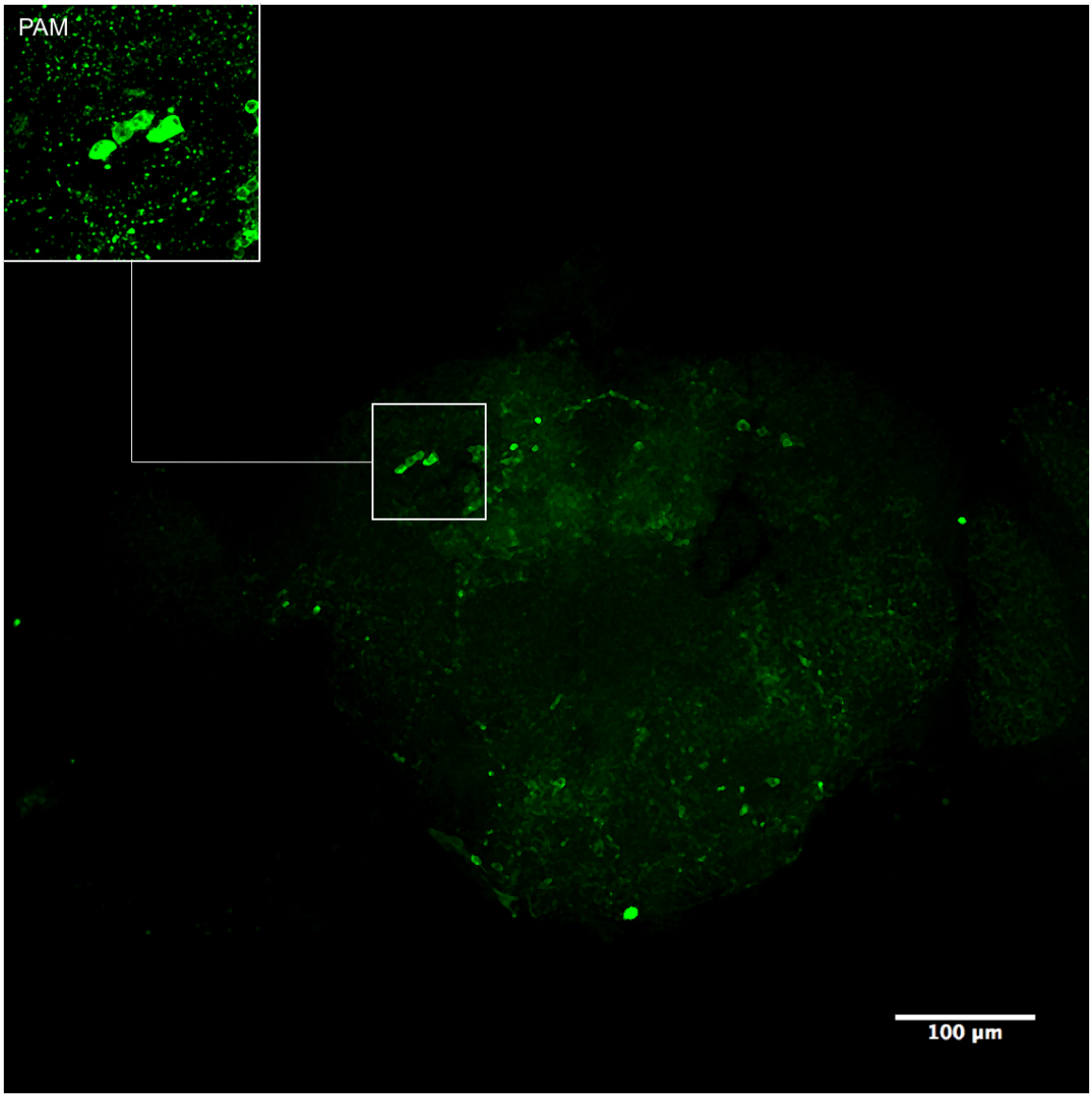

Figure 7.16: Immunostaining of the dopaminergic neurons in the anterior brain region of untreated Moody-Gal4;UAS-Atg18^{RNAi} fly. Representative confocal image of adult fly brains labeled using an anti-TH antibody. The box depicts the dopaminergic neuron cluster PAM. Image magnified 20x , z-stack projection of 59 steps within 29.2 µm section. The zoomed in box is magnified 63x, z-stack projection of 58 steps within 28.7 µm section.

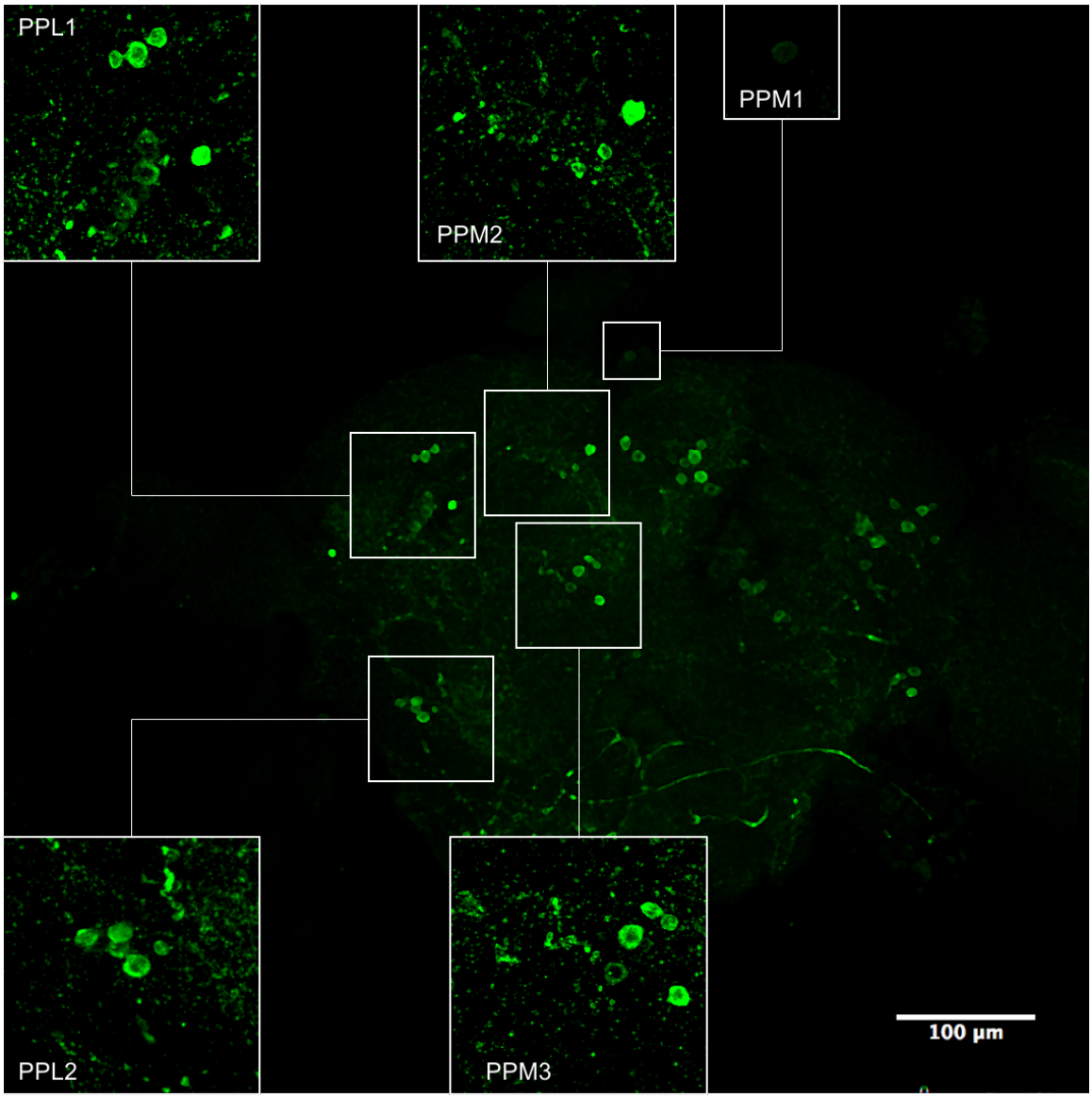

Figure 7.17: : Immunostaining of the dopaminergic neurons in the posterior brain region of untreated Moody-Gal4;UAS-Atg18^{RNAi} fly. Representative confocal image of adult fly brains labeled using an anti-TH antibody. The boxes depict the dopaminergic neuron clusters PPM1, PPM2, PPM3, PPL1 and PPL2. Image magnified 20x, z-stack projection of 62 steps within 30.72 µm section. The zoomed in boxes for the PPM1, PPM2 PPM3 and PPL1 are magnified 63x, z-stack projection of 69 steps within 34.24 µm section. The box for the PPL2 cluster is magnified 63x, z-stack projection of 75 steps within 37.26 µm section.

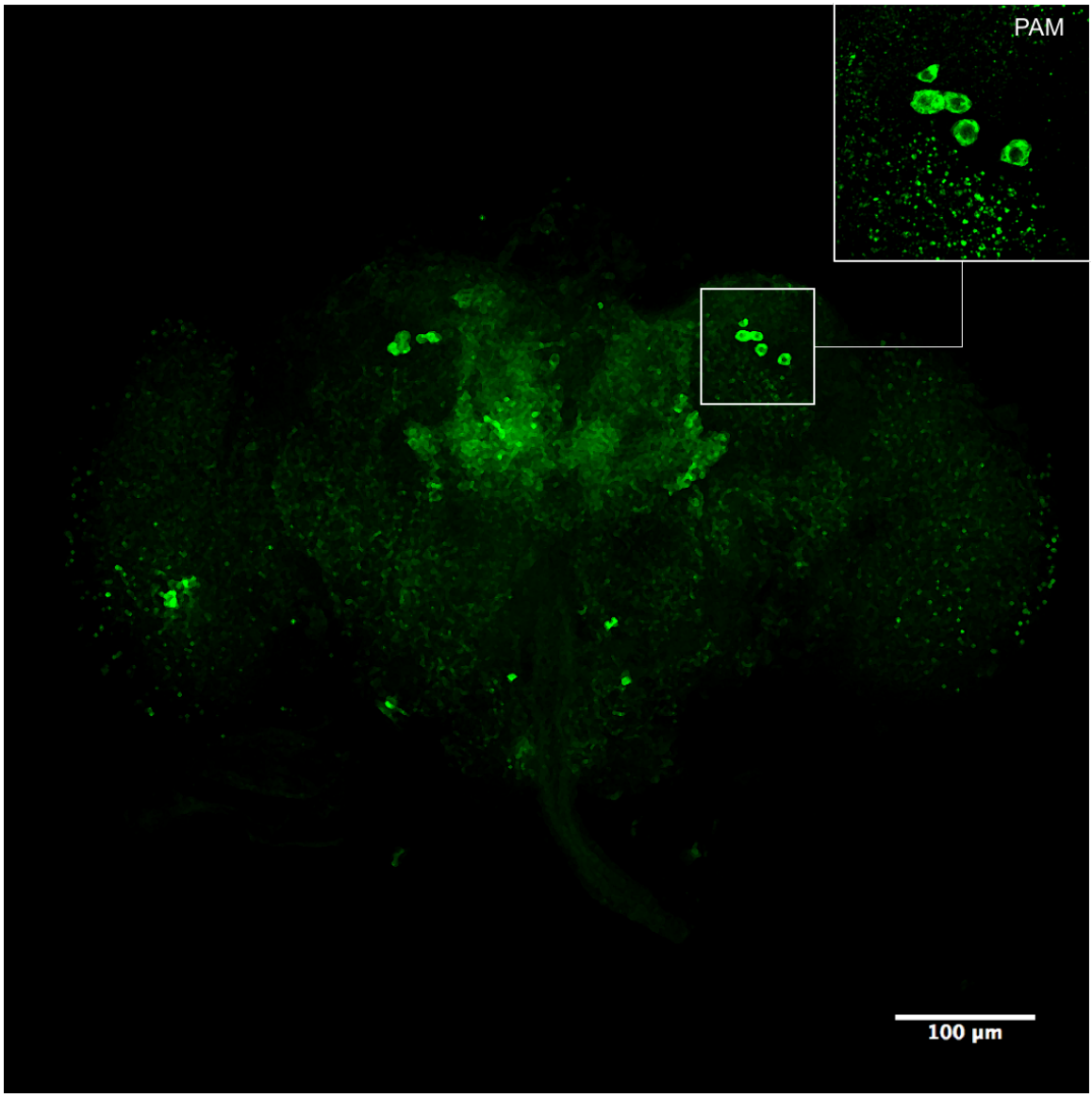

Figure 7.18: Immunostaining of the dopaminergic neurons in the anterior brain region of Moody-Gal4;UAS-Atg18^{RNAi} fly treated with 25 mM paraquat. Representative confocal image of adult fly brains labeled using an anti-TH antibody. The box depicts the dopaminergic neuron cluster PAM. Image magnified 20x , z-stack projection of 47 steps within 23.16 µm section. The zoomed in box is magnified 63x, z-stack projection of 36 steps within 17.62 µm section.

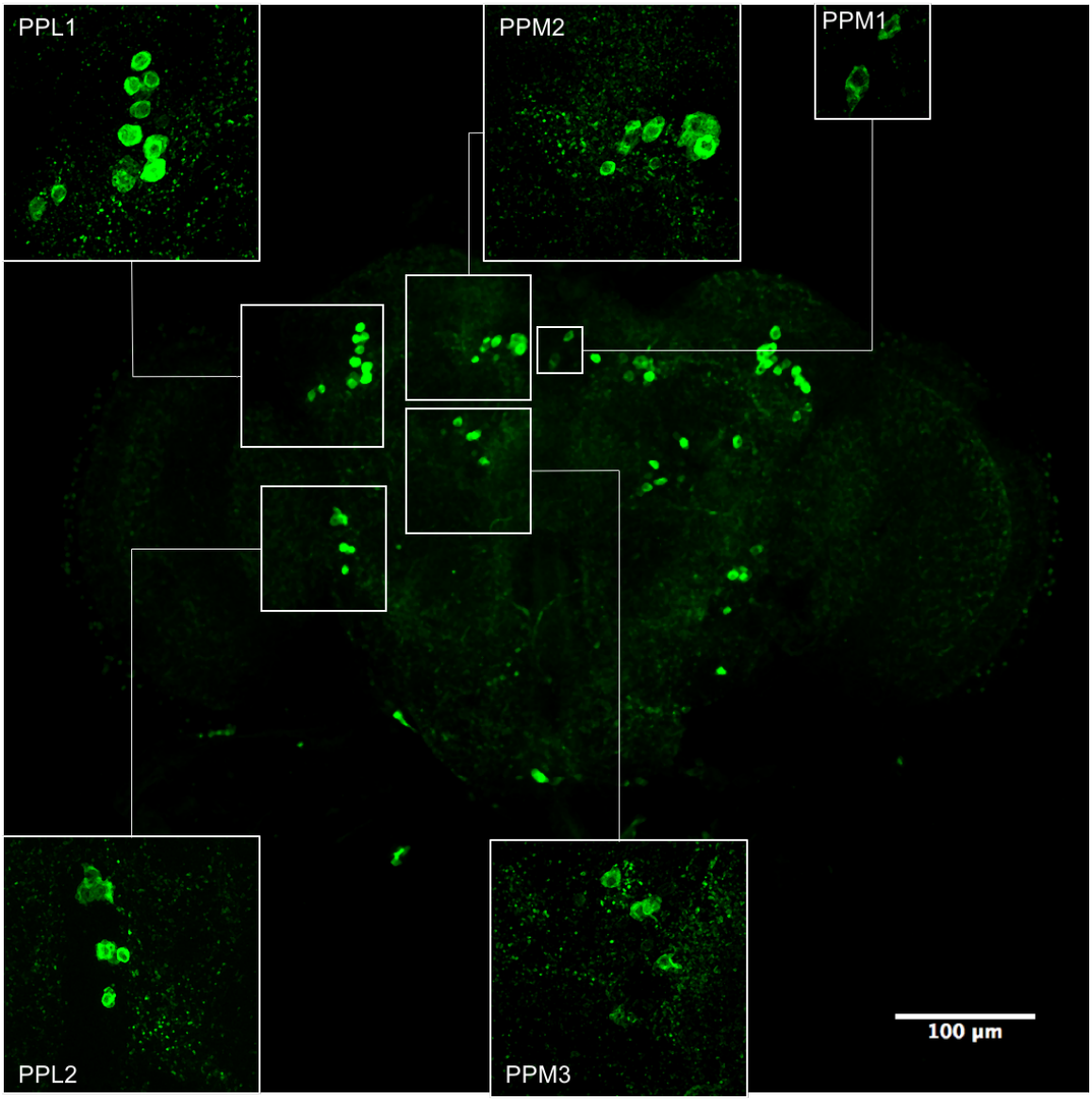

Figure 7.19: Immunostaining of the dopaminergic neurons in the posterior brain region of Moody-Gal4;UAS-Atg18^{RNAi} fly treated with 25 mM paraquat. Representative confocal image of adult fly brains labeled using an anti-TH antibody. The boxes depict the dopaminergic neuron clusters PPM1, PPM2, PPM3, PPL1 and PPL2. Image magnified 20x, z-stack projection of 68 steps within 33.74 µm section. The zoomed in boxes for the PPM1, PPM2 PPM3 and PPL1 are magnified 63x, z-stack projection of 58 steps within 28.71 µm section. The box for the PPL2 cluster is magnified 63x, z-stack projection of 57 steps within 28.2 µm section.

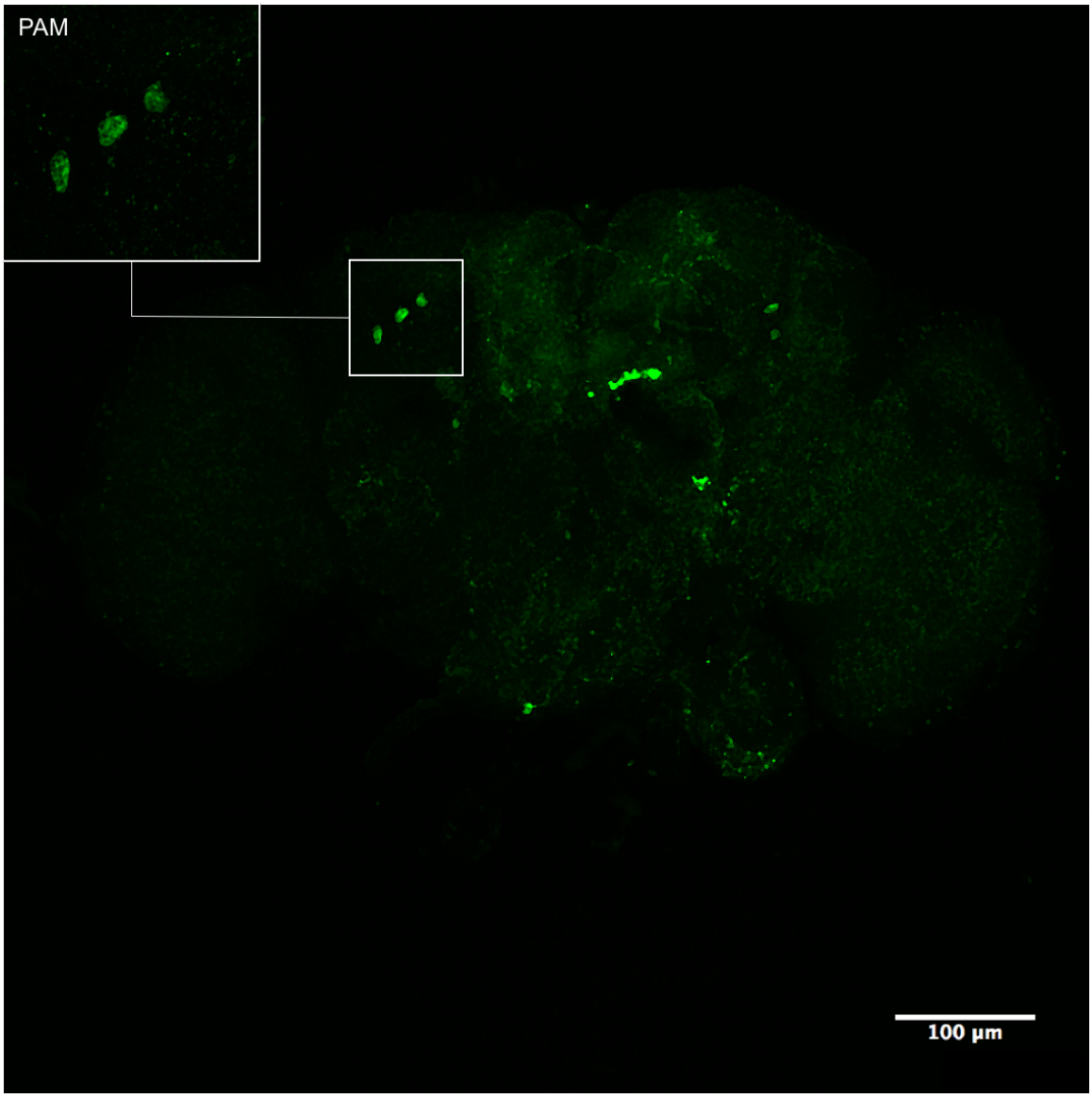

Figure 7.20: Immunostaining of the dopaminergic neurons in the anterior brain region of untreated UAS-Atg18^{RNAi}/+ fly. Representative confocal image of adult fly brains labeled using an anti-TH antibody. The box depicts the dopaminergic neuron cluster PAM. Image magnified 20x , z-stack projection of 66 steps within 32.73 µm section. The zoomed in box is magnified 63x, z-stack projection of 43 steps within 21.15 µm section.

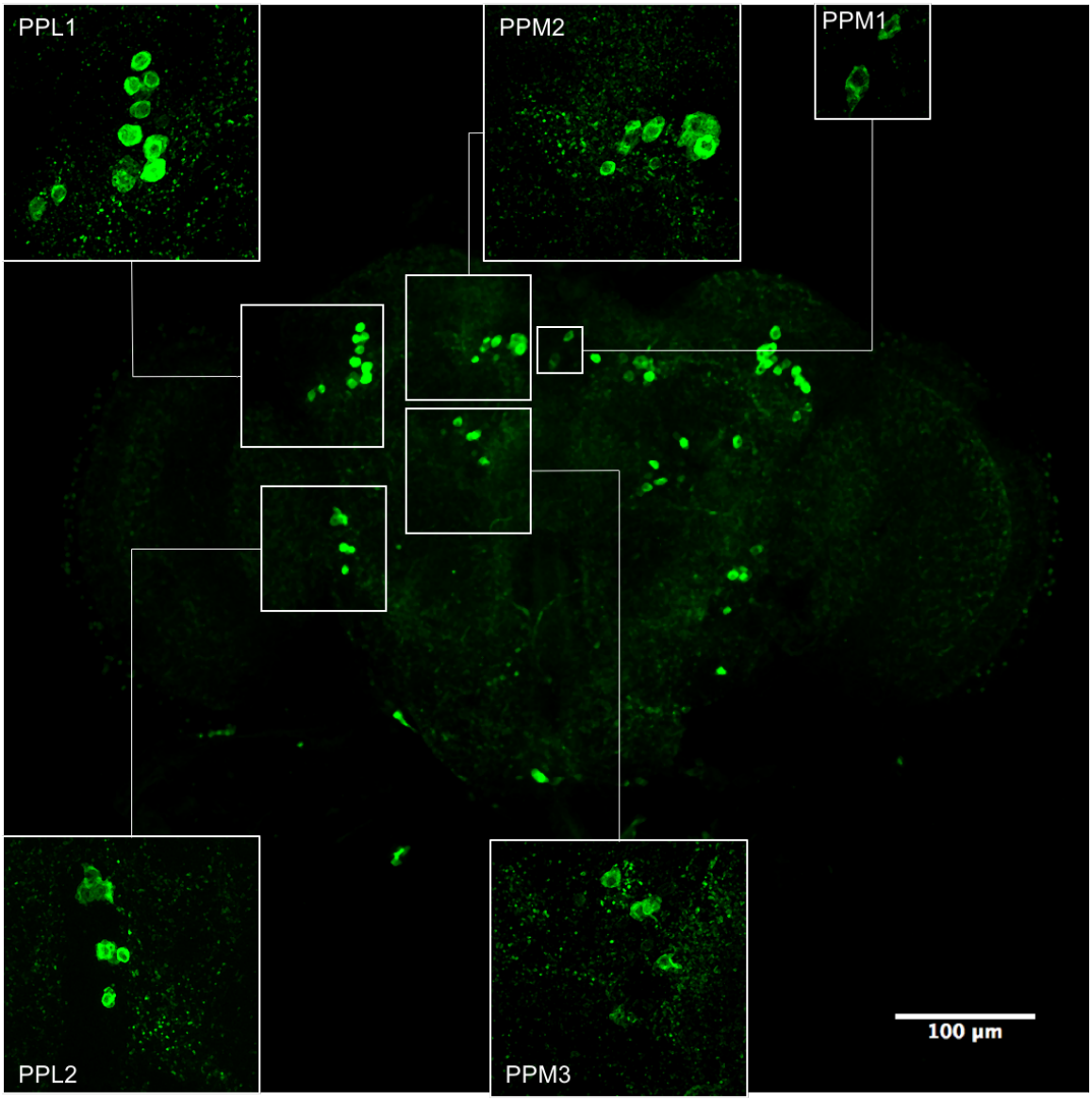

Figure 7.21: Immunostaining of the dopaminergic neurons in the posterior brain region of untreated UAS-Atg18^{RNAi}/+ fly. Representative confocal image of adult fly brains labeled using an anti-TH antibody. The boxes depict the dopaminergic neuron clusters PPM1, PPM2, PPM3, PPL1 and PPL2. Image magnified 20x, z-stack projection of 92 steps within 45 µm section. The zoomed in boxes for the PPM1, PPM2 PPM3 and PPL1 are magnified 63x, z-stack projection of 54 steps within 26.69 µm section. The box for the PPL2 cluster is magnified 63x, z-stack projection of 66 steps within 32.73 µm section.

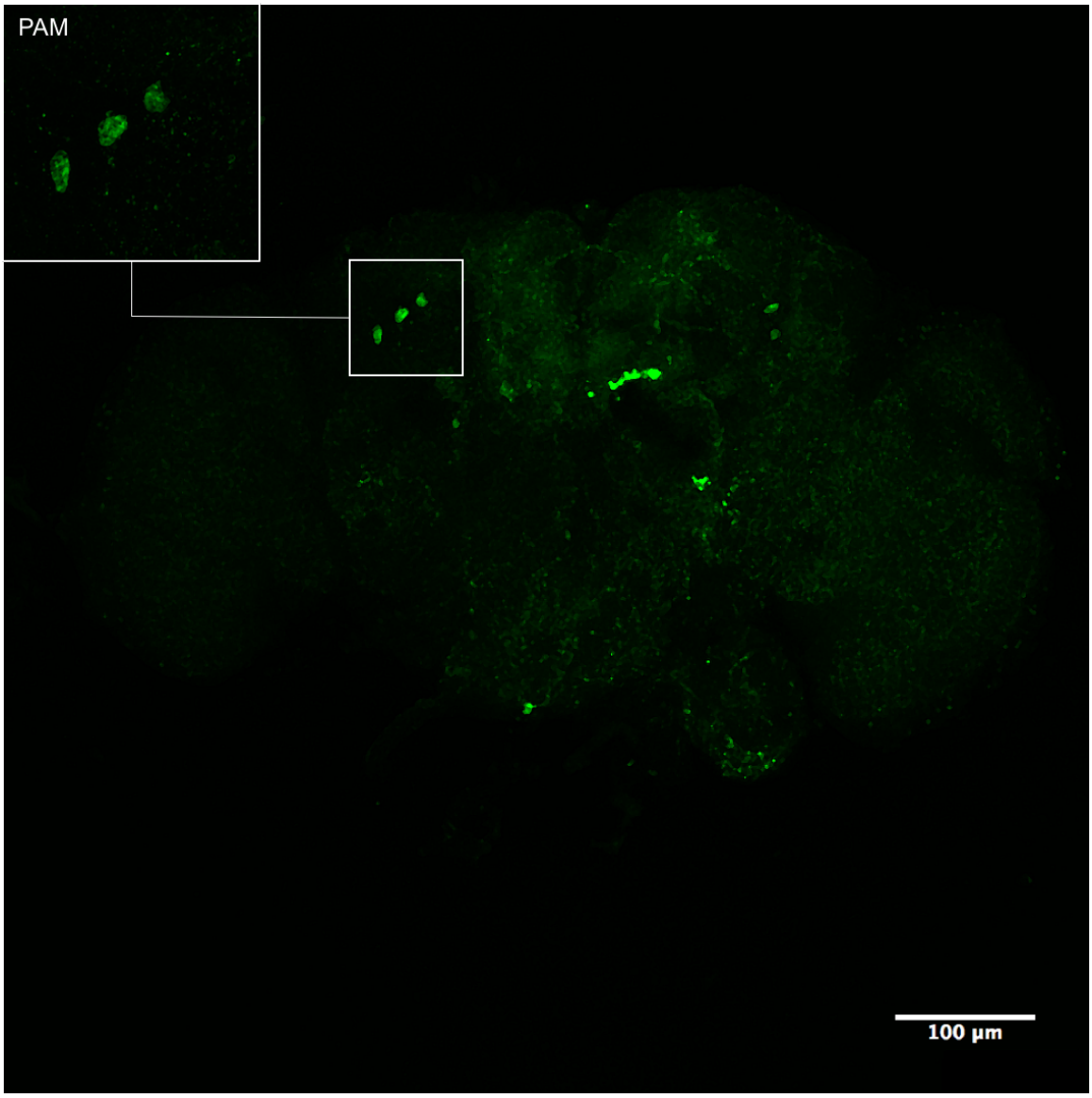

Figure 7.22: Immunostaining of the dopaminergic neurons in the anterior brain region of UAS-Atg18^{RNAi}/+ fly treated with 25 mM paraquat. Representative confocal image of adult fly brains labeled using an anti-TH antibody. The box depicts the dopaminergic neuron cluster PAM. Image magnified 20x , z-stack projection of 71 steps within 35.25 µm section. The zoomed in box is magnified 63x, z-stack projection of 58 steps within 28.7 µm section.

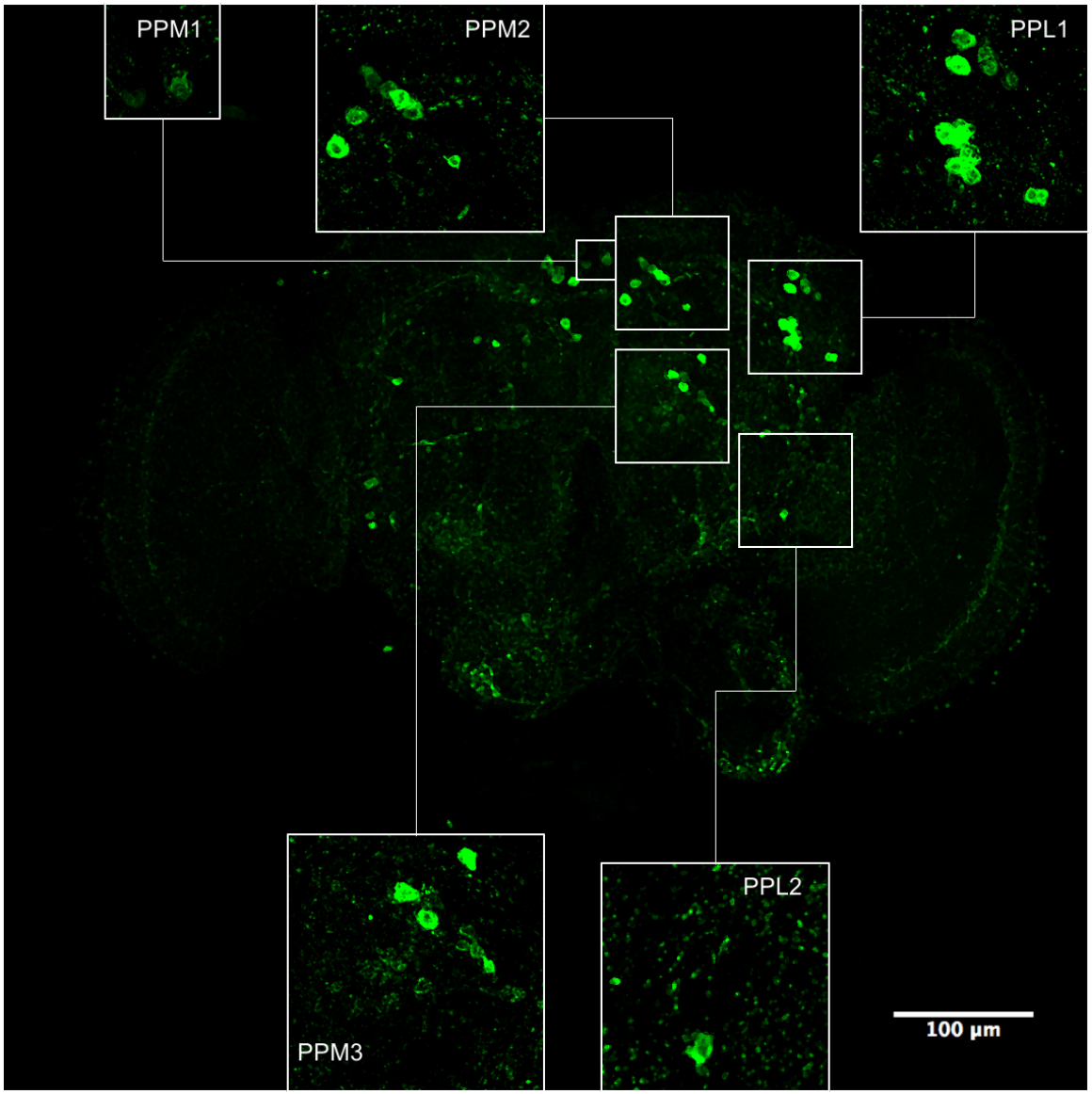

Figure 7.23: Immunostaining of the dopaminergic neurons in the posterior brain region of UAS-Atg18^{RNAi}/+ fly treated with 25 mM paraquat. Representative confocal image of adult fly brains labeled using an anti-TH antibody. The boxes depict the dopaminergic neuron clusters PPM1, PPM2, PPM3, PPL1 and PPL2. Image magnified 20x, z-stack projection of 72 steps within 35.75 µm section. The zoomed in boxes for the PPM1, PPM2 PPM3 and PPL1 are magnified 63x, z-stack projection of 77 steps within 38.27 µm section. The box for the PPL2 cluster is magnified 63x, z-stack projection of 75 steps within 37.26 µm section.

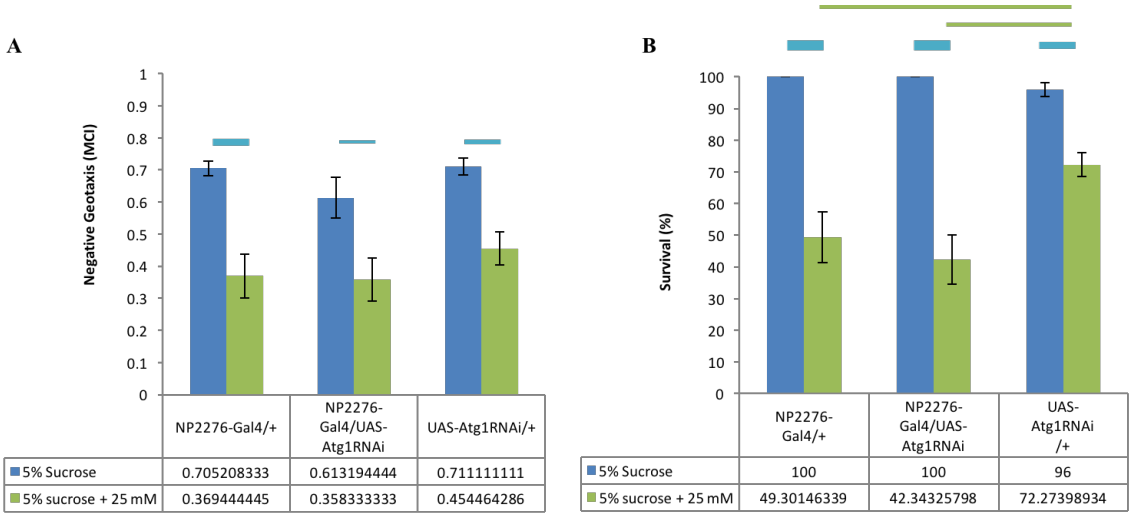

	NP2276-Gal4/+	NP2276-Gal4/UAS-Atg1RNAi	UAS-Atg1RNAi/+
5% Sucrose	0.705208333	0.613194444	0.711111111
5% sucrose + 25 mM	0.369444445	0.358333333	0.454464286

	NP2276-Gal4/+	NP2276-Gal4/UAS-Atg1RNAi	UAS-Atg1RNAi /+
5% Sucrose	100	100	96
5% sucrose + 25 mM	49.30146339	42.34325798	72.27398934

Figure 7.24: Negative Geotaxis and Survival for flies expressing Atg1^{RNAi} in the SPG via the NP2276-Gal4 driver. The experimental and parental flies were exposed to either 5% sucrose solution or 25 mM paraquat in 5% sucrose solution for 24h. **Sample sizes: (A)** NP2276-Gal4/+: 0 mM N=6 25 mM N=6; NP2276-Gal4/UAS-Atg1^{RNAi} 0 mM N=6 25 mM N=3; UAS-Atg1^{RNAi}/+ 0mM N=9 25 mM N=14 **(B)** Survival: NP2276-Gal4/+ 0mM N=12 25 mM N=19; NP2276-Gal4/UAS-Atg1^{RNAi} 0 mM N=8 25 mM N=12; UAS-Atg1^{RNAi}/+ 0 mM N=15 20 mM N=30. Level of statistical significance is depicted by the varying thickness of lines above bars. Each increase of thickness implies a 10-fold increase in significance.

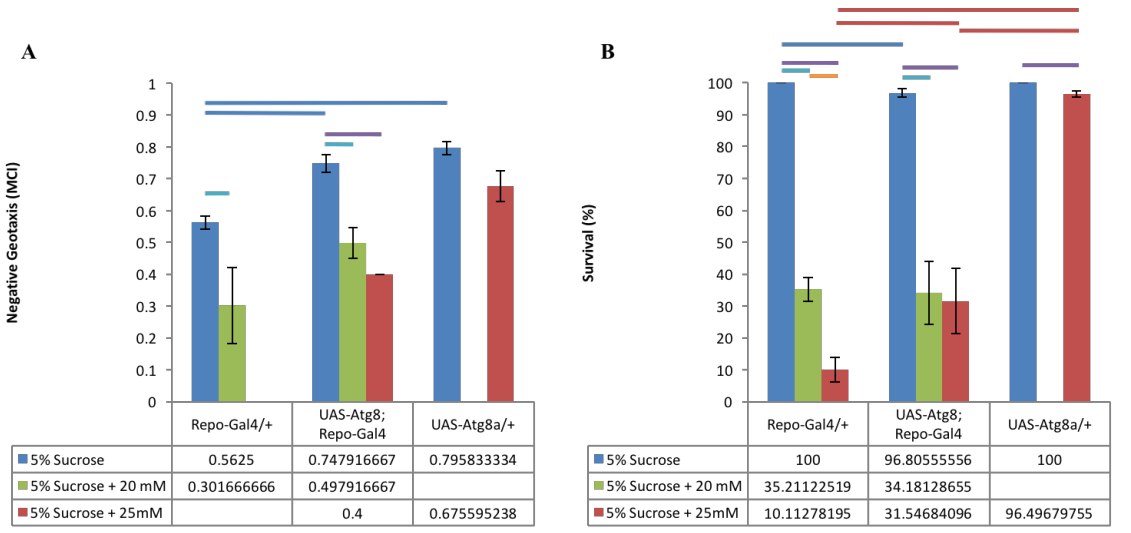

	Repo-Gal4/+	UAS-Atg8; Repo-Gal4	UAS-Atg8a/+
5% Sucrose	0.5625	0.747916667	0.795833334
5% Sucrose + 20 mM	0.301666666	0.497916667	
5% Sucrose + 25mM		0.4	0.675595238

	Repo-Gal4/+	UAS-Atg8; Repo-Gal4	UAS-Atg8a/+
5% Sucrose	100	96.80555556	100
5% Sucrose + 20 mM	35.21122519	34.18128655	
5% Sucrose + 25mM	10.11278195	31.54684096	96.49679755

Figure 7.25: Negative Geotaxis and Survival for flies expressing Atg8a in all glia. The experimental and parental flies were exposed to either 5% sucrose solution or 25 mM paraquat in 5% sucrose solution for 24h. **Sample sizes: (A)** Repo-Gal4/+: 0 mM N=6 25 mM N=6; Repo-Gal4/UAS-Atg8a 0 mM N=6 25 mM N=3; UAS-Atg8a/+ 0mM N=9 25 mM N=14 **(B)** Survival: Repo-Gal4/+ 0mM N=12 25 mM N=19; Repo-Gal4/UAS-Atg8a 0 mM N=8 25 mM N=12; UAS-Atg8a/+ 0 mM N=15 20 mM N=30. Level of statistical significance is depicted by the varying thickness of lines above bars. Each increase of thickness implies a 10-fold increase in significance.

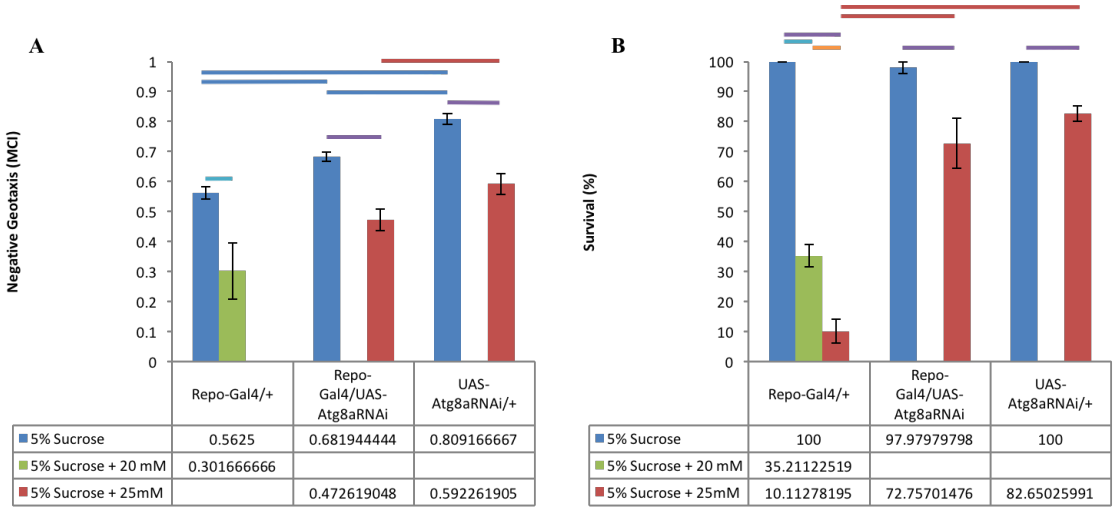

	Repo-Gal4/+	Repo-Gal4/UAS-Atg8aRNAi	UAS-Atg8aRNAi/+
5% Sucrose	0.5625	0.681944444	0.809166667
5% Sucrose + 20 mM	0.301666666		
5% Sucrose + 25mM		0.472619048	0.592261905

	Repo-Gal4/+	Repo-Gal4/UAS-Atg8aRNAi	UAS-Atg8aRNAi/+
5% Sucrose	100	97.97979798	100
5% Sucrose + 20 mM	35.21122519		
5% Sucrose + 25mM	10.11278195	72.75701476	82.65025991

Figure 7.26: Negative Geotaxis and Survival for flies expressing Atg8a^{RNAi} in all glia. The experimental and parental flies were exposed to either 5% sucrose solution or 25 mM paraquat in 5% sucrose solution for 24h. **Sample sizes: (A)** Repo-Gal4/+: 0 mM N=6 25 mM N=6; Repo-Gal4/UAS-Atg8a^{RNAi} 0 mM N=6 25 mM N=3; UAS-Atg8a^{RNAi}/+ 0mM N=9 25 mM N=14 **(B)** Survival: Repo-Gal4/+ 0mM N=12 25 mM N=19; Repo-Gal4/UAS-Atg8a^{RNAi} 0 mM N=8 25 mM N=12; UAS-Atg8a^{RNAi}/+ 0 mM N=15 20 mM N=30. Level of statistical significance is depicted by the varying thickness of lines above bars. Each increase of thickness implies a 10-fold increase in significance.

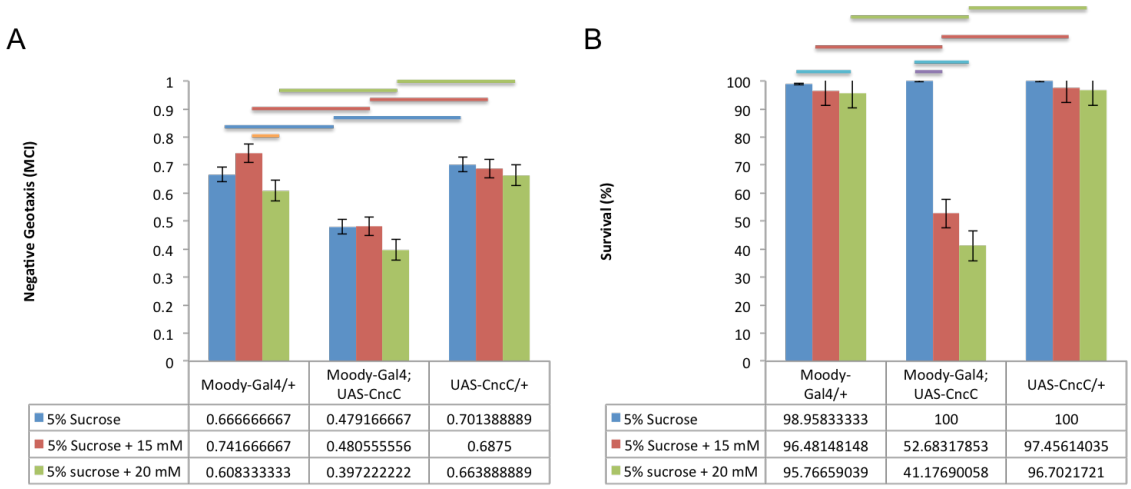

	Moody-Gal4/+	Moody-Gal4; UAS-CncC	UAS-CncC/+
5% Sucrose	0.666666667	0.479166667	0.701388889
5% Sucrose + 15 mM	0.741666667	0.480555556	0.6875
5% sucrose + 20 mM	0.608333333	0.397222222	0.663888889

	Moody-Gal4/+	Moody-Gal4; UAS-CncC	UAS-CncC/+
5% Sucrose	98.95833333	100	100
5% Sucrose + 15 mM	96.48148148	52.68317853	97.45614035
5% sucrose + 20 mM	95.76659039	41.17690058	96.7021721

Figure 7.27: Negative Geotaxis and Survival for the flies expressing CncC in SPG. The flies were exposed to 5% sucrose, 15 mM paraquat in 5% sucrose and 20 mM paraquat in 5% sucrose for 24 h. **Sample sizes: (A)** Negative Geotaxis: Moody-Gal4/+ N=6 for all treatments; Moody-Gal4;UAS-CncC cross: 0 mM N=6; 15 mM and 20 mM N=3; UAS-CncC/+ N=6 for all treatments. **(B)** Survival: Moody-Gal4/+0 mM and 15 mM N=7; 20 mM N=8; Moody-Gal4;UAS-CncC cross: 0 mM N=6; 15 mM and 20 mM N=4; UAS-CncC/+ 0 mM and 15 mM N=7; 20 mM N=8.

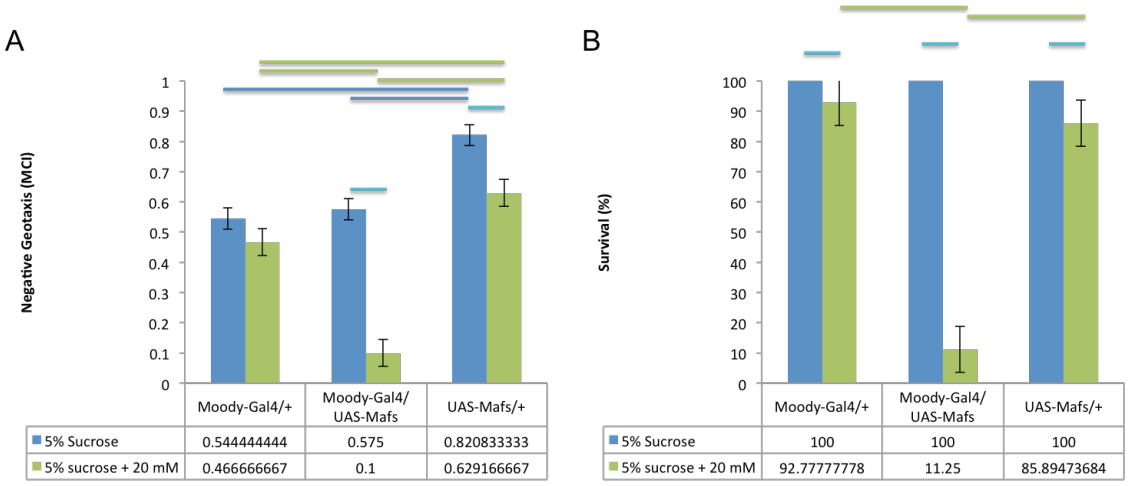

Figure 7.28 Negative Geotaxis and Survival for flies expressing MafS in the SPG. The flies were exposed to 5% sucrose, 15 mM paraquat in 5% sucrose and 20 mM paraquat in 5% sucrose for 24 h. **Sample sizes: (A)** Negative Geotaxis: Moody-Gal4/+: N=6 for all treatments; Moody-Gal4;UAS-MafS cross: 0 mM N=6; 20 mM N=1; UAS-MafS/+ N=6 for all treatments. **(B)** Survival: Moody-Gal4/+ cross: 0 mM N=5; 20 mM N=9; Moody-Gal4;UAS-MafS cross: 0 mM N=5; 20 mM N=11; UAS-MafS/+0 mM N=5; 20 mM N=7.

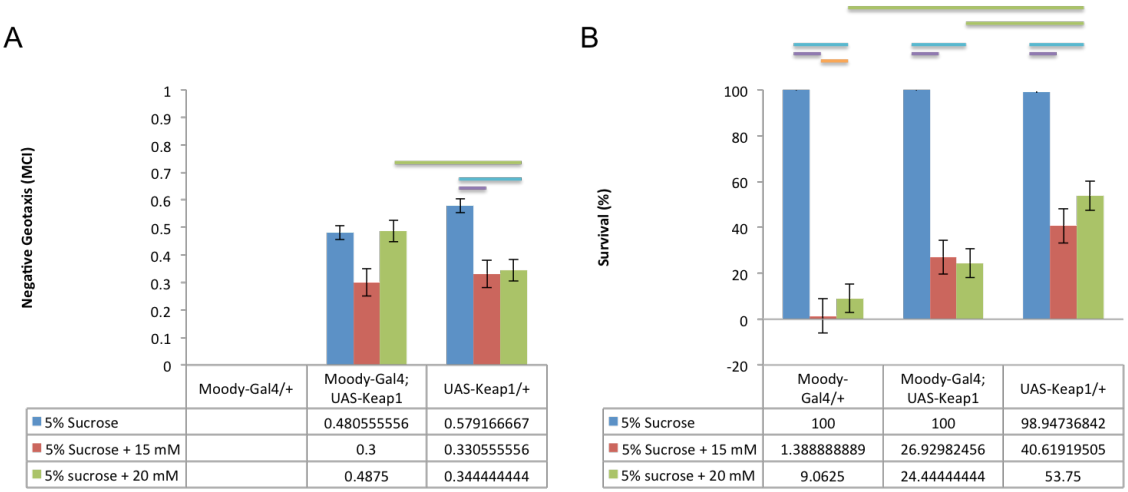

Figure 7.29 Negative Geotaxis and Survival for flies expressing Keap1 in the SPG. The flies were exposed to 5% sucrose, 15 mM paraquat in 5% sucrose and 20 mM paraquat in 5% sucrose for 24 h. **Sample sizes: (A)** Negative Geotaxis: Moody-Gal4/+: N=0 for all treatments; Moody-Gal4;UAS-Keap1 cross: 0 mM N=6; 15 mM and 20 mM N=3; UAS-Keap1/+ cross: 0 mM N=6; 15 mM and 20 mM N=3. **(B)** Survival: Moody-Gal4 /+ 0 mM N=3; 15 mM and 20 mM N=4; Moody-Gal4;UAS-Keap1 0 mM and 15 mM N=5; 20 mM N=6; UAS-Keap1/+ 0 mM and 15 mM N=5; 20 mM N=4.

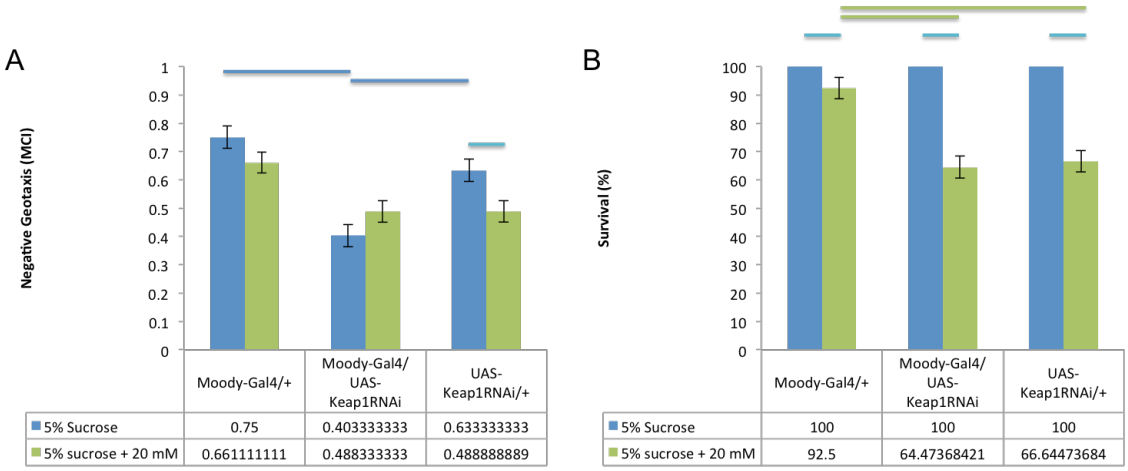

Figure 7.30 Negative Geotaxis and Survival for flies expressing Keap1^{RNAi} in the SPG. The flies were exposed to 5% sucrose, 15 mM paraquat in 5% sucrose and 20 mM paraquat in 5% sucrose for 24 h. **Sample sizes: (A)** Negative Geotaxis: Moody-Gal4/+ N=6 for all treatments; Moody-Gal4/UAS-Keap1^{RNAi} N=5 for all treatments; UAS-Keap1^{RNAi}/+ N=6 for all treatments. **(B)** Survival: Moody-Gal4/+ 0 mM N=4; 20 mM N=11; Moody-Gal4/UAS-Keap1^{RNAi} cross: 0 mM N=4; 20 mM N=5; UAS-Keap1^{RNAi}/+0 mM N=4; 20 mM N=5.

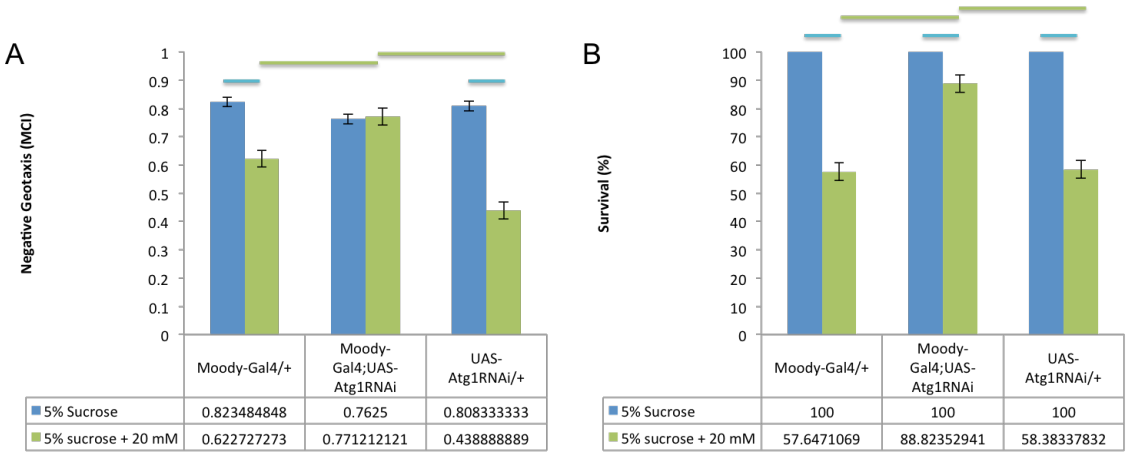

Figure 7.31 Negative Geotaxis and Survival for flies expressing Atg1^{RNAi} in the SPG. The flies were exposed to 5% sucrose, 15 mM paraquat in 5% sucrose and 20 mM paraquat in 5% sucrose for 24 h. **Sample sizes: (A)** Negative Geotaxis: Moody-Gal4/+ N=11 for all treatments; Moody-Gal4;UAS-Atg^{RNAi} 0 mM N=11; 20 mM N=12; UAS-Atg1^{RNAi}/+ 0 mM N=9; 20 mM N=10; **(B)** Survival: Moody-Gal4/+ 0 mM N=7; 20 mM N=4; Moody-Gal4;UAS-Atg1^{RNAi} cross: 0 mM N=9; 20 mM N=17; UAS-Atg1^{RNAi}/+ cross: 0 mM N=7; 20 mM N=13.

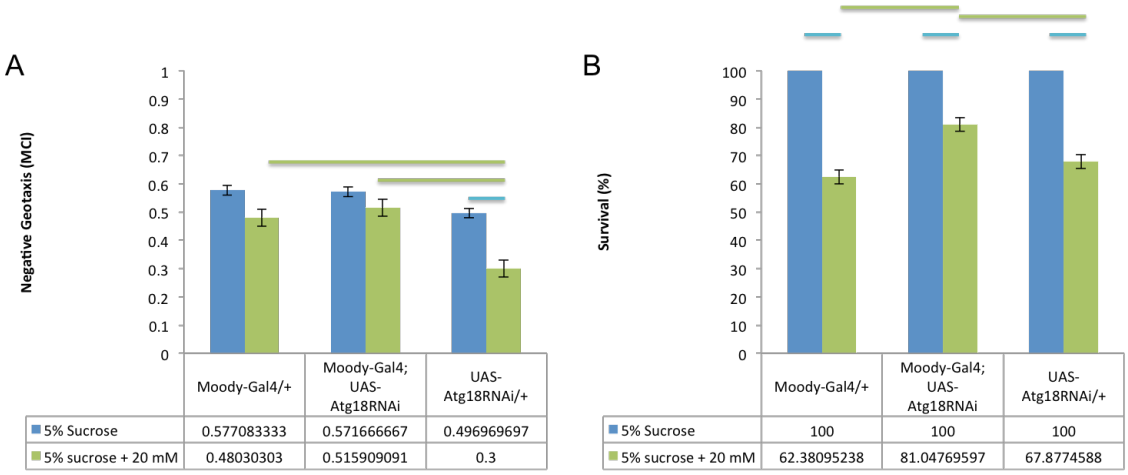

Figure 7.32 Negative Geotaxis and Survival for flies expressing Atg18^{RNAi} in SPG. The flies were exposed to 5% sucrose, 15 mM paraquat in 5% sucrose and 20 mM paraquat in 5% sucrose for 24 h. **Sample sizes: (A)** Negative Geotaxis: Moody-Gal4/+ 0 mM N=11; 20 mM N=12; Moody-Gal4;UAS-Atg18^{RNAi} cross: 0 mM N=10; 20 mM N=11; UAS- Atg18^{RNAi}/+ cross: 0 mM N=7; 20 mM N=11; **(B)** Survival: Moody-Gal4/+ 0 mM N=8; 20 mM N=14; Moody-Gal4;UAS-Atg18^{RNAi} cross: 0 mM N=6; 20 mM N=23; UAS-Atg18^{RNAi}/+ cross: 0 mM N=8; 20 mM N=21.

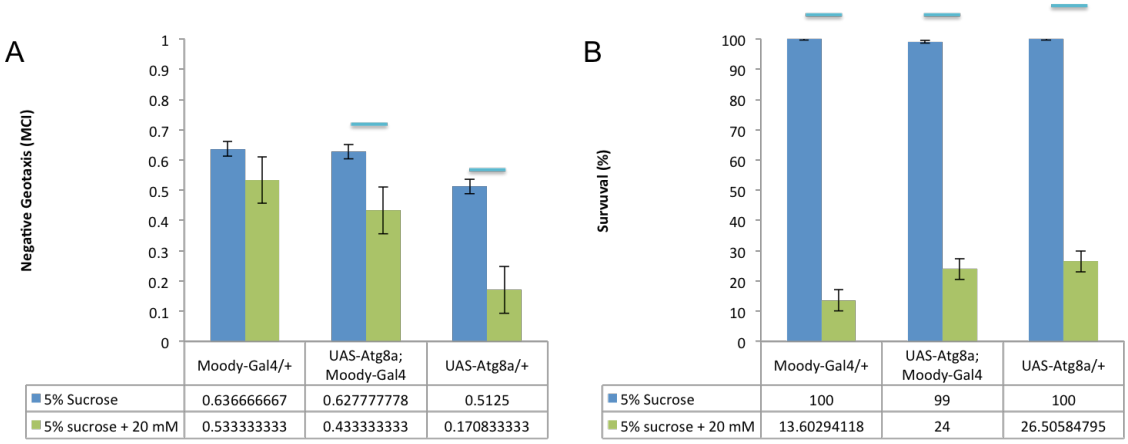

Figure 7.33 Negative Geotaxis and Survival for flies expressing Atg8a in SPG. The flies were exposed to 5% sucrose, 15 mM paraquat in 5% sucrose and 20 mM paraquat in 5% sucrose for 24 h. **Sample sizes: (A)** Negative Geotaxis: Moody-Gal4/+ 0 mM N=5; 20 mM N=1; Moody-Gal4;UAS-Atg8a cross: 0 mM N=6; 20 mM N=2; UAS-Atg8a/+ 0 mM N=2; 20 mM N=6; **(B)** Survival: Moody-Gal4/+ 0 mM N=3; 20 mM N=4; Moody-Gal4;UAS-Atg8a cross: N=5 for all treatments; UAS-Atg8a/+ N=5 for all treatments.

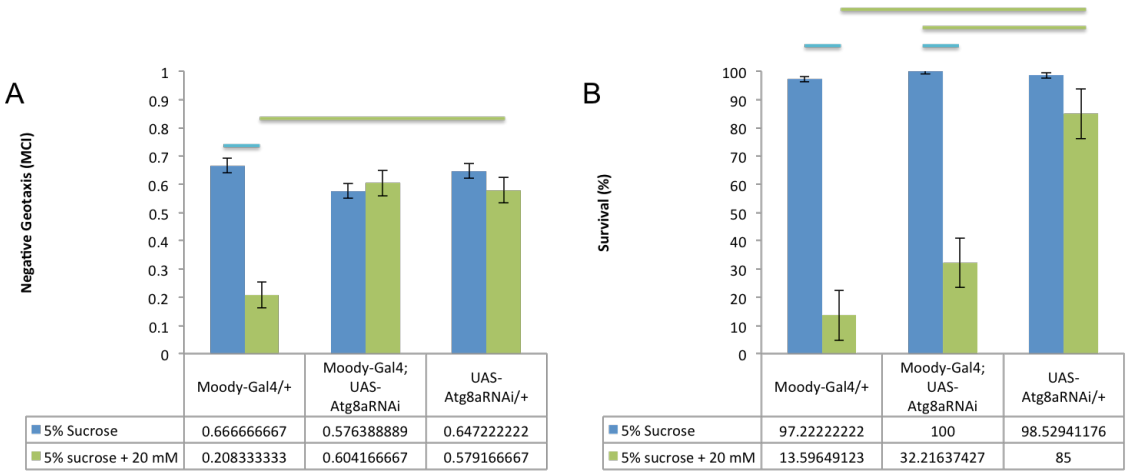

Figure 7.34 Negative Geotaxis and Survival for flies expressing Atg8a^{RNAi} in SPG. The flies were exposed to 5% sucrose, 15 mM paraquat in 5% sucrose and 20 mM paraquat in 5% sucrose for 24 h. **Sample sizes: (A)** Negative Geotaxis: Moody-Gal4/+ 0 mM N=6; 20 mM N=1; Moody-Gal4;UAS-Atg8a^{RNAi} 0 mM N=6; 20 mM N=2; UAS-Atg8a^{RNAi}/+ N=6 for all treatments; **(B)** Survival: Moody-Gal4/+ 0 mM N=4; 20 mM N=6; Moody-Gal4;UAS-Atg8a^{RNAi} 0 mM N=4; 20 mM N=6; UAS-Atg8a^{RNAi}/+ cross: N=5 for all treatments.

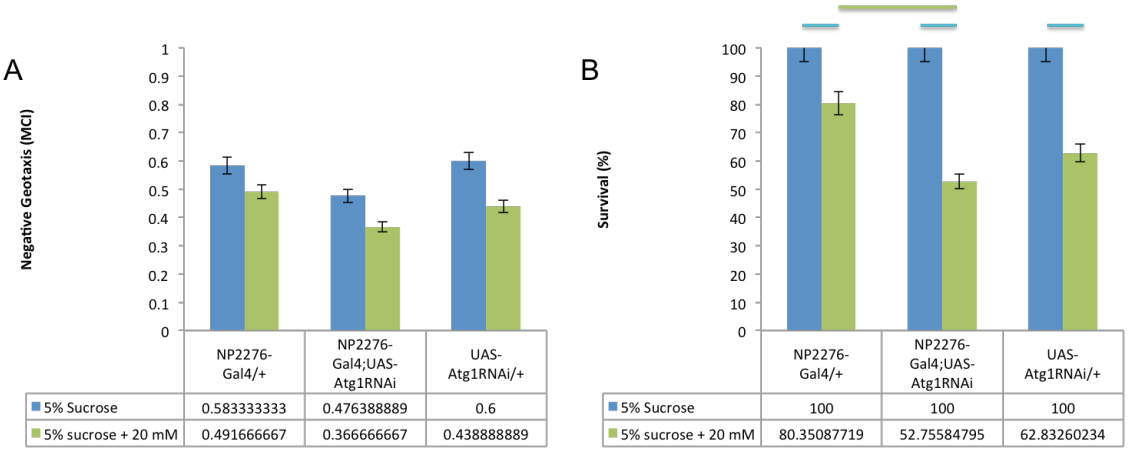

Figure 7.35 Negative Geotaxis and Survival for flies expressing Atg1^{RNAi} in the SPG using the NP2276-Gal4 driver. The flies were exposed to 5% sucrose, 15 mM paraquat in 5% sucrose and 20 mM paraquat in 5% sucrose for 24 h. **Sample sizes: (A)** Negative Geotaxis: NP2276-Gal4/+ N=6 for all treatments; NP2276-Gal4;UAS-Atg1^{RNAi} 0 mM N=6; 20 mM N=3; UAS- Atg1^{RNAi}/+ cross: N=6 for all treatments **(B)** Survival: NP2276-Gal4/+ 0 mM N=4; 20 mM N=6; NP2276-Gal4;UAS-Atg1^{RNAi} cross: N=4 for all treatments; UAS-Atg1^{RNAi}/+ cross: 0 mM N=4; 20 mM N=8.

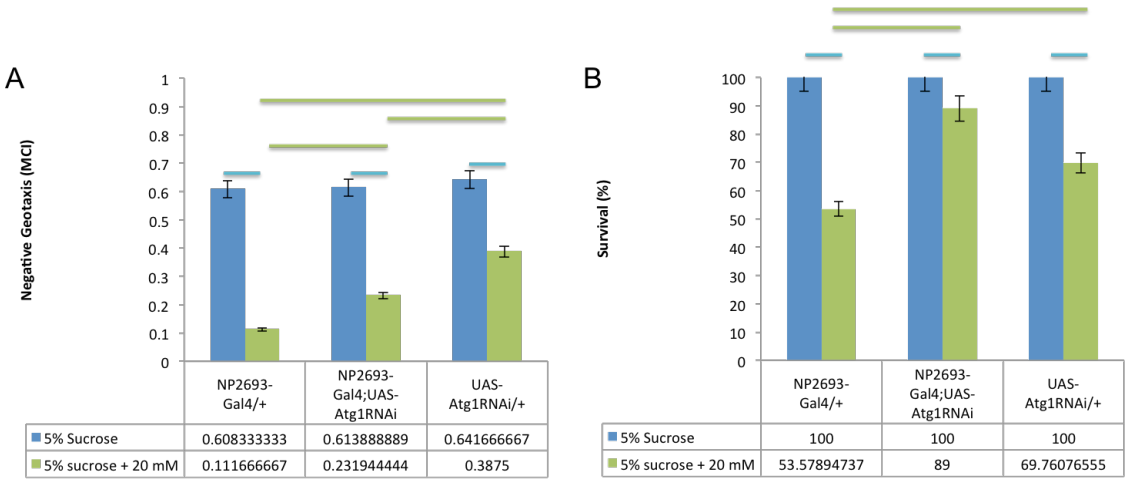

Figure 7.36 Negative Geotaxis and Survival for flies expressing Atg1^{RNAi} in the PNG The flies were exposed to 5% sucrose, 15 mM paraquat in 5% sucrose and 20 mM paraquat in 5% sucrose for 24 h. **Sample sizes: (A)** Negative Geotaxis: NP2693-Gal4/+ N=6 for all treatments; NP2693-Gal4;UAS-Atg1^{RNAi} N=6 for all treatments; UAS-Atg1^{RNAi}/+ 0 mM N=6; 20 mM N=5; **(B)** Survival: NP2693-Gal4/+ 0 mM N=3; 20 mM N=5; NP2693-Gal4;UAS-Atg1^{RNAi} cross: 0 mM N=4; 20 mM N=5; UAS-Atg1^{RNAi}/+ 0 mM N=6; 20 mM N=11.

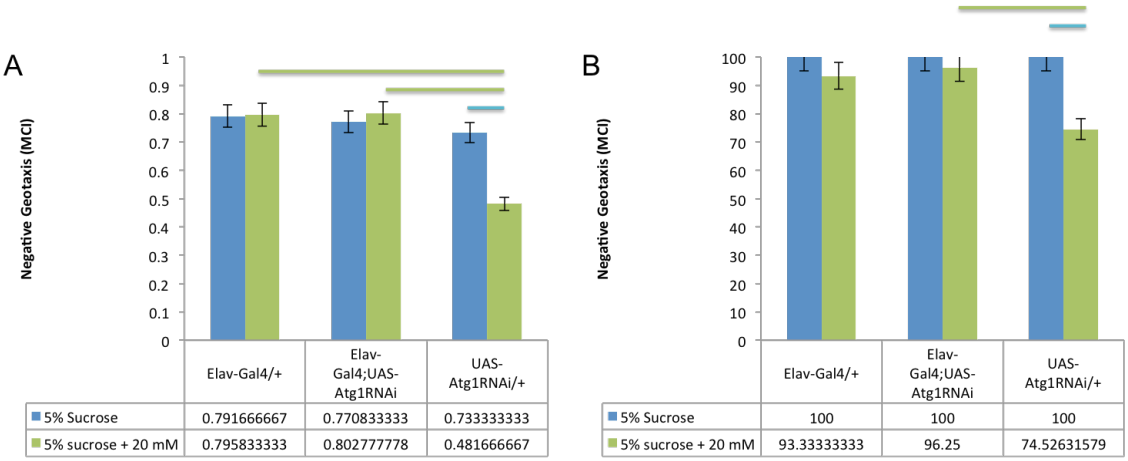

Figure 7.37 Negative Geotaxis and Survival for flies expressing Atg1^{RNAi} in all neurons. The flies were exposed to 5% sucrose, 15 mM paraquat in 5% sucrose and 20 mM paraquat in 5% sucrose for 24 h. **Sample sizes: (A)** Negative Geotaxis: elav-Gal4/+: N=6 for all treatments; elav-Gal4;UAS-Atg1^{RNAi} N=6 for all treatments; UAS- Atg1^{RNAi}/+ 0 mM N=6; 20 mM N=5; **(B)** Survival: elav-Gal4/+ 0 mM N=3; 20 mM N=4; elav-Gal4;UAS-Atg1^{RNAi} cross: N=4 for all treatments; UAS-Atg1^{RNAi}/+ 0 mM N=4; 20 mM N=5.

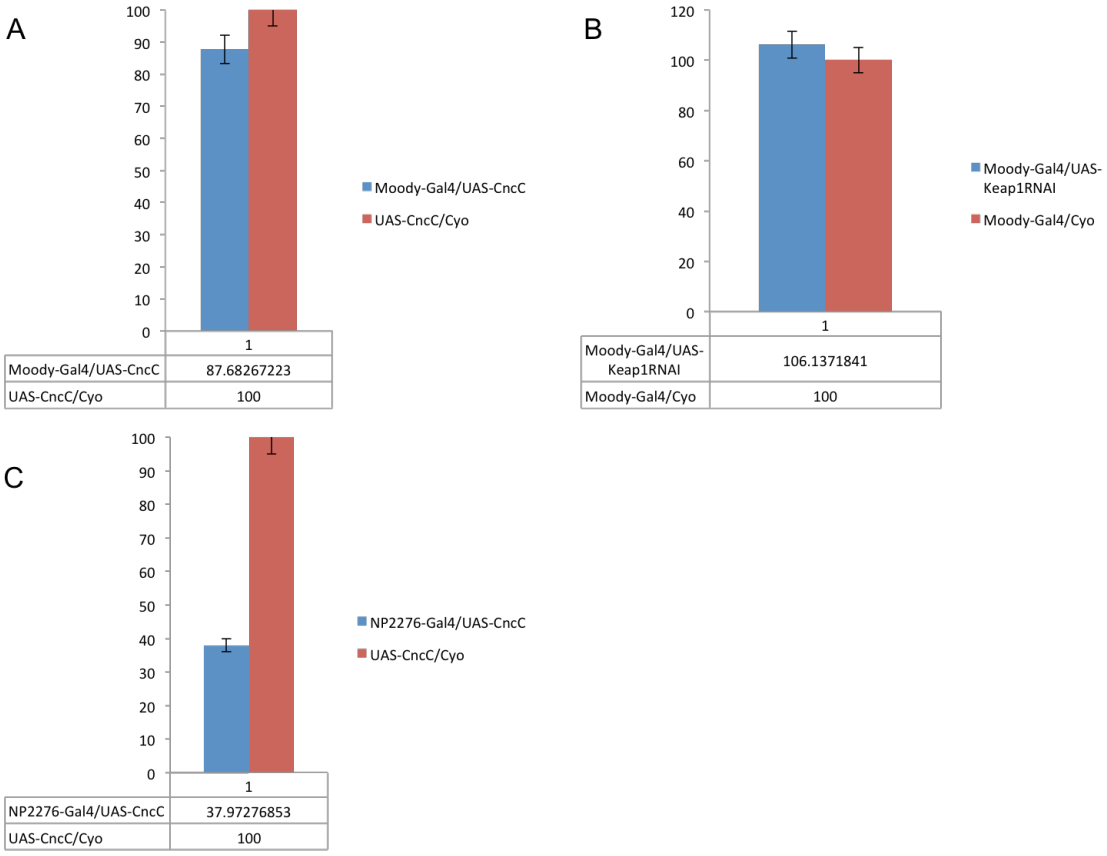

Figure 7.38 Developmental Lethality for crosses that overexpress CncC in the SPG. (A) Developmental lethality ratio between Moody-Gal4/UAS-CncC VS. UAS-CncC/Cyo; **(B)** Developmental lethality ratio between Moody-Gal4/UAS-Keap1^{RNAi} VS. Moody-Gal4/Cyo; **(C)** Developmental lethality ratio between NP2276-Gal4/UAS-CncC VS. UAS-CncC/Cyo. For all assays the rations are normalized so that the internal controls are 100

7.4 Alternative Methods

7.4.1 Negative Geotaxis Assay

Negative geotaxis assay was performed in the same way as outlined in section 2.4 except that 10 flies per vial were used per sample.

7.4.2 CO_2 anesthesia exposure

The CO_2 anesthesia exposure experiment was performed on 1-4 day old w^{1118} male flies grown at 25^0 C. The flies were anesthetized with CO_2 on the fly pad for either 0 min, 2 min or 5 min. The flies were then tested using the negative geotaxis assay at 10 min, 20 min, 30 min, 40 min, 50 min, 60 min and 90 min.

7.4.3 Developmental Lethality Assay

The developmental lethality assay was performed in order to detect toxic levels of overexpression of certain proteins on flies during development. In the case of fly socks that already contain a balancer chromosome, the flies were simply crossed with the Gal4 stock and left to grow at 25^0 C until eclosion. Once the flies eclosed, the number of flies of each genotype was counted and recorded every 1-2 days up until 10 days after eclosion. Fly stocks that did not contain balancer chromosomes were first crossed with the appropriate balancer stocks, and then the progeny from these crosses were crossed with the Gal4 stocks. The same growing and counting procedure was applied for these flies. A total of 6 individual replicate crosses were produced for each assay. The recorded data was then analyzed by adding the number of flies of a particular genotype for all the 6 replicate crosses together. The genotype containing the balancer chromosome was considered an internal control and the other genotype containing the UAS/Gal4 construct

was considered the experimental genotype. The total number of internal control flies was standardized to be 100, while the total number of experimental flies was divided by the total number of internal control flies and then multiplied by 100 in order to provide a ratio out of 100.